

T2K neutrino oscillation results

Ciro Riccio

WIN2019 - The 27th International Workshop
on Weak Interactions and Neutrinos

June 4th, 2019



UNIVERSITÀ DEGLI STUDI
DI NAPOLI FEDERICO II



Overview

Overview

- Neutrino oscillations

Overview

- Neutrino oscillations
- T2K experimental setup

Overview

- Neutrino oscillations
- T2K experimental setup
- Oscillation analysis strategy

Overview

- Neutrino oscillations
- T2K experimental setup
- Oscillation analysis strategy
- T2K latest results

Overview

- Neutrino oscillations
- T2K experimental setup
- Oscillation analysis strategy
- T2K latest results
- Conclusions

Neutrino oscillations

Neutrino mixing described by the PMNS matrix: 3 mixing angles and 1 complex CPV phase

$$\begin{pmatrix} \nu_e \\ \nu_\mu \\ \nu_\tau \end{pmatrix} = \begin{pmatrix} 1 & 0 & 0 \\ 0 & c_{23} & s_{23} \\ 0 & -s_{23} & c_{23} \end{pmatrix} \begin{pmatrix} c_{13} & 0 & s_{13}e^{-i\delta_{CP}} \\ 0 & 1 & 0 \\ -s_{13}e^{i\delta_{CP}} & 0 & c_{13} \end{pmatrix} \begin{pmatrix} c_{12} & s_{12} & 0 \\ -s_{12} & c_{12} & 0 \\ 0 & 0 & 1 \end{pmatrix} \begin{pmatrix} \nu_1 \\ \nu_2 \\ \nu_3 \end{pmatrix}$$

$$\Delta m_{ji}^2 = m_j^2 - m_i^2 \quad c_{ij} = \cos \theta_{ij} \quad s_{ij} = \sin \theta_{ij}$$

Neutrino oscillations

Neutrino mixing described by the PMNS matrix: 3 mixing angles
and 1 complex CPV phase

$$\begin{pmatrix} \nu_e \\ \nu_\mu \\ \nu_\tau \end{pmatrix} = \begin{pmatrix} 1 & 0 & 0 \\ 0 & c_{23} & s_{23} \\ 0 & -s_{23} & c_{23} \end{pmatrix} \begin{pmatrix} c_{13} & 0 & s_{13}e^{-i\delta_{CP}} \\ 0 & 1 & 0 \\ -s_{13}e^{i\delta_{CP}} & 0 & c_{13} \end{pmatrix} \begin{pmatrix} c_{12} & s_{12} & 0 \\ -s_{12} & c_{12} & 0 \\ 0 & 0 & 1 \end{pmatrix} \begin{pmatrix} \nu_1 \\ \nu_2 \\ \nu_3 \end{pmatrix}$$

Atmospheric and
accelerator

$$\theta_{23} \sim 50^\circ$$

$$|\Delta m_{32}^2| \sim 2.5 \times 10^{-3} \text{ eV}^2$$

$$\Delta m_{ji}^2 = m_j^2 - m_i^2 \quad c_{ij} = \cos \theta_{ij} \quad s_{ij} = \sin \theta_{ij}$$

Neutrino oscillations

Neutrino mixing described by the PMNS matrix: 3 mixing angles and 1 complex CPV phase

$$\begin{pmatrix} \nu_e \\ \nu_\mu \\ \nu_\tau \end{pmatrix} = \begin{pmatrix} 1 & 0 & 0 \\ 0 & c_{23} & s_{23} \\ 0 & -s_{23} & c_{23} \end{pmatrix} \begin{pmatrix} c_{13} & 0 & s_{13}e^{-i\delta_{CP}} \\ 0 & 1 & 0 \\ -s_{13}e^{i\delta_{CP}} & 0 & c_{13} \end{pmatrix} \begin{pmatrix} c_{12} & s_{12} & 0 \\ -s_{12} & c_{12} & 0 \\ 0 & 0 & 1 \end{pmatrix} \begin{pmatrix} \nu_1 \\ \nu_2 \\ \nu_3 \end{pmatrix}$$

Atmospheric and
accelerator
 $\theta_{23} \sim 50^\circ$
 $|\Delta m_{32}^2| \sim 2.5 \times 10^{-3} \text{ eV}^2$

Reactor and accelerator
 $\theta_{13} \sim 8^\circ$
Accelerator only $\delta_{CP} = ??$

$$\Delta m_{ji}^2 = m_j^2 - m_i^2 \quad c_{ij} = \cos \theta_{ij} \quad s_{ij} = \sin \theta_{ij}$$

Neutrino oscillations

Neutrino mixing described by the PMNS matrix: 3 mixing angles and 1 complex CPV phase

$$\begin{pmatrix} \nu_e \\ \nu_\mu \\ \nu_\tau \end{pmatrix} = \begin{pmatrix} 1 & 0 & 0 \\ 0 & c_{23} & s_{23} \\ 0 & -s_{23} & c_{23} \end{pmatrix} \begin{pmatrix} c_{13} & 0 & s_{13}e^{-i\delta_{CP}} \\ 0 & 1 & 0 \\ -s_{13}e^{i\delta_{CP}} & 0 & c_{13} \end{pmatrix} \begin{pmatrix} c_{12} & s_{12} & 0 \\ -s_{12} & c_{12} & 0 \\ 0 & 0 & 1 \end{pmatrix} \begin{pmatrix} \nu_1 \\ \nu_2 \\ \nu_3 \end{pmatrix}$$

Atmospheric and
accelerator
 $\theta_{23} \sim 50^\circ$
 $|\Delta m_{32}^2| \sim 2.5 \times 10^{-3} \text{ eV}^2$

Reactor and accelerator
 $\theta_{13} \sim 8^\circ$
Accelerator only $\delta_{CP} = ??$

Solar and
reactor
 $\theta_{12} \sim 34^\circ$
 $\Delta m_{12}^2 \sim 7.5 \times 10^{-5} \text{ eV}^2$

$$\Delta m_{ji}^2 = m_j^2 - m_i^2 \quad c_{ij} = \cos \theta_{ij} \quad s_{ij} = \sin \theta_{ij}$$

Neutrino oscillations

Neutrino mixing described by the PMNS matrix: 3 mixing angles and 1 complex CPV phase

$$\begin{pmatrix} \nu_e \\ \nu_\mu \\ \nu_\tau \end{pmatrix} = \begin{pmatrix} 1 & 0 & 0 \\ 0 & c_{23} & s_{23} \\ 0 & -s_{23} & c_{23} \end{pmatrix} \begin{pmatrix} c_{13} & 0 & s_{13}e^{-i\delta_{CP}} \\ 0 & 1 & 0 \\ -s_{13}e^{i\delta_{CP}} & 0 & c_{13} \end{pmatrix} \begin{pmatrix} c_{12} & s_{12} & 0 \\ -s_{12} & c_{12} & 0 \\ 0 & 0 & 1 \end{pmatrix} \begin{pmatrix} \nu_1 \\ \nu_2 \\ \nu_3 \end{pmatrix}$$

Atmospheric and
accelerator
 $\theta_{23} \sim 50^\circ$
 $|\Delta m_{32}^2| \sim 2.5 \times 10^{-3} \text{ eV}^2$

Reactor and accelerator
 $\theta_{13} \sim 8^\circ$
Accelerator only $\delta_{CP} = ??$

Solar and
reactor
 $\theta_{12} \sim 34^\circ$
 $\Delta m_{12}^2 \sim 7.5 \times 10^{-5} \text{ eV}^2$

Inferred from event rate: $P(\nu_\alpha \rightarrow \nu_\beta) = P(E, L, \Delta m^2, \theta)$

$$\Delta m_{ji}^2 = m_j^2 - m_i^2 \quad c_{ij} = \cos \theta_{ij} \quad s_{ij} = \sin \theta_{ij}$$

Neutrino oscillations

Neutrino mixing described by the PMNS matrix: 3 mixing angles and 1 complex CPV phase

$$\begin{pmatrix} \nu_e \\ \nu_\mu \\ \nu_\tau \end{pmatrix} = \begin{pmatrix} 1 & 0 & 0 \\ 0 & c_{23} & s_{23} \\ 0 & -s_{23} & c_{23} \end{pmatrix} \begin{pmatrix} c_{13} & 0 & s_{13}e^{-i\delta_{CP}} \\ 0 & 1 & 0 \\ -s_{13}e^{i\delta_{CP}} & 0 & c_{13} \end{pmatrix} \begin{pmatrix} c_{12} & s_{12} & 0 \\ -s_{12} & c_{12} & 0 \\ 0 & 0 & 1 \end{pmatrix} \begin{pmatrix} \nu_1 \\ \nu_2 \\ \nu_3 \end{pmatrix}$$

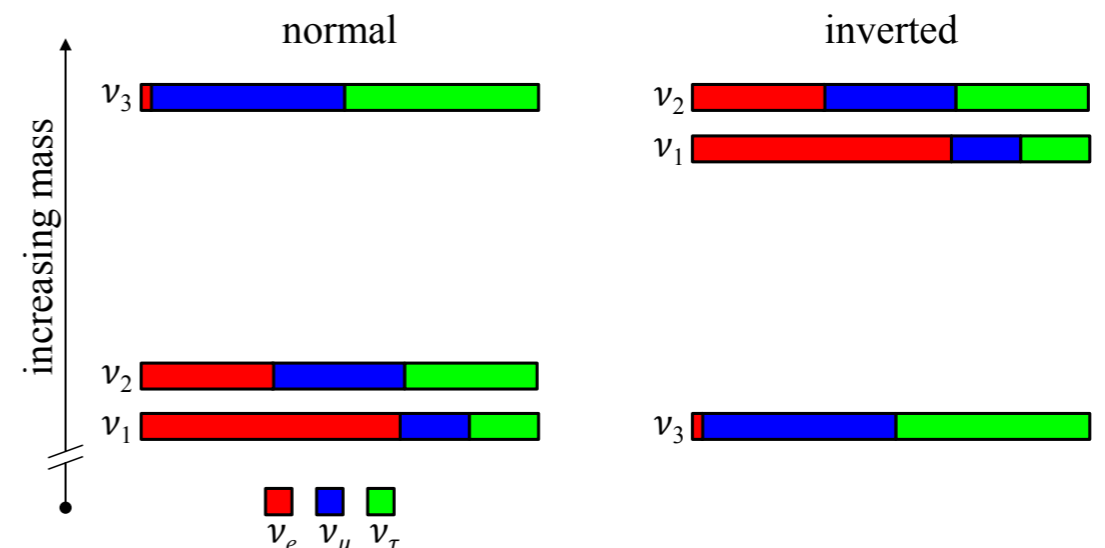
Atmospheric and
accelerator
 $\theta_{23} \sim 50^\circ$
 $|\Delta m_{32}^2| \sim 2.5 \times 10^{-3} \text{ eV}^2$

Reactor and accelerator
 $\theta_{13} \sim 8^\circ$
Accelerator only $\delta_{CP} = ??$

Solar and
reactor
 $\theta_{12} \sim 34^\circ$
 $\Delta m_{12}^2 \sim 7.5 \times 10^{-5} \text{ eV}^2$

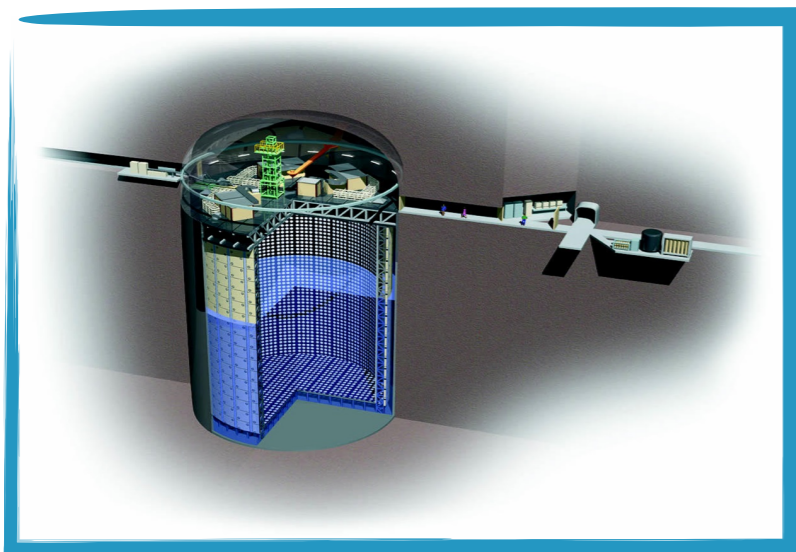
Inferred from event rate: $P(\nu_\alpha \rightarrow \nu_\beta) = P(E, L, \Delta m^2, \theta)$

Open questions: δ_{CP} , θ_{23} octant and mass ordering

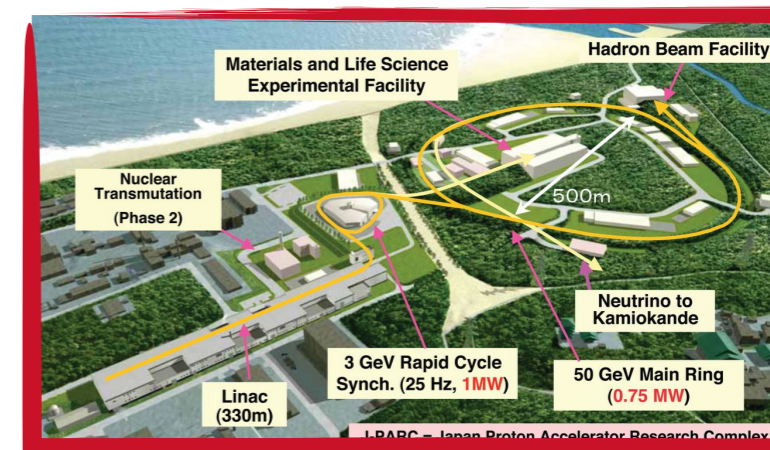


$$\Delta m_{ji}^2 = m_j^2 - m_i^2 \quad c_{ij} = \cos \theta_{ij} \quad s_{ij} = \sin \theta_{ij}$$

The T2K experiment

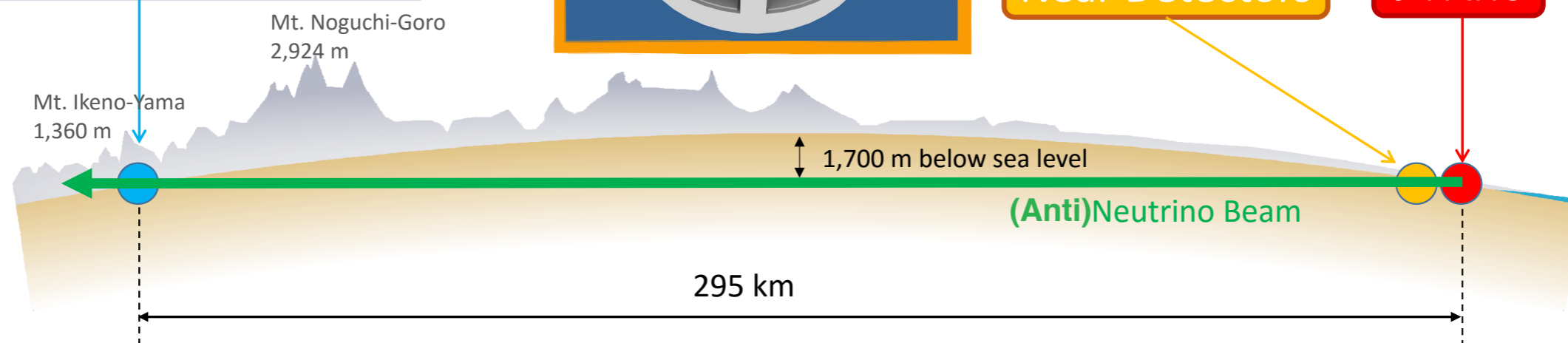


Super-Kamiokande

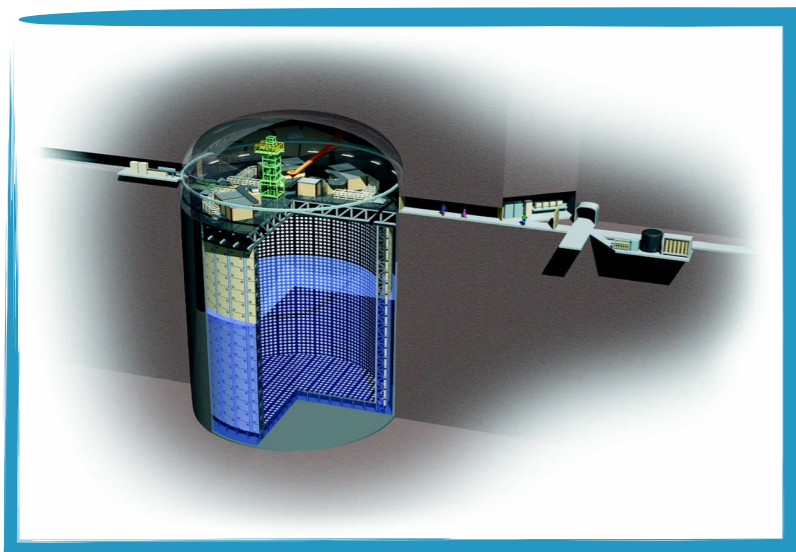


Near Detectors

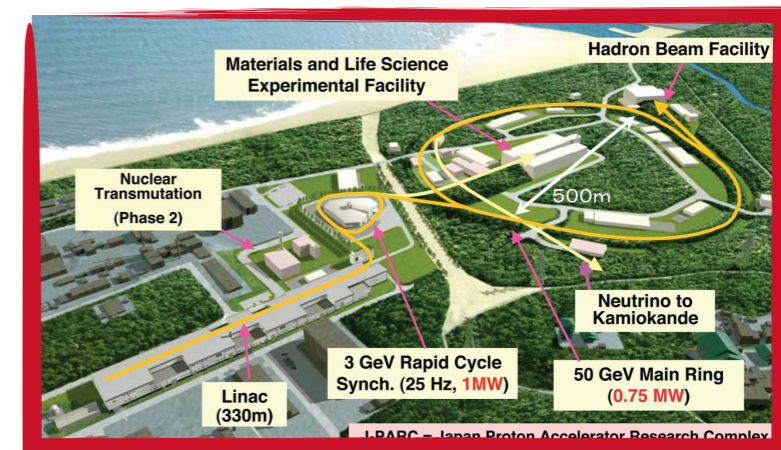
J-PARC



The T2K experiment

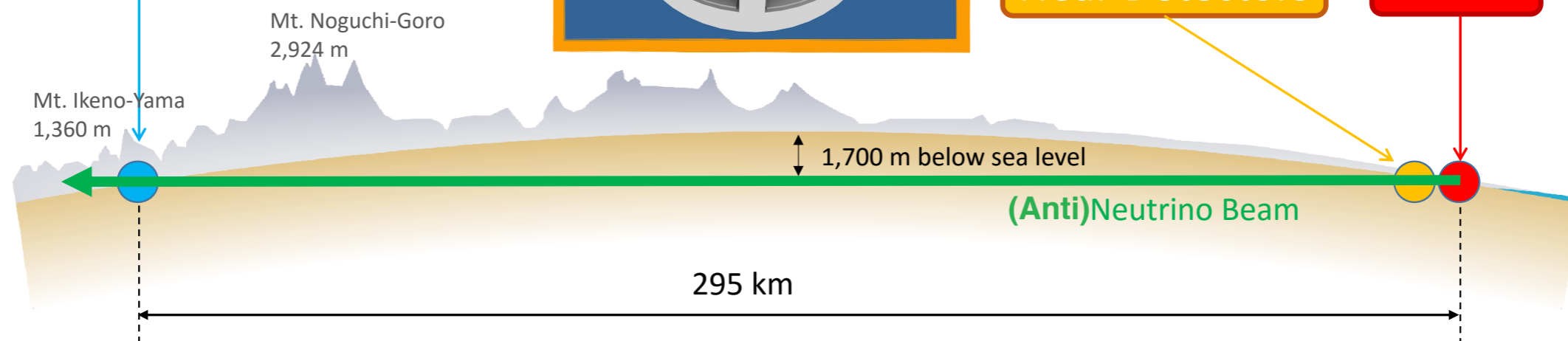


Super-Kamiokande



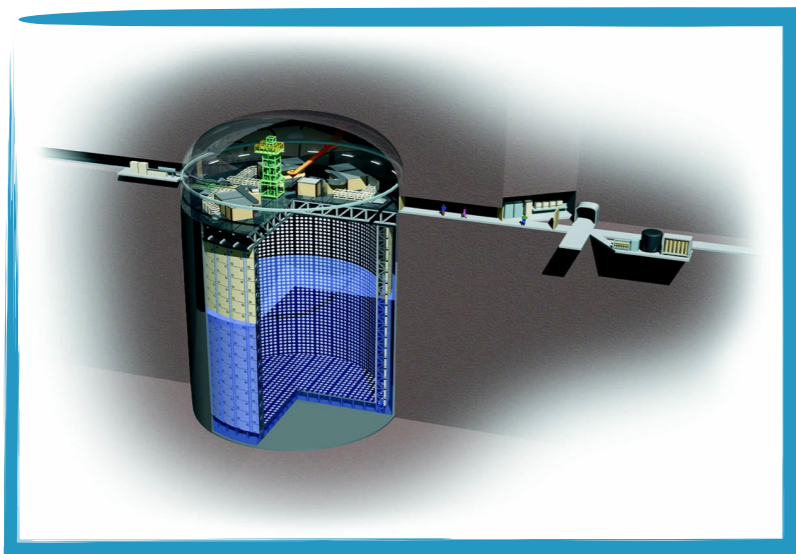
Near Detectors

J-PARC

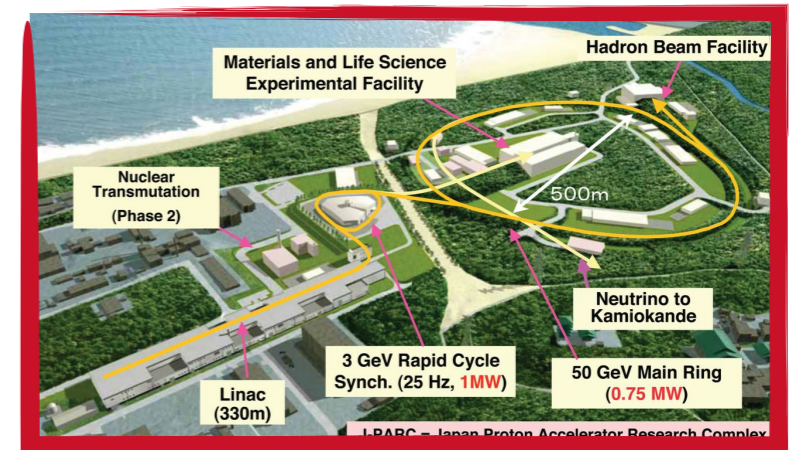


Physics goals:

The T2K experiment

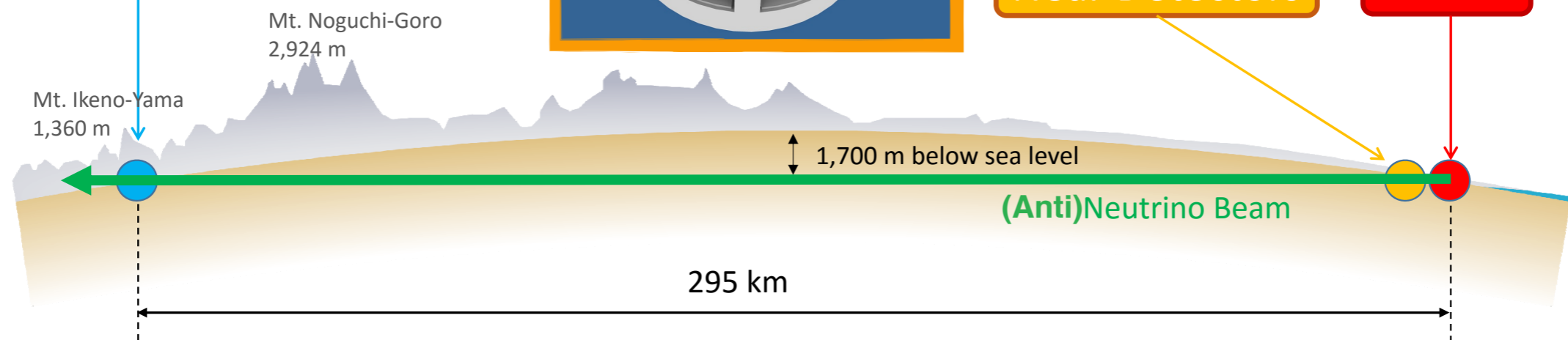


Super-Kamiokande



Near Detectors

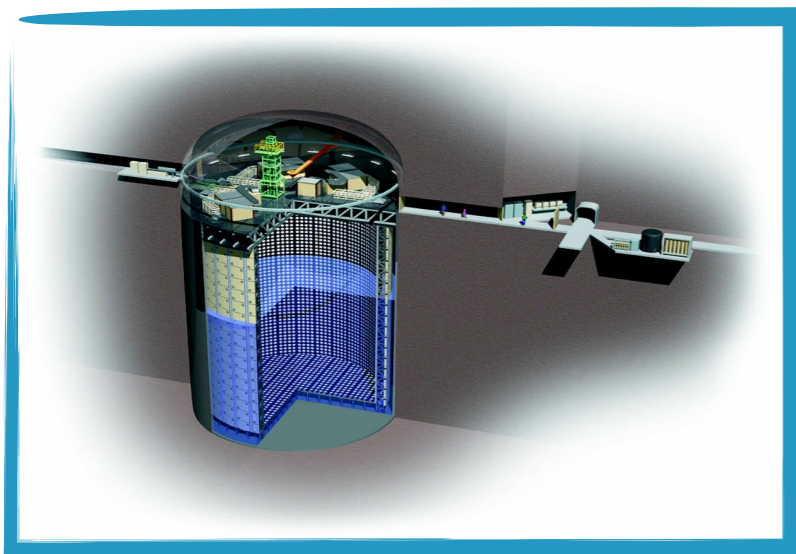
J-PARC



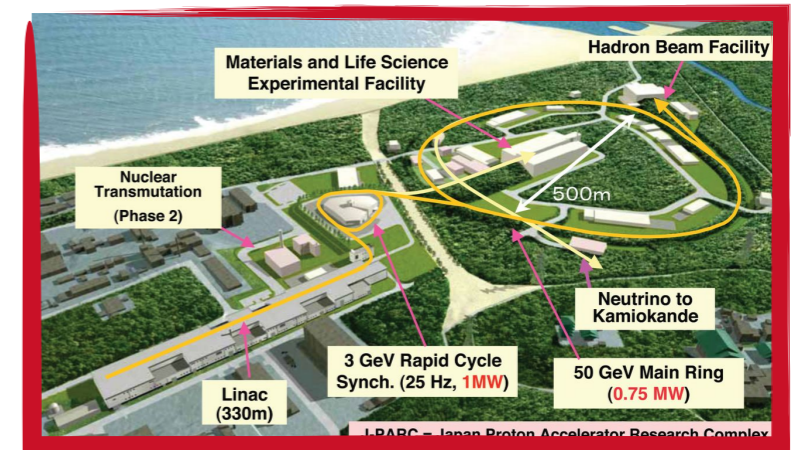
Physics goals:

- Precise measurement of θ_{23} , $|\Delta m_{32}^2|$

The T2K experiment

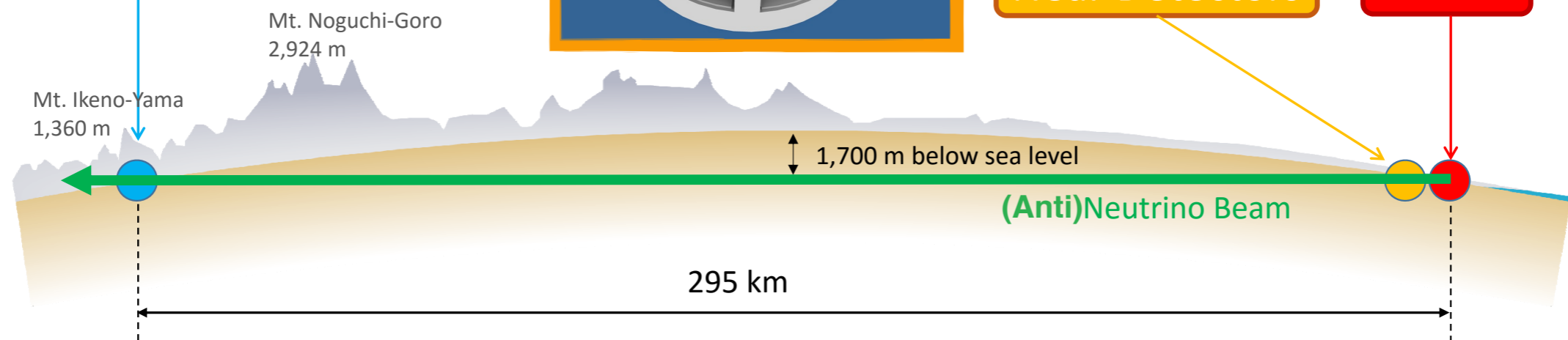


Super-Kamiokande



Near Detectors

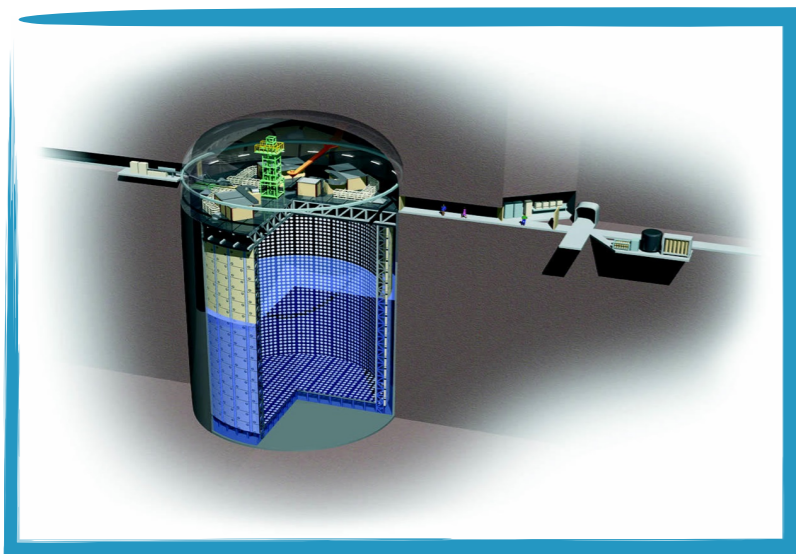
J-PARC



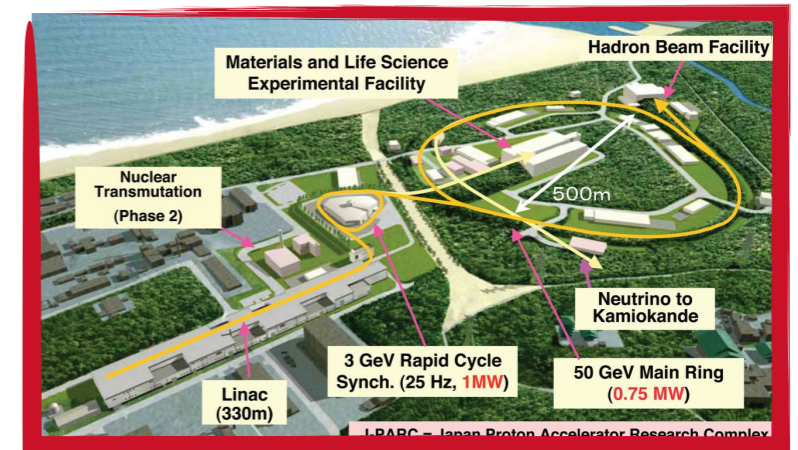
Physics goals:

- Precise measurement of θ_{23} , $|\Delta m_{32}^2|$
- Determine θ_{13} and δ_{CP}

The **T2K** experiment

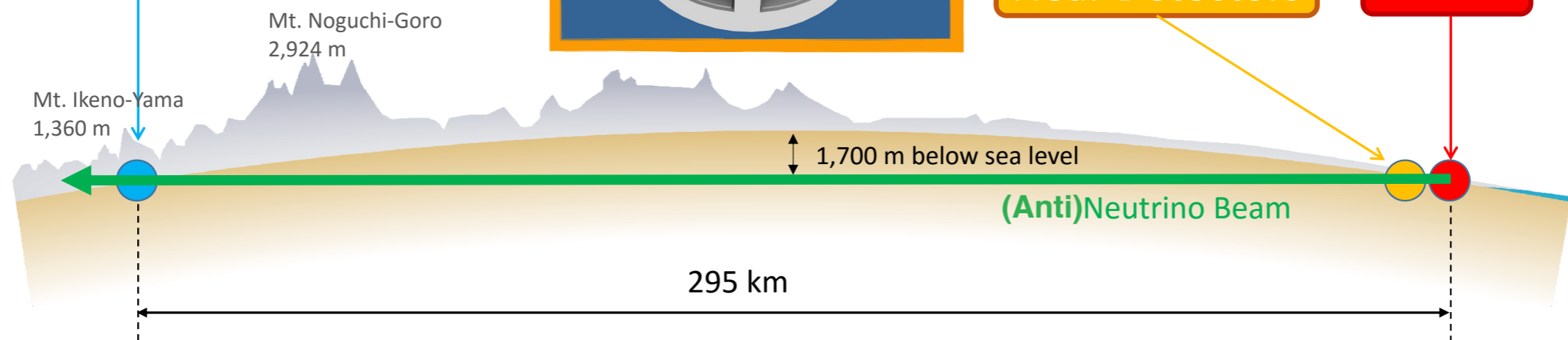


Super-Kamiokande



Near Detectors

J-PARC



Physics goals:

- Precise measurement of θ_{23} , $|\Delta m_{32}^2|$
- Determine θ_{13} and δ_{CP}
- ν cross section measurements at the near detectors

Oscillations measurements at T2K

Oscillations measurements at T2K

Long baseline accelerator-based experiments are sensitive to:

Oscillations measurements at

Long baseline accelerator-based experiments are sensitive to:

- Atmospheric parameters ($\theta_{23}, \Delta m_{32}^2$) through ν_{μ} disappearance

$$P(\bar{\nu}_{\mu} \rightarrow \bar{\nu}_{\mu}) \approx 1 - \sin^2 2\theta_{23} \sin^2 \left(\frac{\Delta m_{32}^2 L}{4E} \right)$$

Oscillations measurements at

Long baseline accelerator-based experiments are sensitive to:

- Atmospheric parameters ($\theta_{23}, \Delta m_{32}^2$) through ν_{μ} disappearance

$$P(\bar{\nu}_{\mu} \rightarrow \bar{\nu}_{\mu}) \approx 1 - \sin^2 2\theta_{23} \sin^2 \left(\frac{\Delta m_{32}^2 L}{4E} \right)$$

- (θ_{13}, δ_{CP}) depends on the $\nu_e/\bar{\nu}_e$ appearance

$$P(\bar{\nu}_{\mu} \rightarrow \bar{\nu}_e) \approx \sin^2 2\theta_{13} \sin^2 \theta_{23} \sin^2 \left(\frac{\Delta m_{32}^2 L}{4E} \right) (\mp) O(\delta_{CP})$$

Oscillations measurements at

Long baseline accelerator-based experiments are sensitive to:

- Atmospheric parameters ($\theta_{23}, \Delta m_{32}^2$) through ν_{μ} disappearance

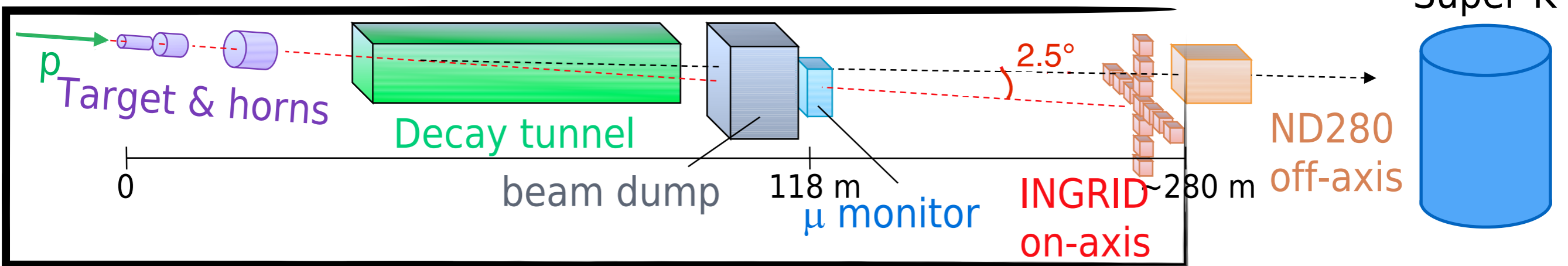
$$P(\bar{\nu}_{\mu} \rightarrow \bar{\nu}_{\mu}) \approx 1 - \sin^2 2\theta_{23} \sin^2 \left(\frac{\Delta m_{32}^2 L}{4E} \right)$$

- (θ_{13}, δ_{CP}) depends on the $\nu_e/\bar{\nu}_e$ appearance

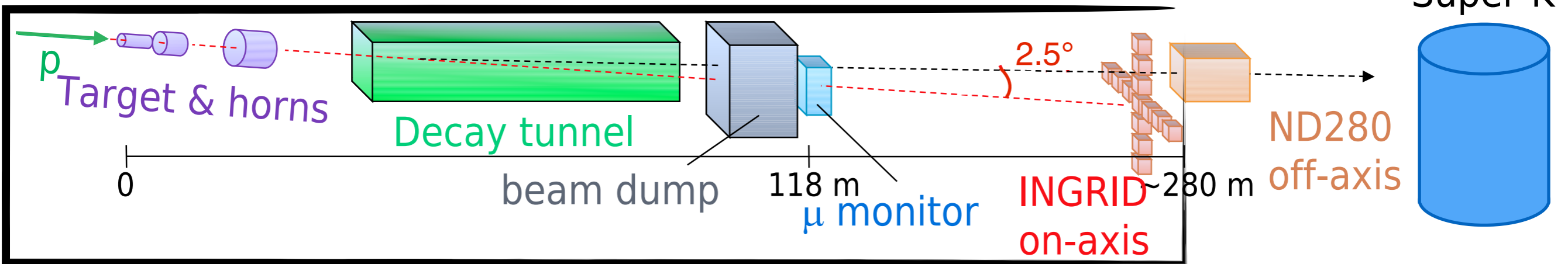
$$P(\bar{\nu}_{\mu} \rightarrow \bar{\nu}_e) \approx \sin^2 2\theta_{13} \sin^2 \theta_{23} \sin^2 \left(\frac{\Delta m_{32}^2 L}{4E} \right) (\mp) O(\delta_{CP})$$

In the case of T2K δ_{CP} change the appearance probability by $\pm 30\%$ while the mass ordering has a $\sim 10\%$ effects

T2K Beam

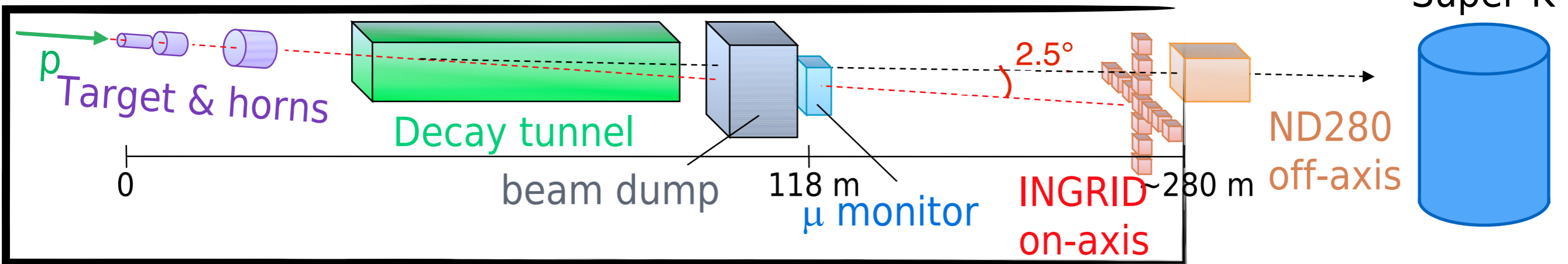


T2K Beam



30 GeV proton beam from J-PARC Main Ring extracted onto a graphite target producing hadrons (mainly pions and kaons)

T2K Beam

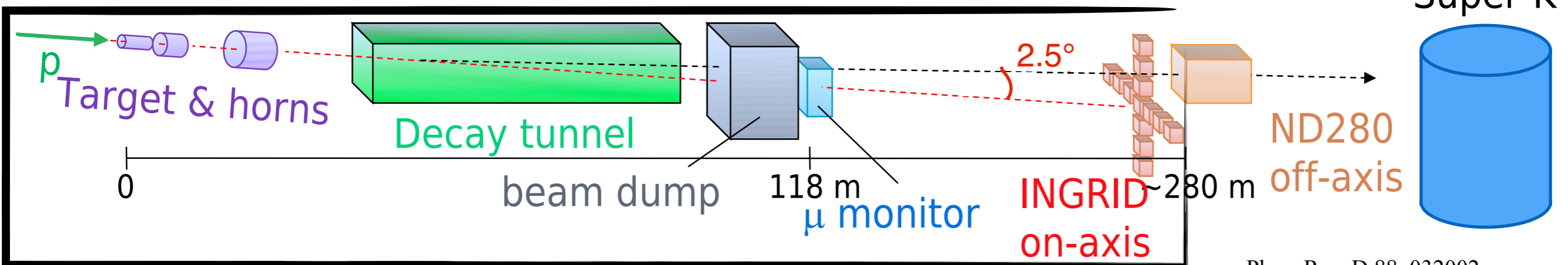


30 GeV proton beam from J-PARC Main Ring extracted onto a graphite target producing hadrons (mainly pions and kaons)

Hadrons are focused and selected in charge by 3 electromagnetic horns:

- ν_μ beam created by π^+ and $\bar{\nu}_\mu$ beam by π^- decay

T2K Beam

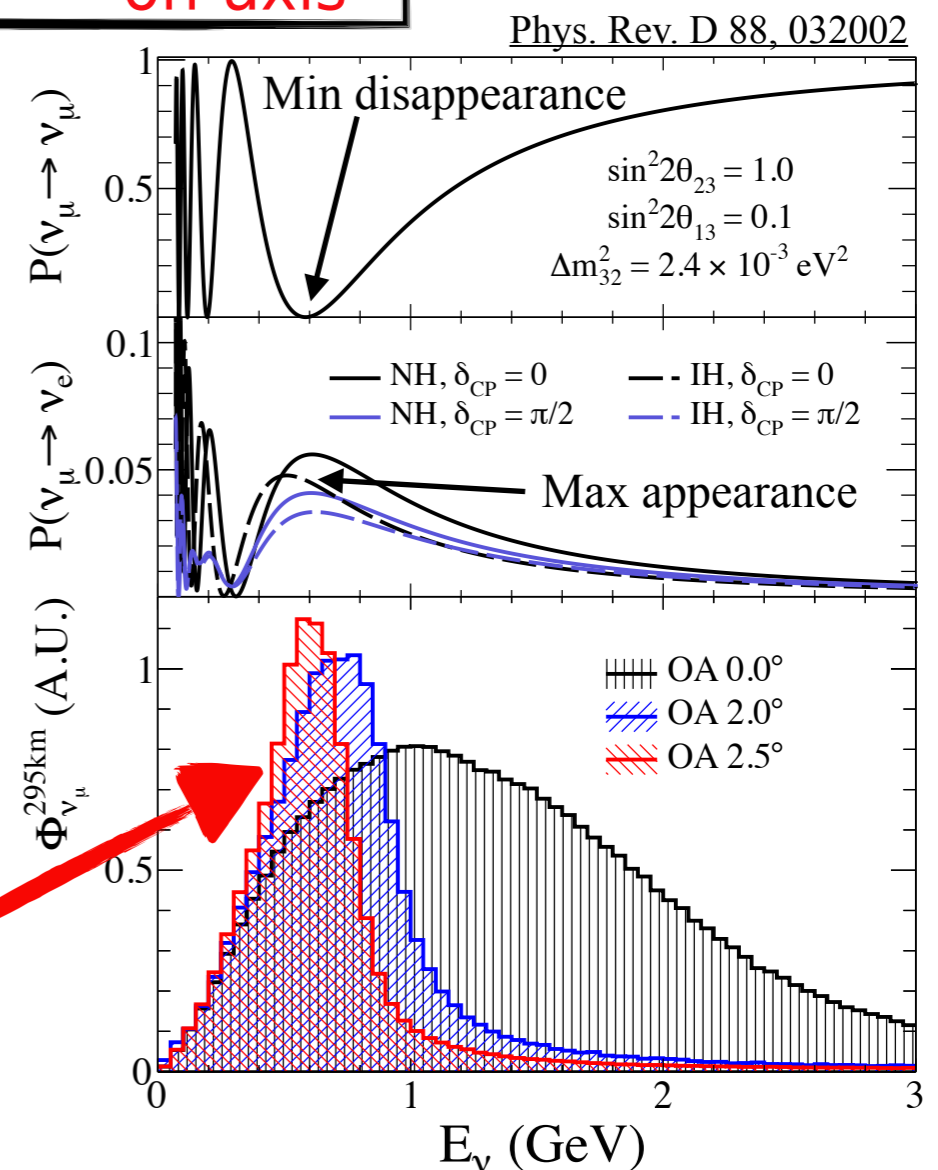


30 GeV proton beam from J-PARC Main Ring extracted onto a graphite target producing hadrons (mainly pions and kaons)

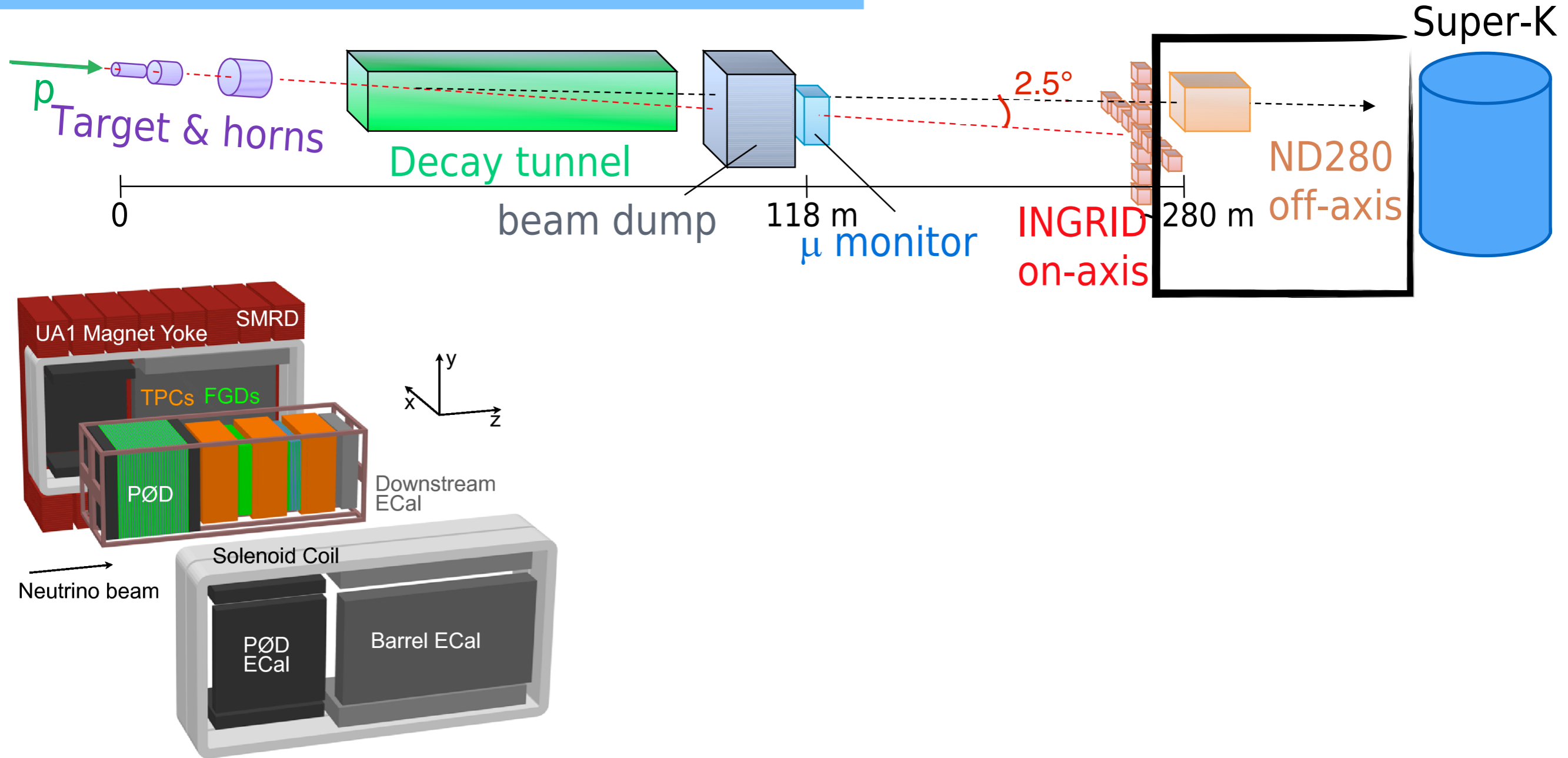
Hadrons are focused and selected in charge by 3 electromagnetic horns:

- ν_μ beam created by π^+ and $\bar{\nu}_\mu$ beam by π^- decay

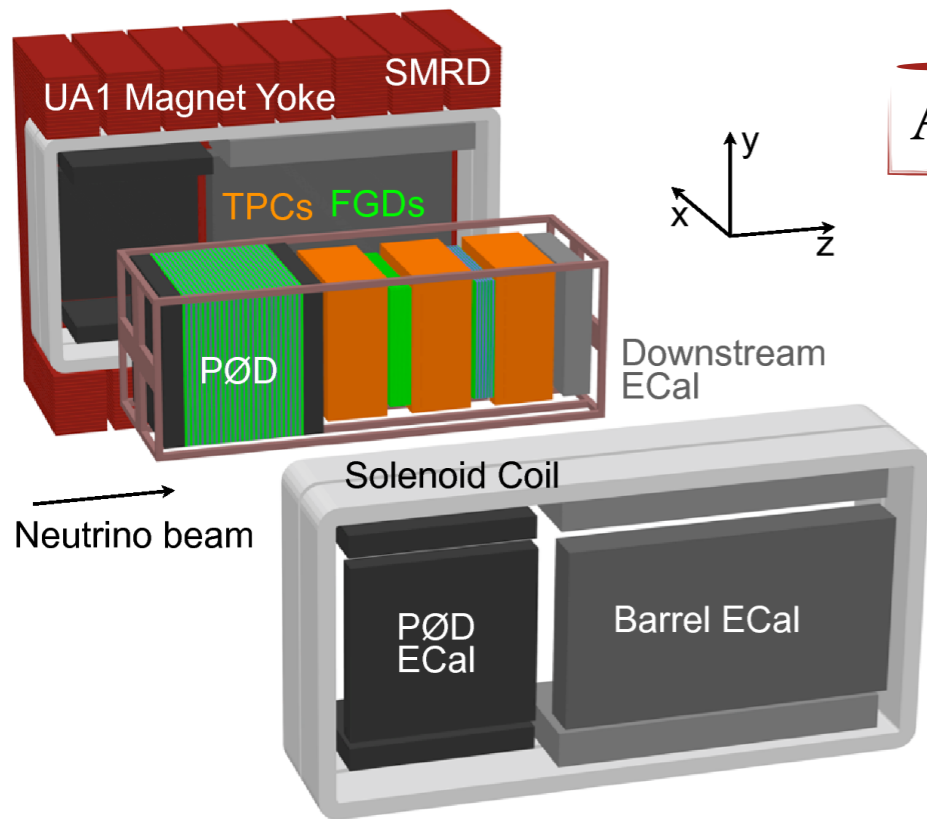
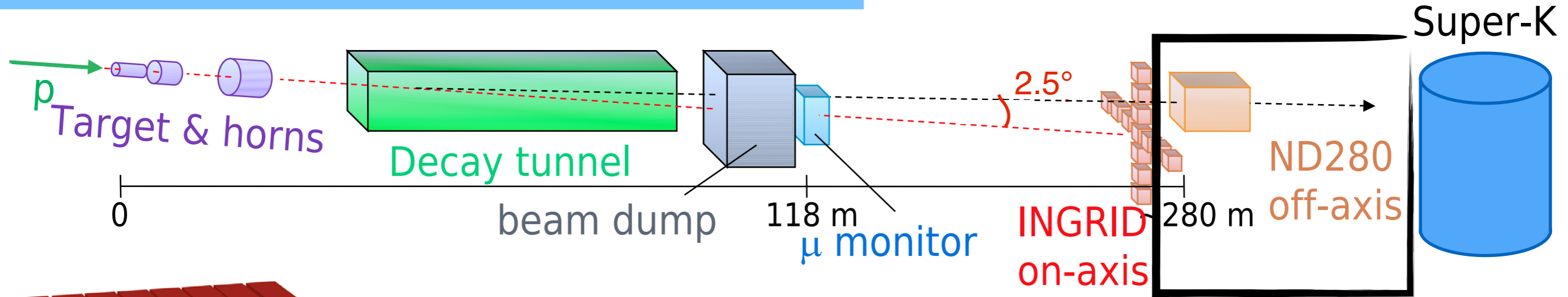
Detectors 2.5° off the direction of the beam centered around **0.6 GeV**. Off-axis method reduce high energy tail and maximize oscillation detection probabilities



The off-axis near detector (ND280)

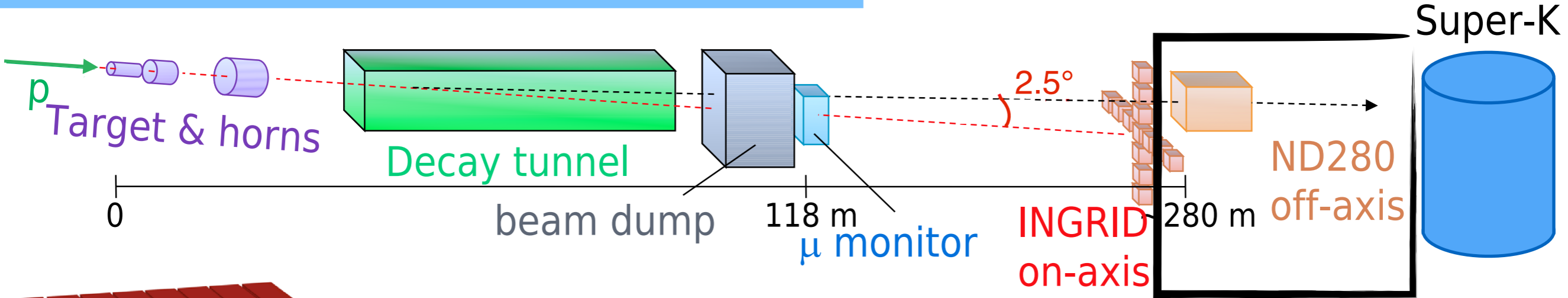


The off-axis near detector (ND280)



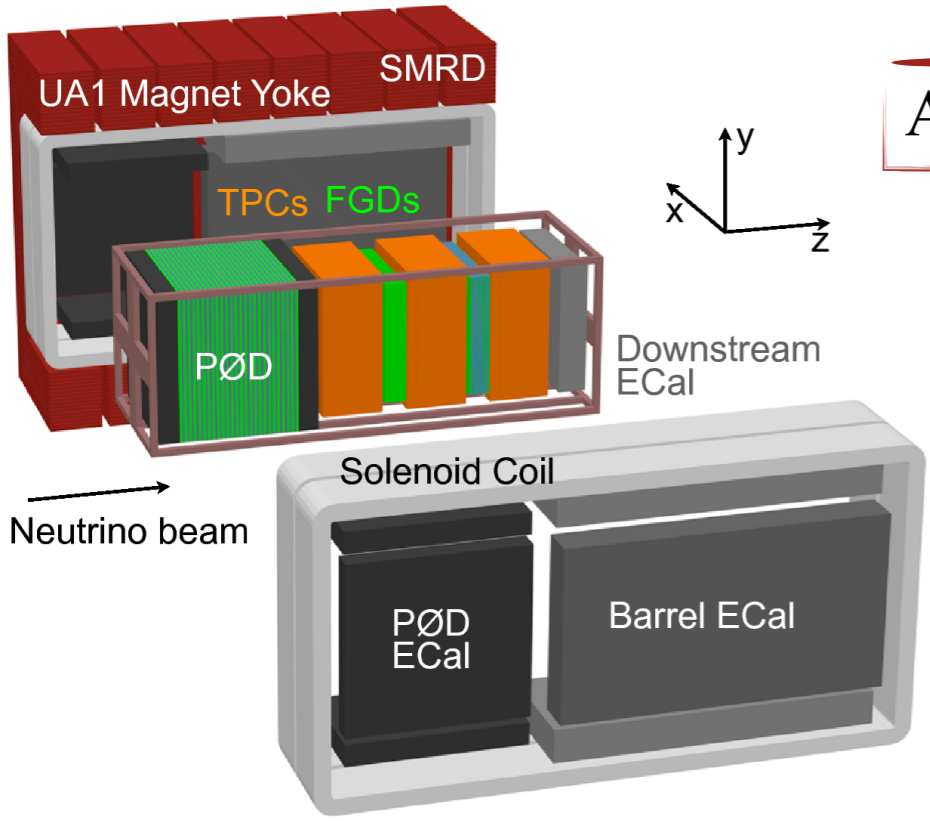
A large dipole magnet (UA1) produces 0.2 T.

The off-axis near detector (ND280)

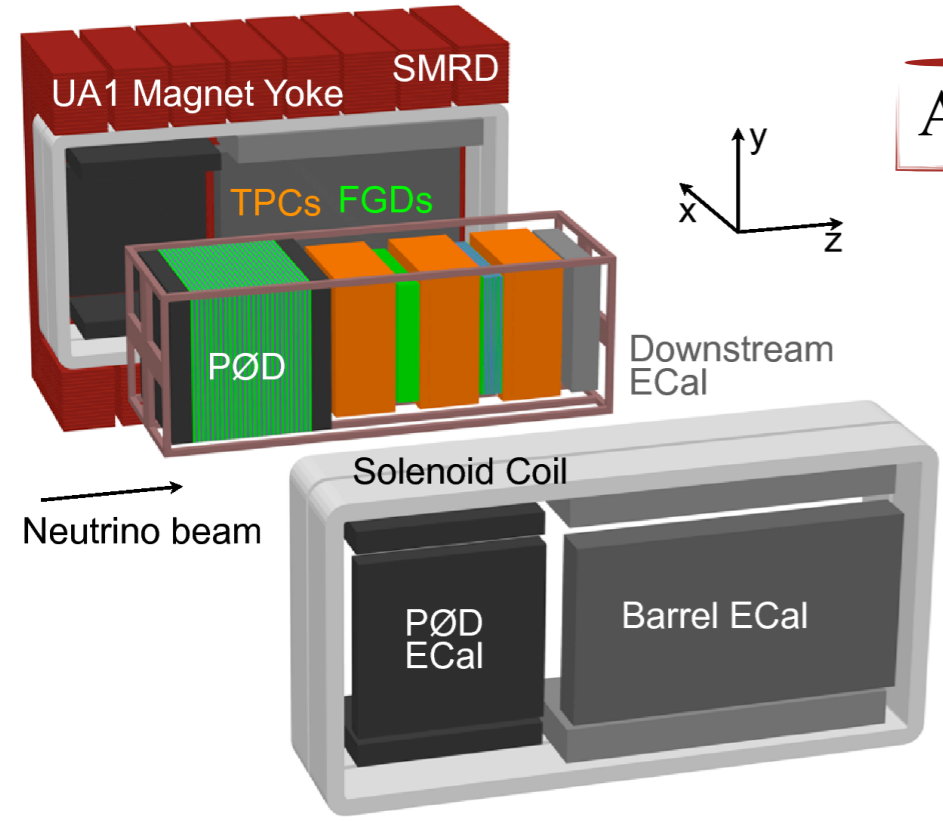
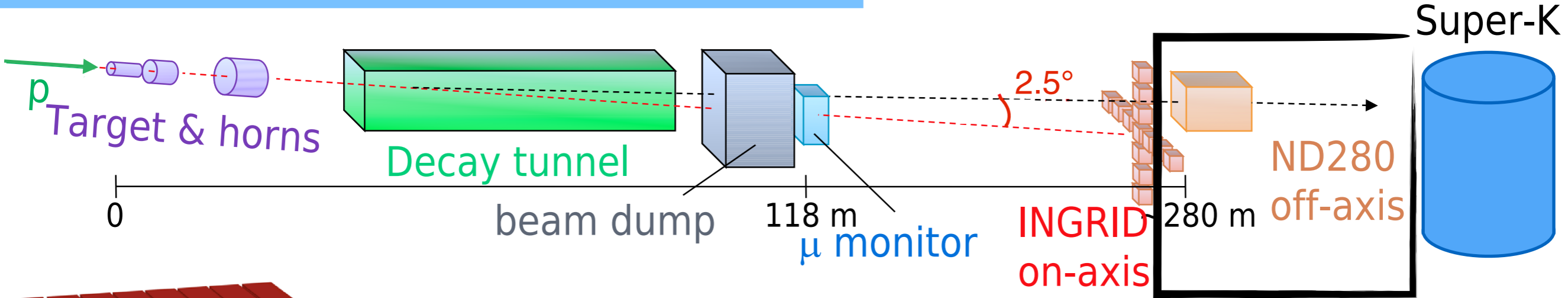


A large dipole magnet (UA1) produces 0.2 T.

Side muon range detector (SMRD): plastic scintillators instrumenting the magnet iron slice



The off-axis near detector (ND280)

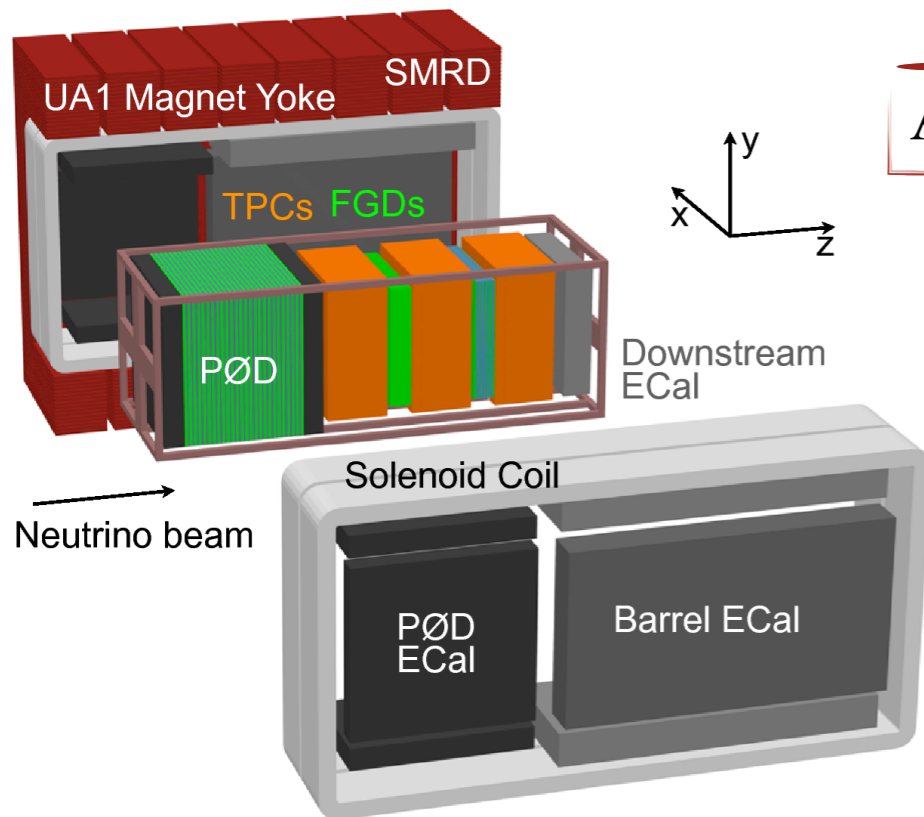
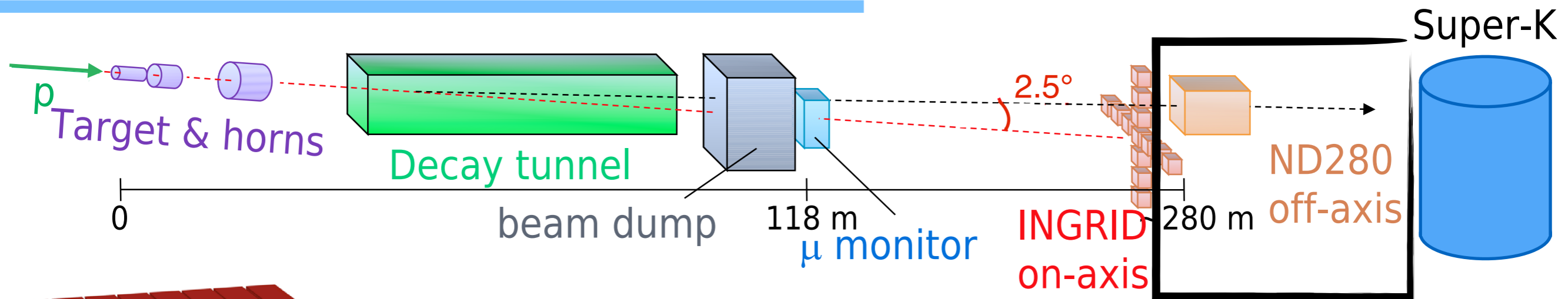


A large dipole magnet (UA1) produces 0.2 T.

Side muon range detector (SMRD): plastic scintillators instrumenting the magnet iron slice

π^0 detector (PØD): xy layers plastic scintillator alternated with water layers

The off-axis near detector (ND280)



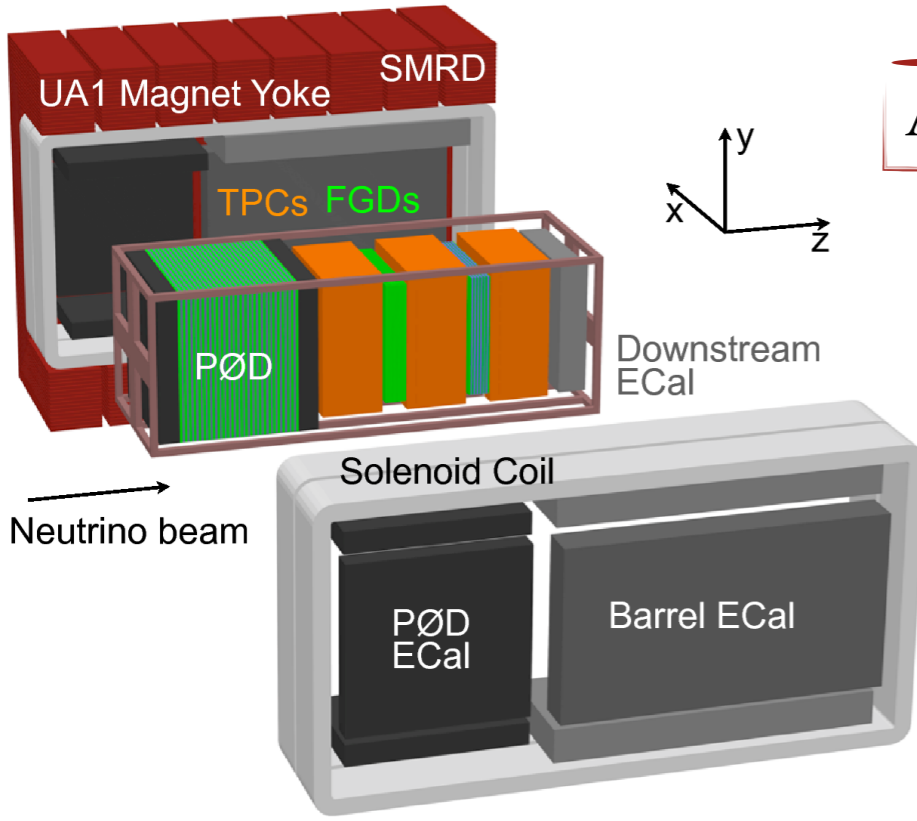
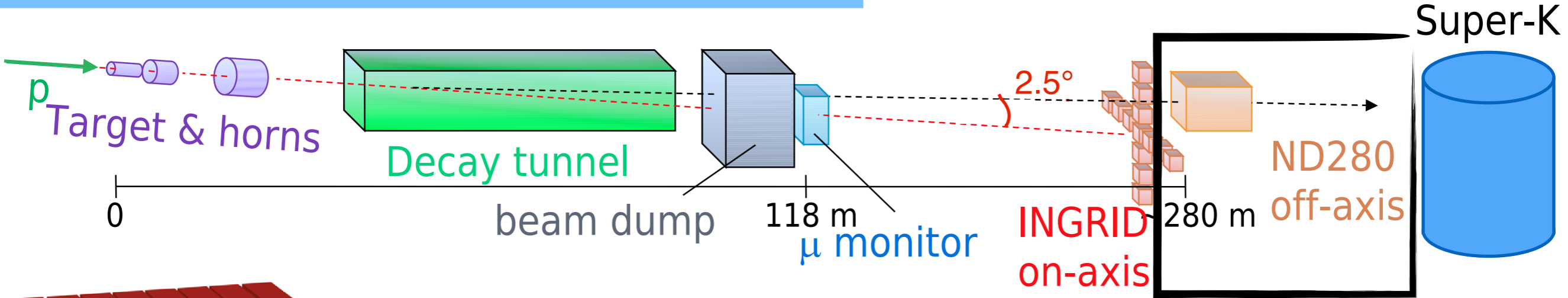
A large dipole magnet (UA1) produces 0.2 T.

Side muon range detector (SMRD): plastic scintillators instrumenting the magnet iron slice

π^0 detector (PØD): xy layers plastic scintillator alternated with water layers

3 Time projection chambers (TPC): reconstruct momentum and charge, PID based on ionization

The off-axis near detector (ND280)



A large dipole magnet (UA1) produces 0.2 T.

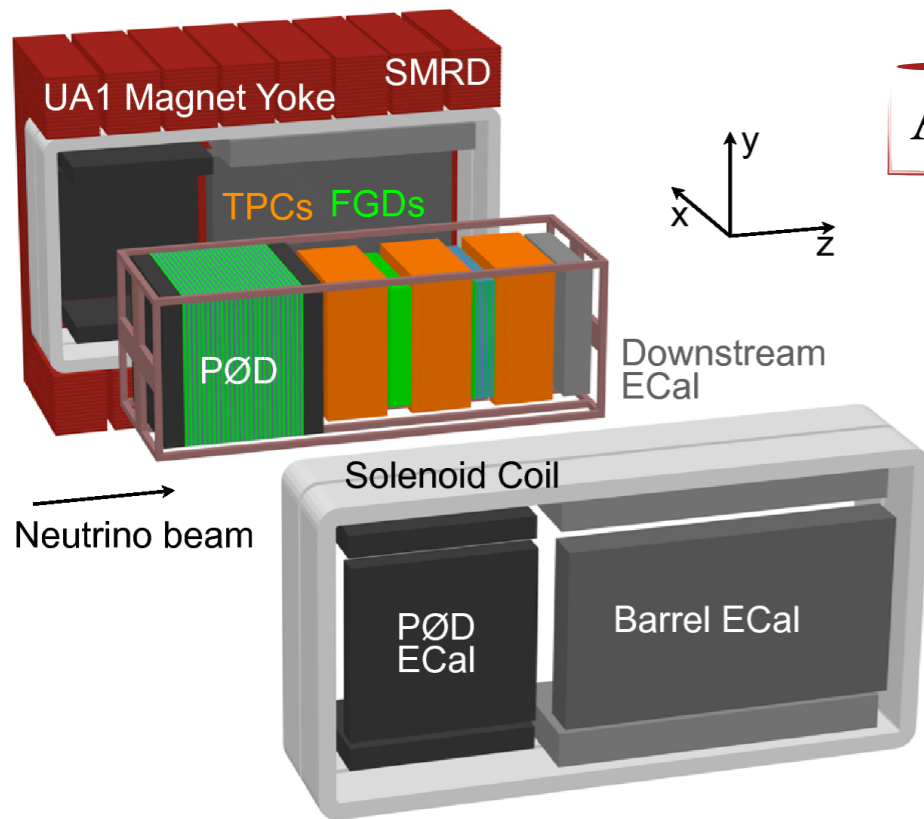
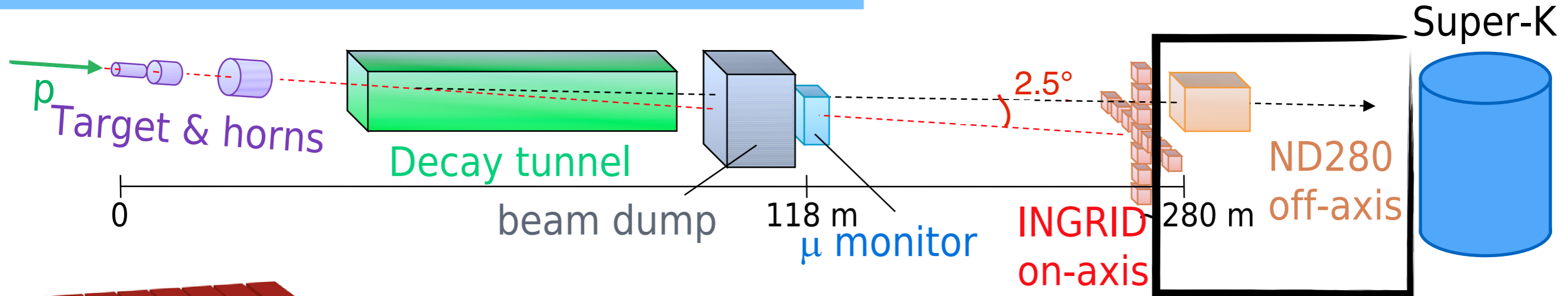
Side muon range detector (SMRD): plastic scintillators instrumenting the magnet iron slice

π^0 detector (PØD): xy layers plastic scintillator alternated with water layers

3 Time projection chambers (TPC): reconstruct momentum and charge, PID based on ionization

2 Fine-grained detectors (FGD): upstream constituted of xy layers of plastic scintillator, the other is alternated with water layers

The off-axis near detector (ND280)



A large dipole magnet (UA1) produces 0.2 T.

Side muon range detector (SMRD): plastic scintillators instrumenting the magnet iron slice

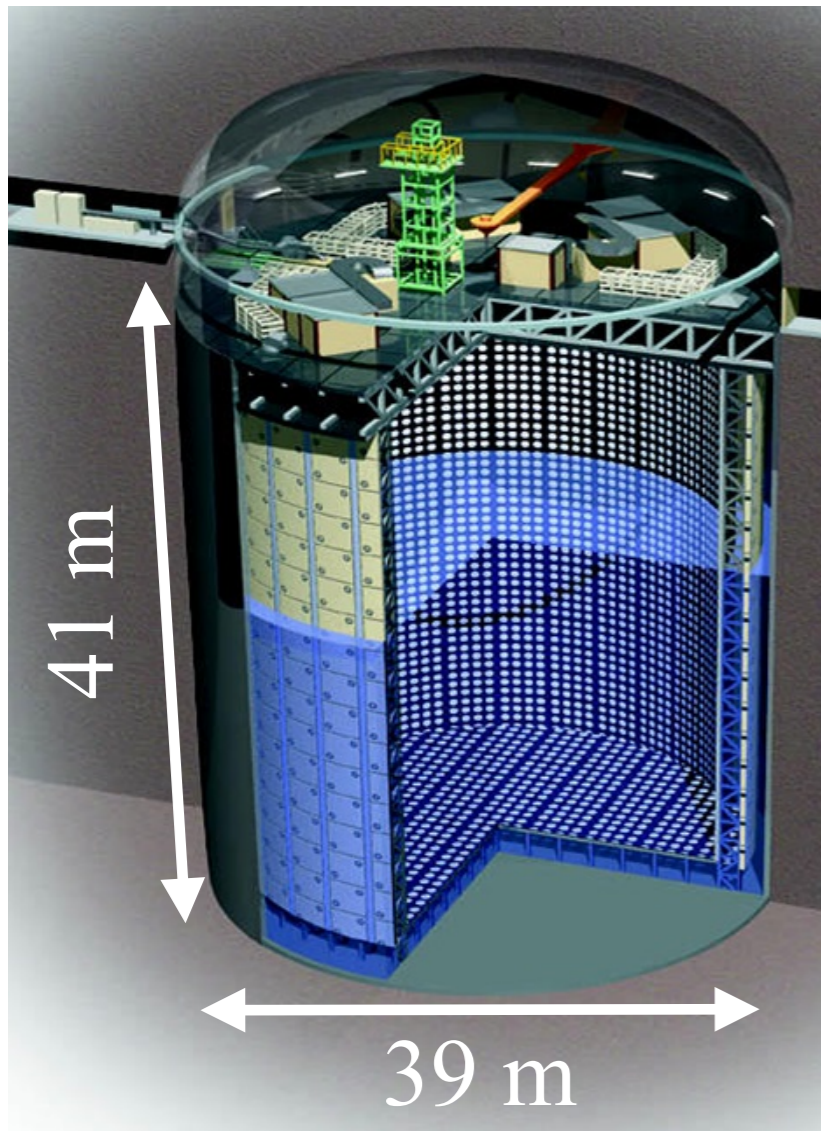
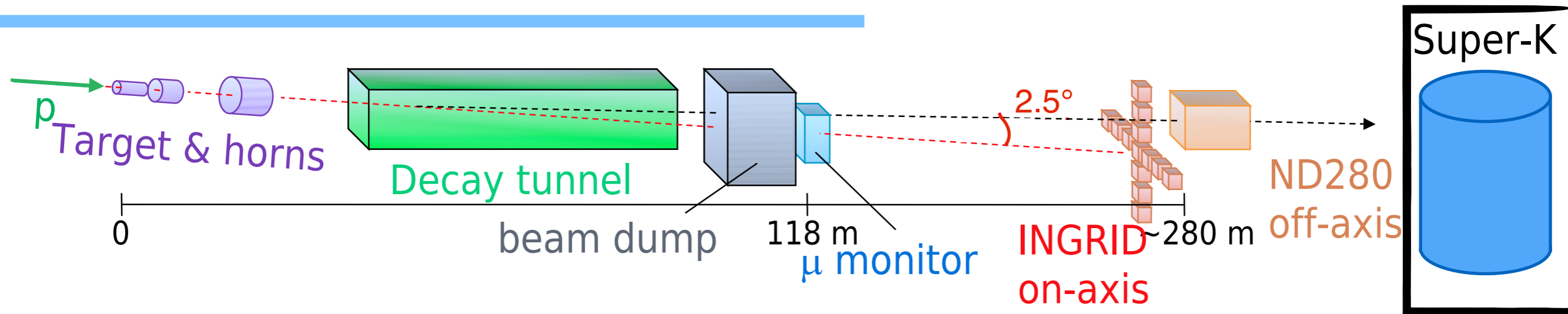
π^0 detector (PØD): xy layers plastic scintillator alternated with water layers

3 Time projection chambers (TPC): reconstruct momentum and charge, PID based on ionization

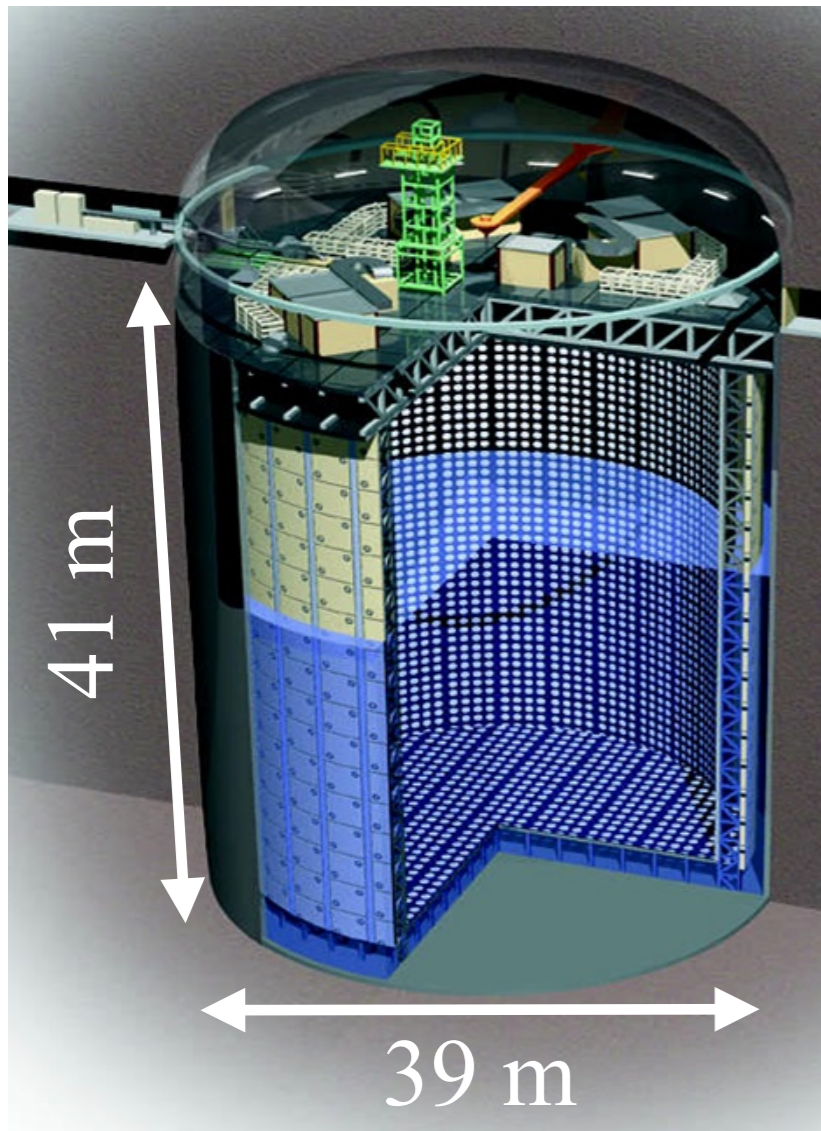
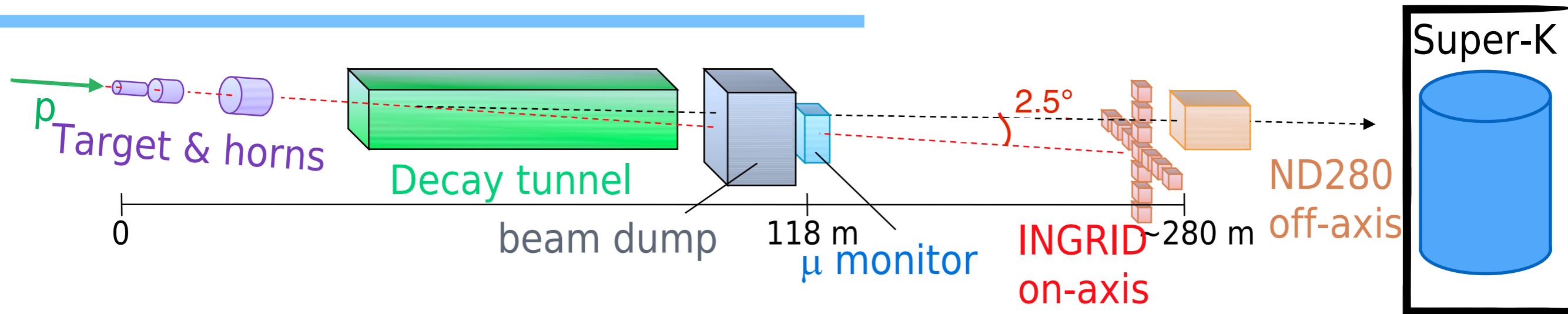
2 Fine-grained detectors (FGD): upstream constituted of xy layers of plastic scintillator, the other is alternated with water layers

An electromagnetic calorimeter (ECal) is used to distinguish tracks from showers

Super-Kamiokande (SK)

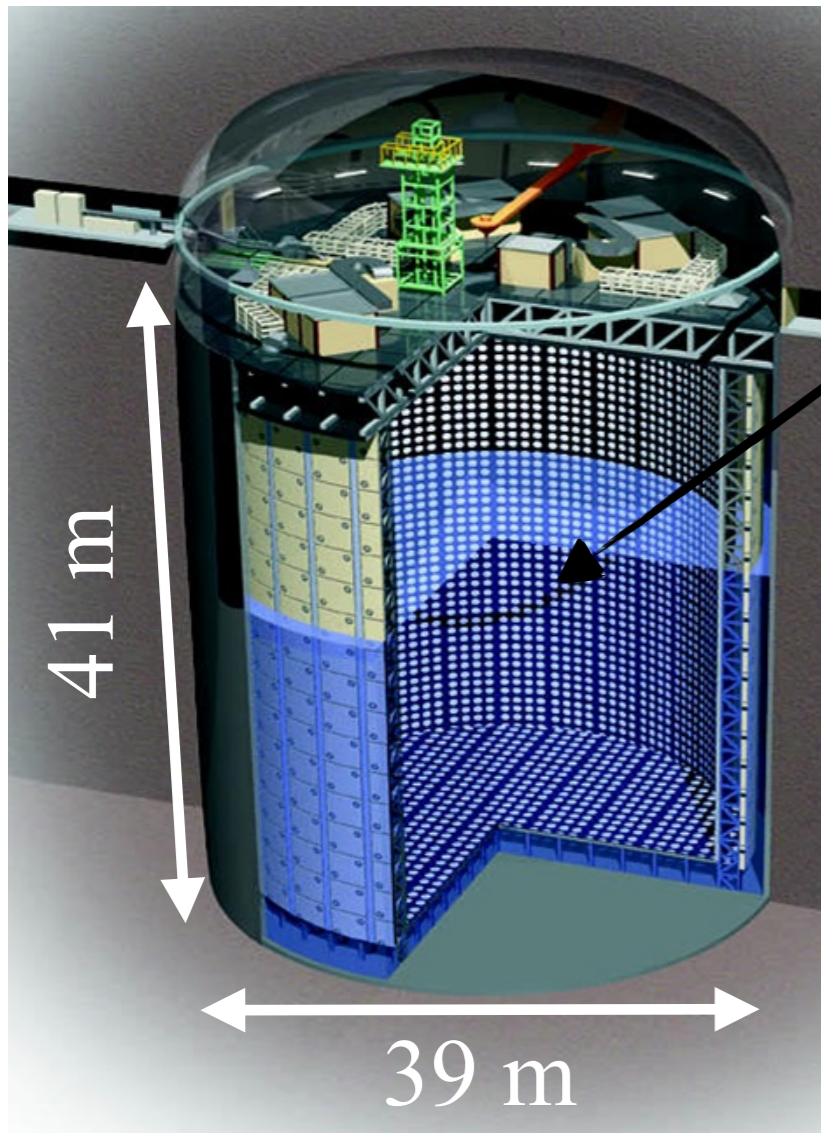
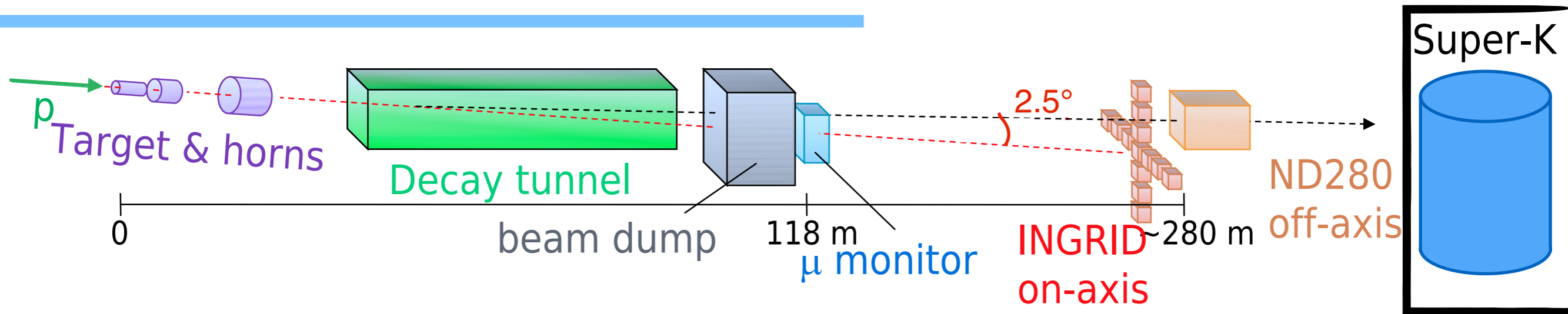


Super-Kamiokande (SK)



SK is a 50 kton water Cherenkov detector

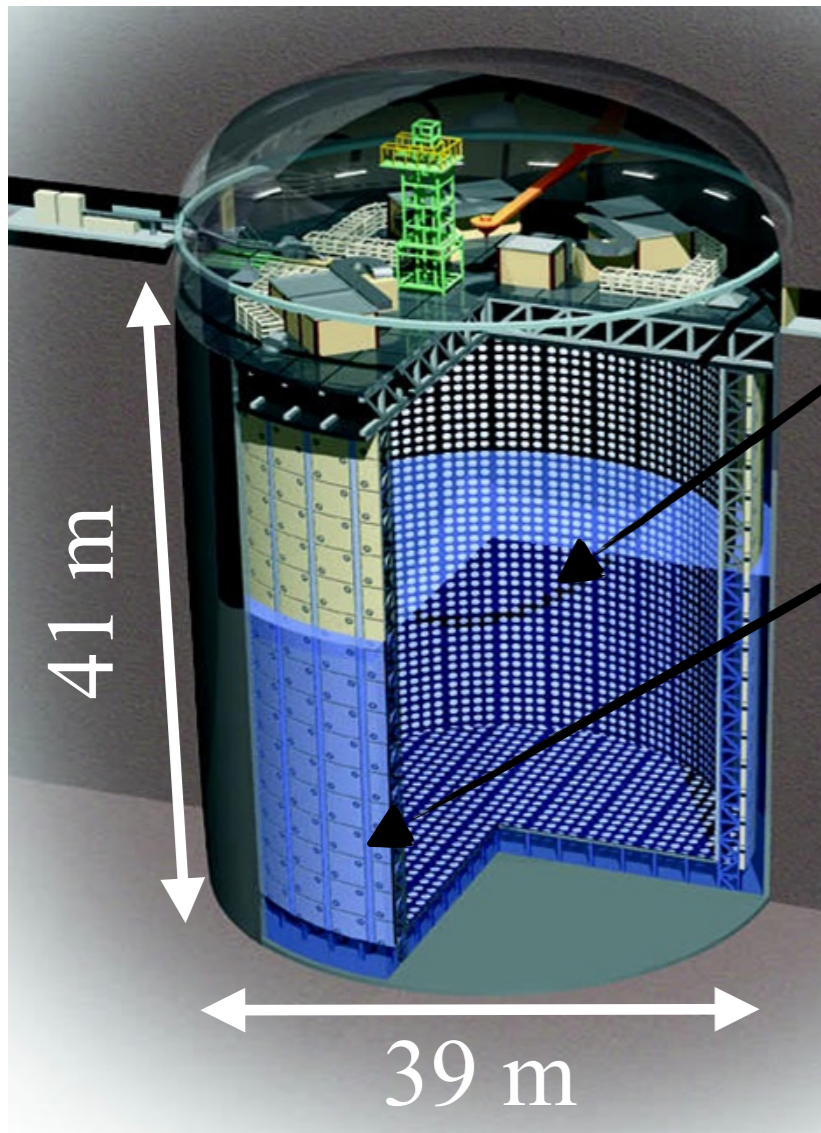
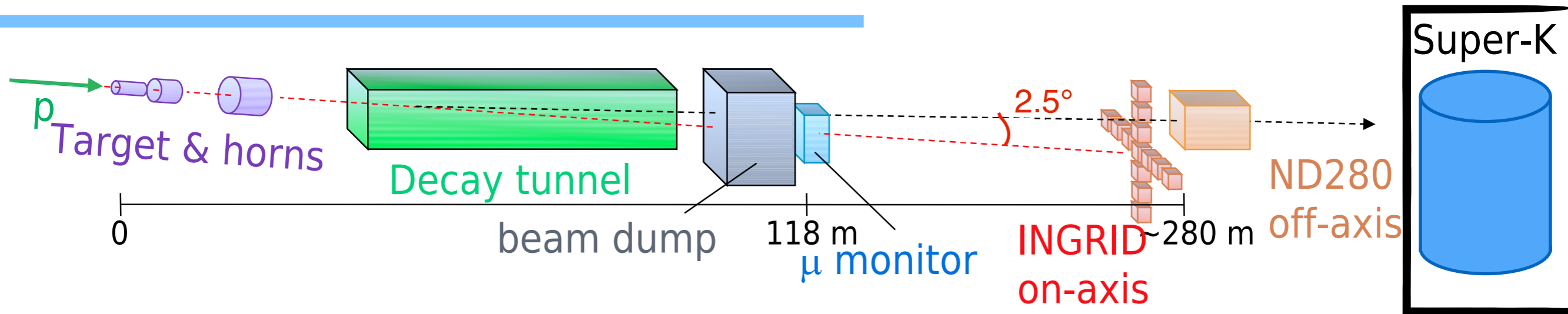
Super-Kamiokande (SK)



SK is a 50 kton water Cherenkov detector

Inner detector ~11000
20 inch PMTs

Super-Kamiokande (SK)

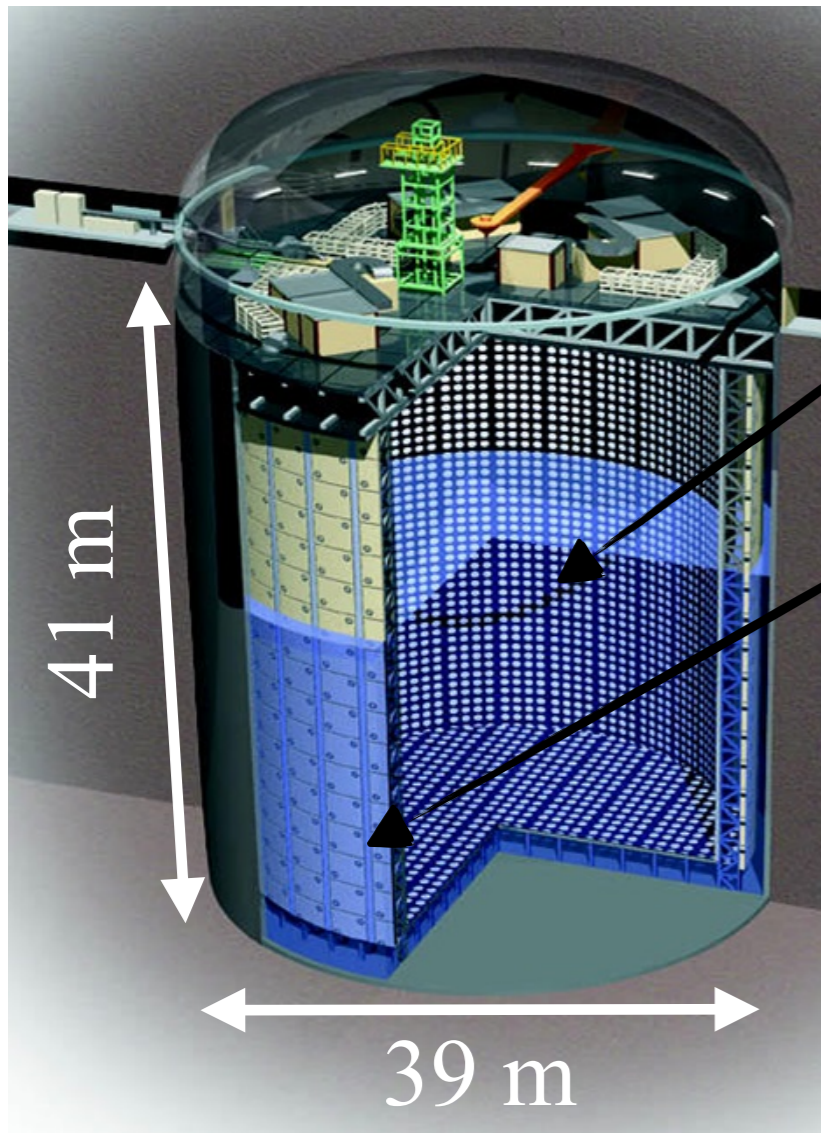
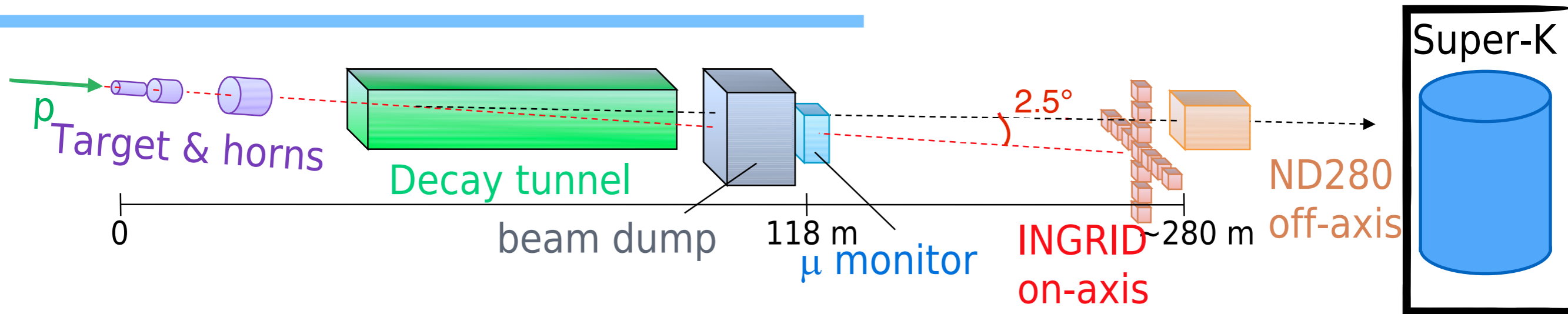


SK is a 50 kton water Cherenkov detector

Inner detector ~11000
20 inch PMTs

Outer detector ~2000
8 inch PMTs

Super-Kamiokande (SK)

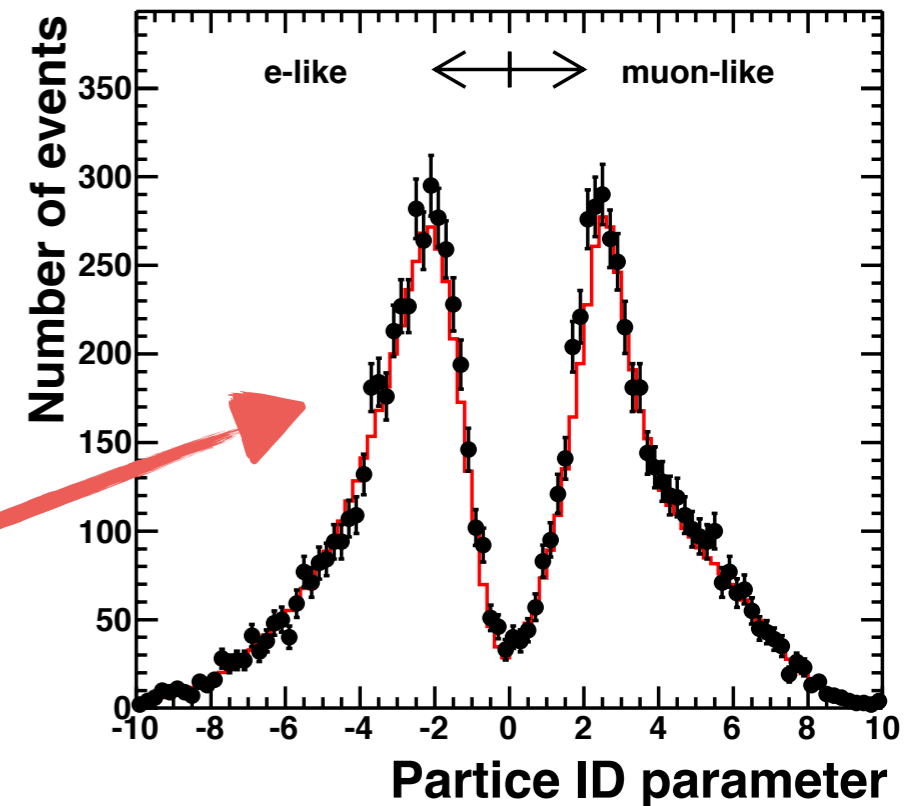


SK is a 50 kton water Cherenkov detector

Inner detector ~11000
20 inch PMTs

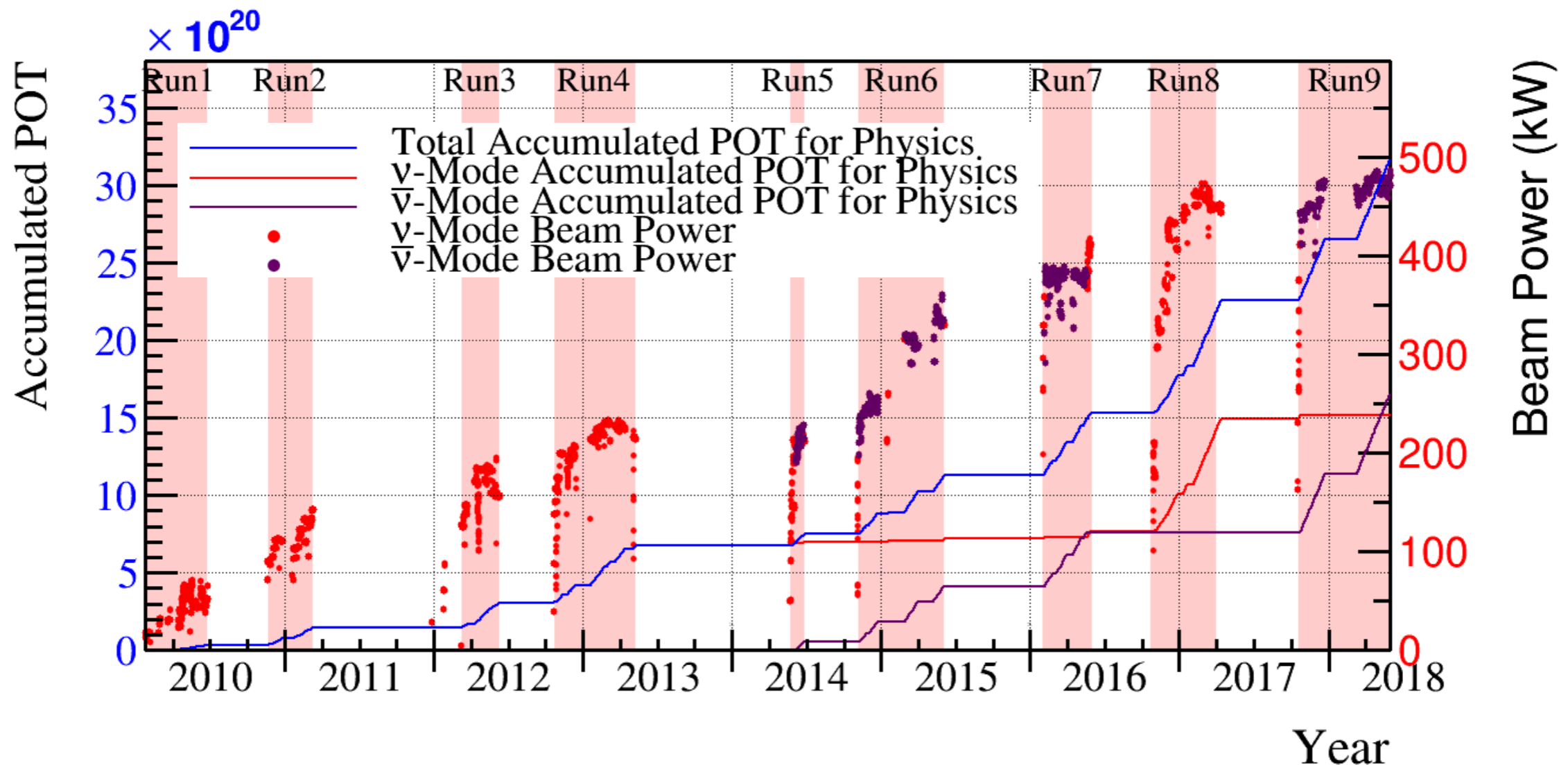
Outer detector ~2000
8 inch PMTs

Very good μ/e separation



Collected data

- Total proton on target (POT) collected: 3.1×10^{21} POT: 1.5×10^{21} POT in ν mode and 1.6×10^{21} POT in $\bar{\nu}$ mode
- Beam power 500 kW!



T2K oscillation analysis strategy

T2K oscillation analysis strategy

Flux prediction:

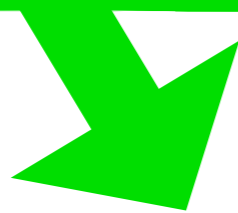
proton beam measurements and
external hadron production
measurements

Neutrino interactions model:

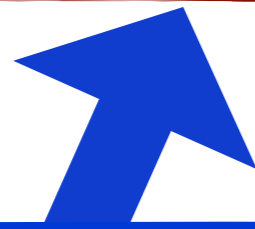
tuned using external data

T2K oscillation analysis strategy

Flux prediction:
proton beam measurements and
external hadron production
measurements



ND280 measurements:
select CC ν_μ and $\bar{\nu}_\mu$ interactions
constrain flux and cross sections



Neutrino interactions model:
tuned using external data

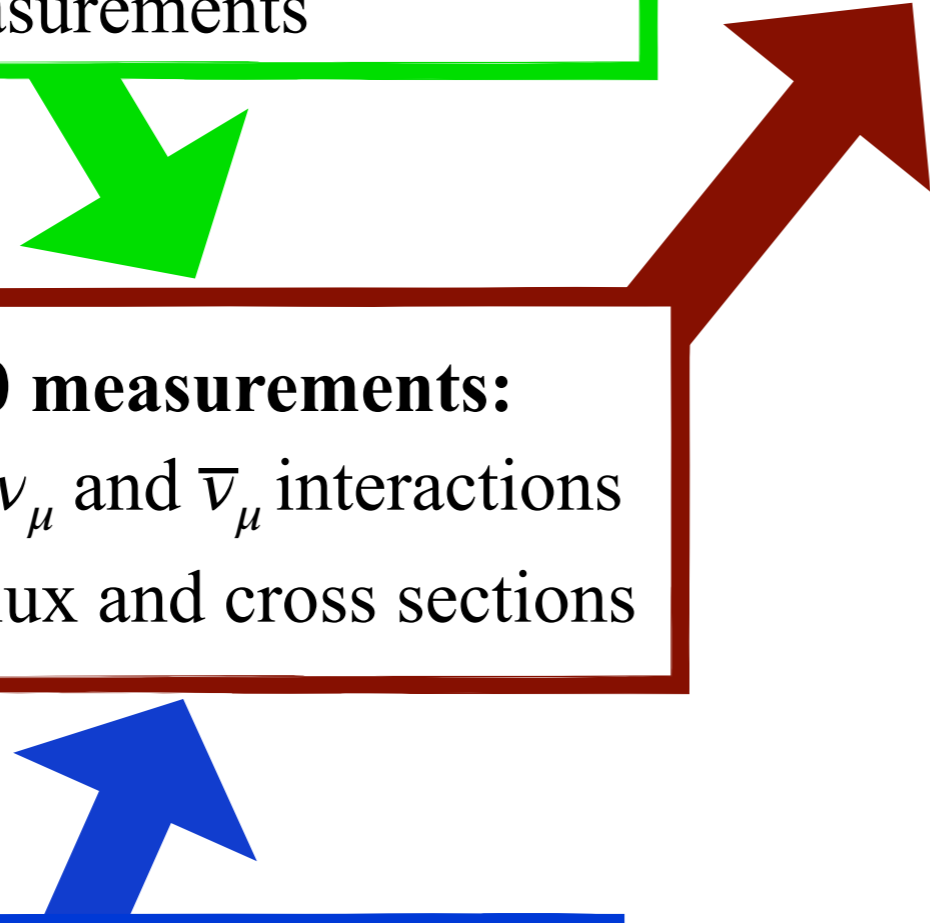
T2K oscillation analysis strategy

Flux prediction:
proton beam measurements and
external hadron production
measurements

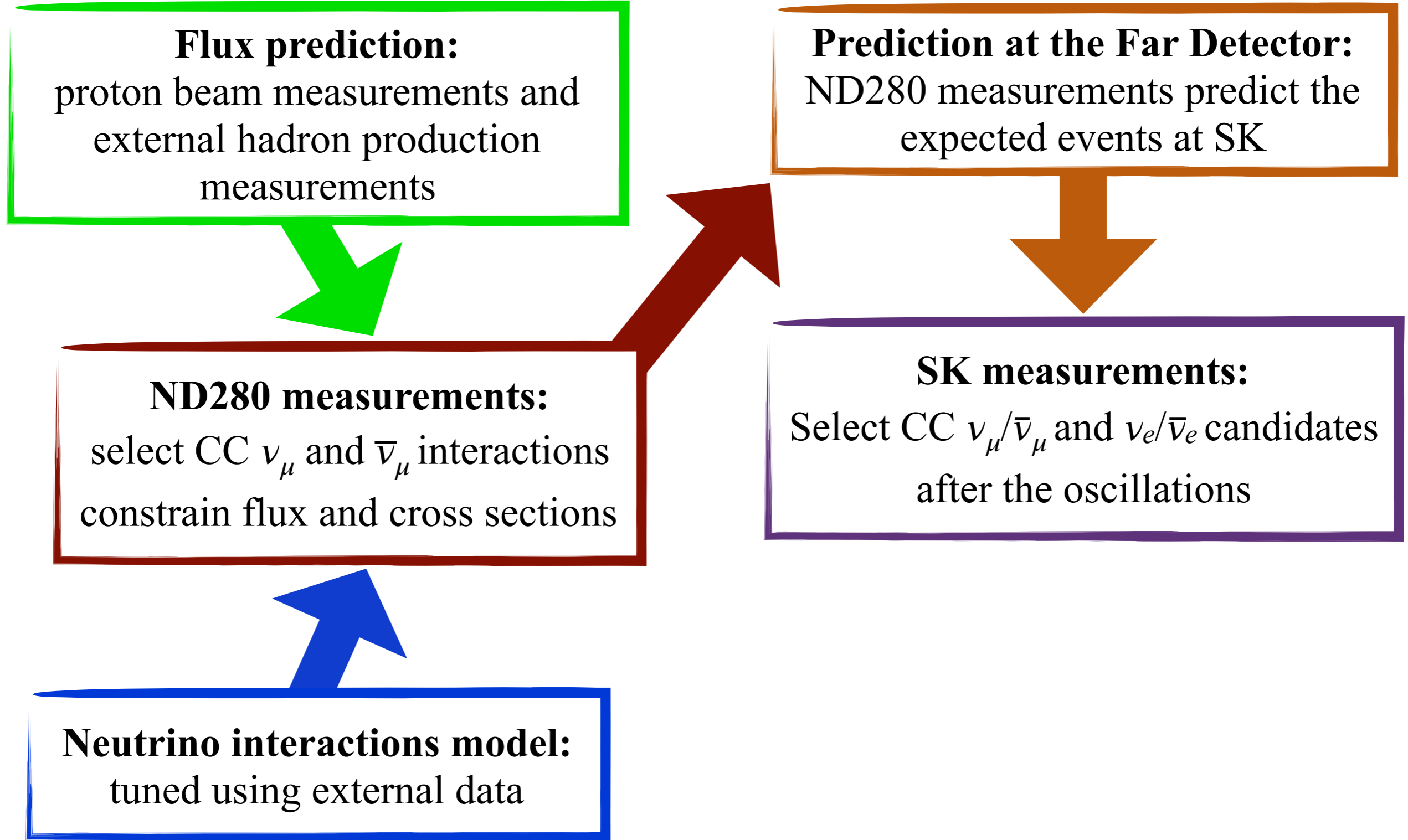
Prediction at the Far Detector:
ND280 measurements predict the
expected events at SK

ND280 measurements:
select CC ν_μ and $\bar{\nu}_\mu$ interactions
constrain flux and cross sections

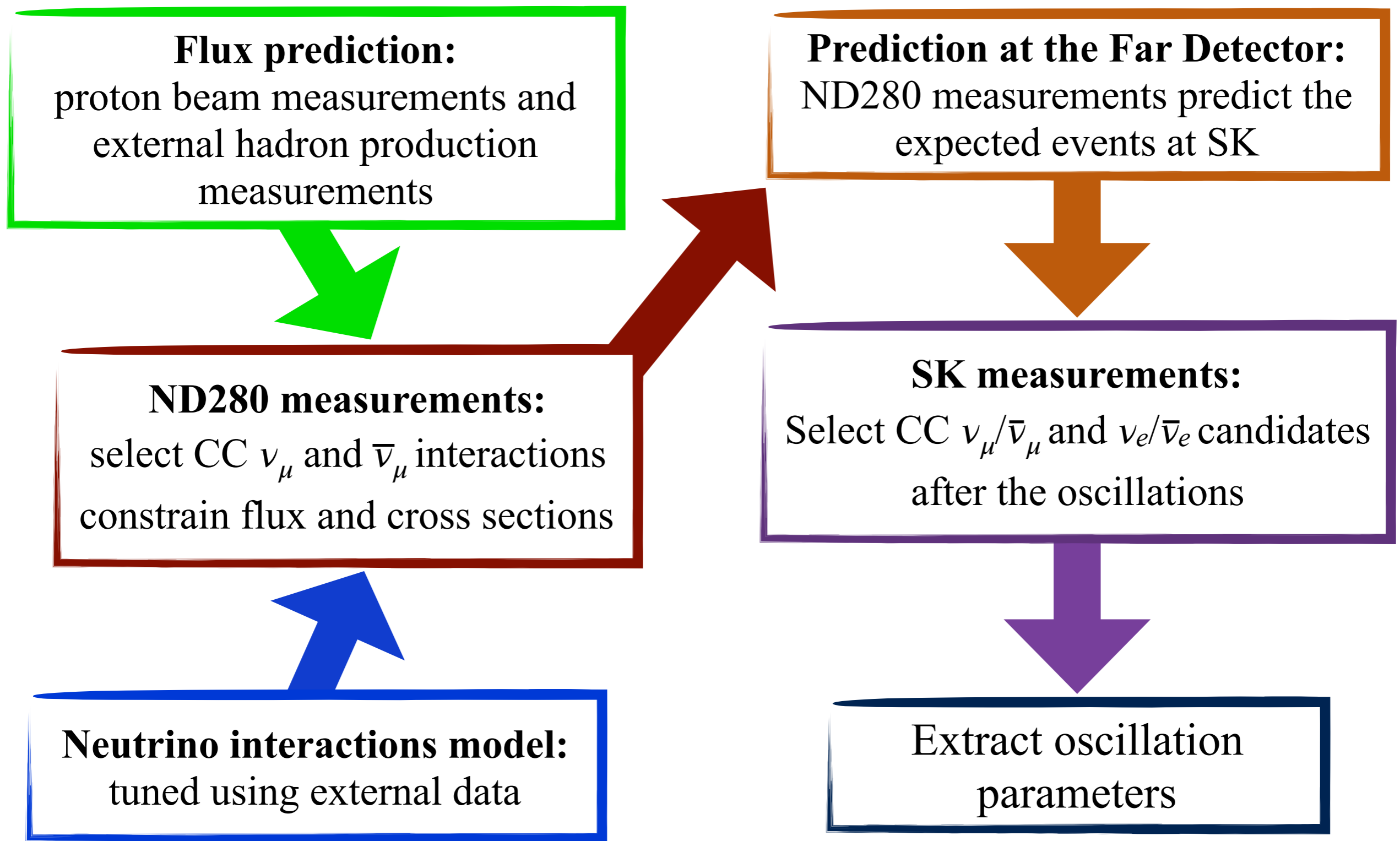
Neutrino interactions model:
tuned using external data



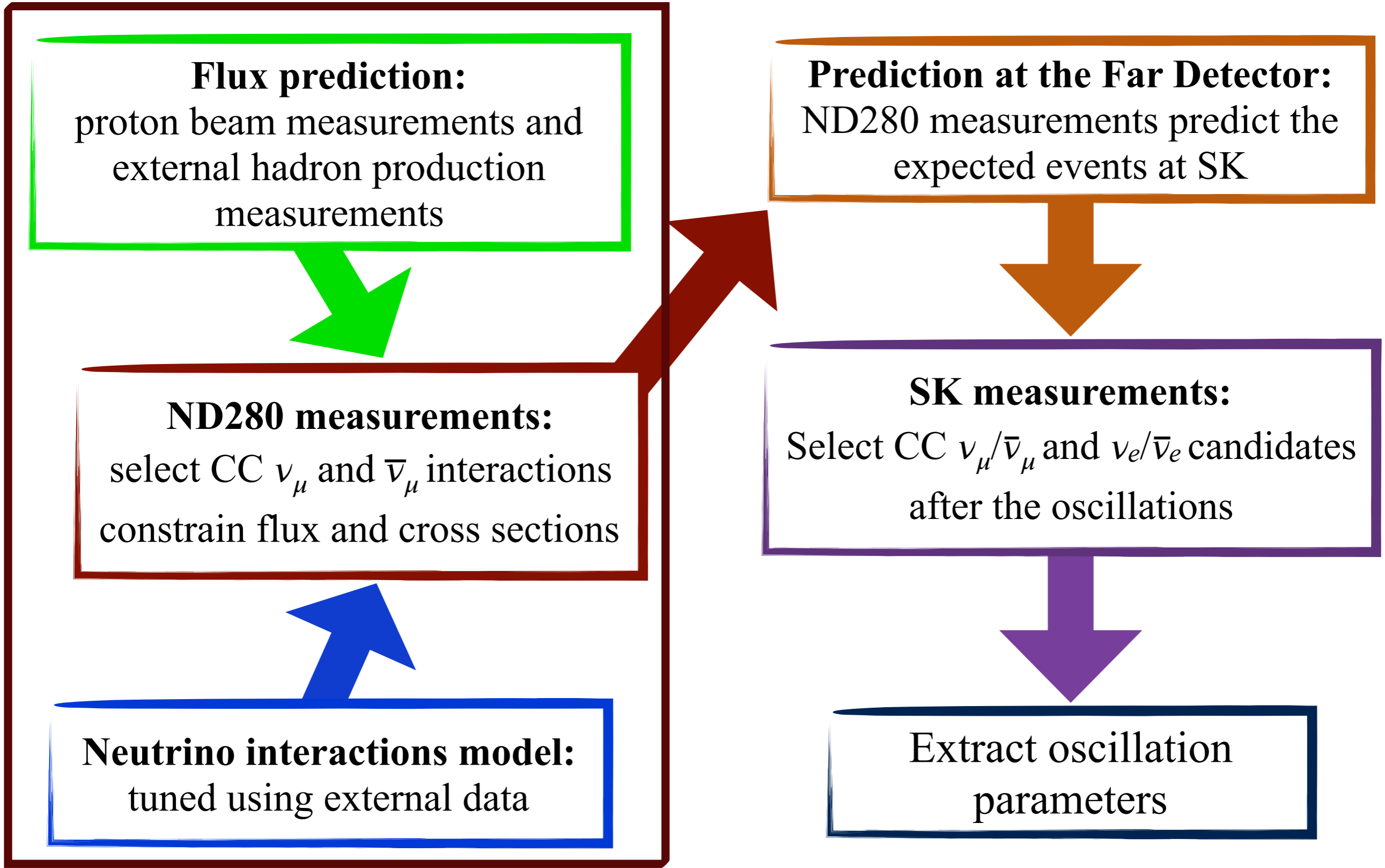
T2K oscillation analysis strategy



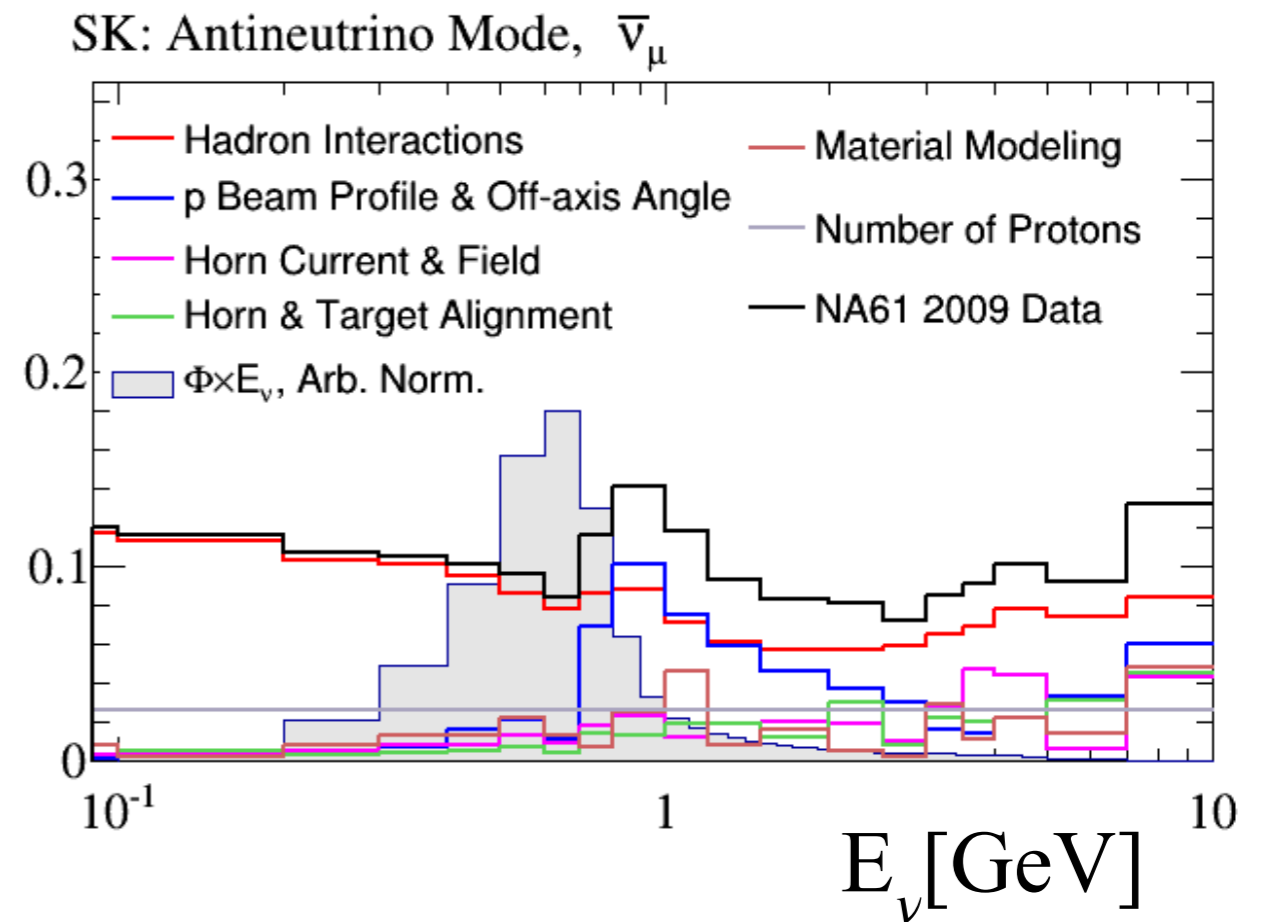
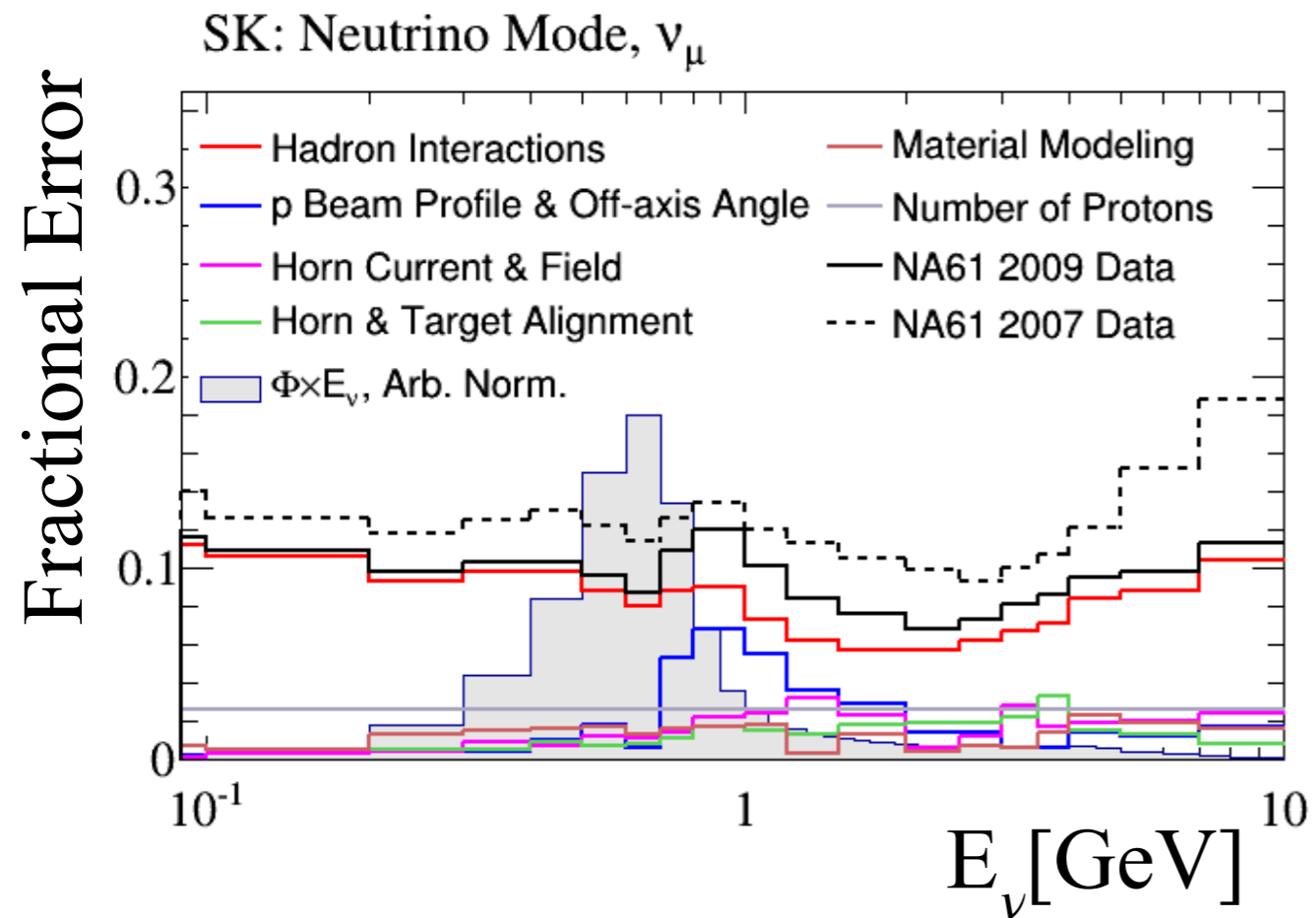
T2K oscillation analysis strategy



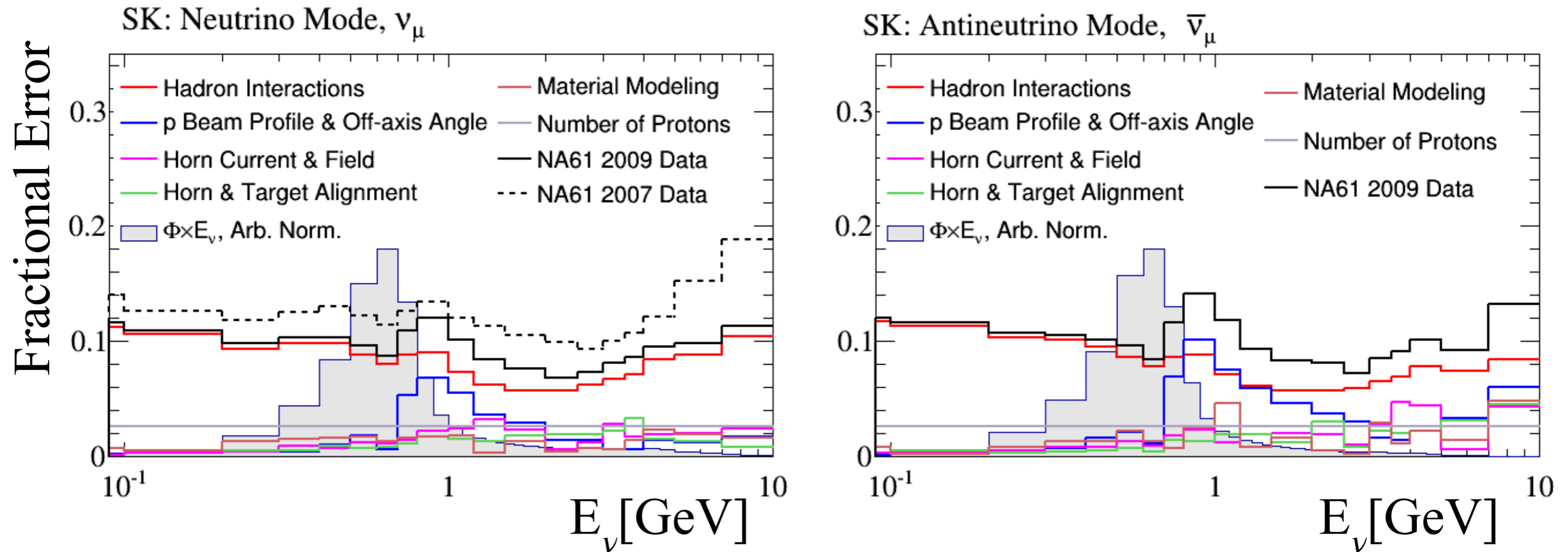
T2K oscillation analysis strategy



Neutrino fluxes

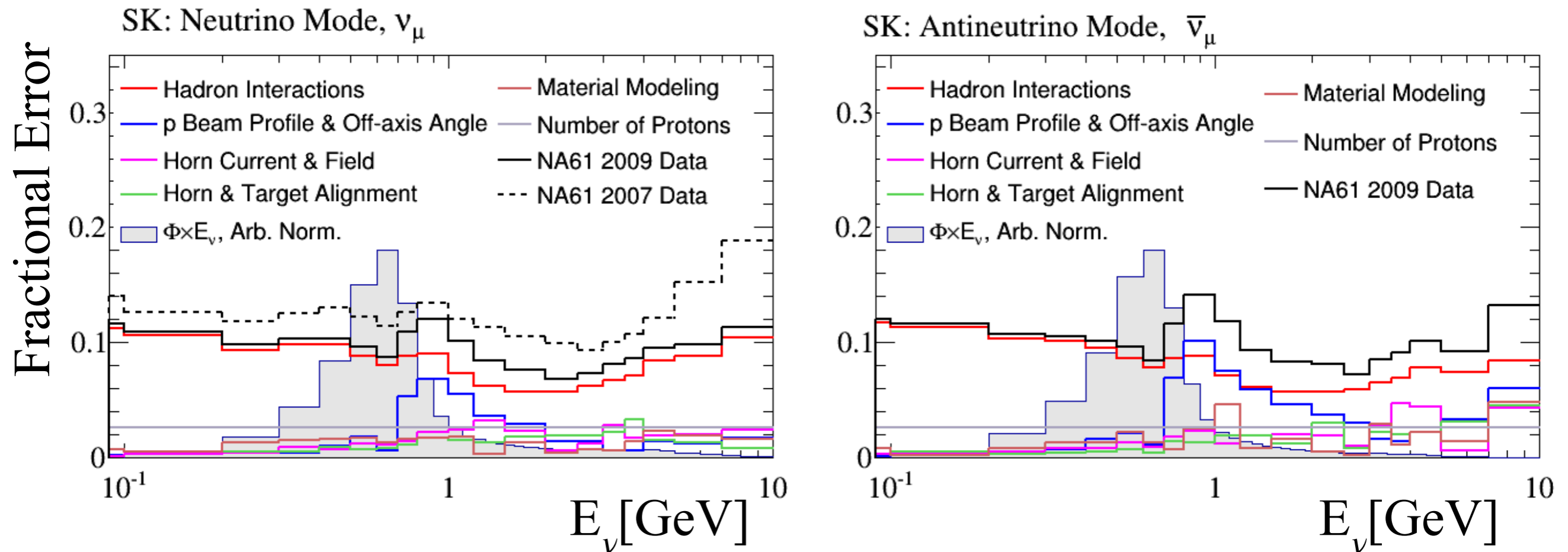


Neutrino fluxes



Fluxes known with uncertainties smaller than 10% based on NA61/SHINE thin-target measurements

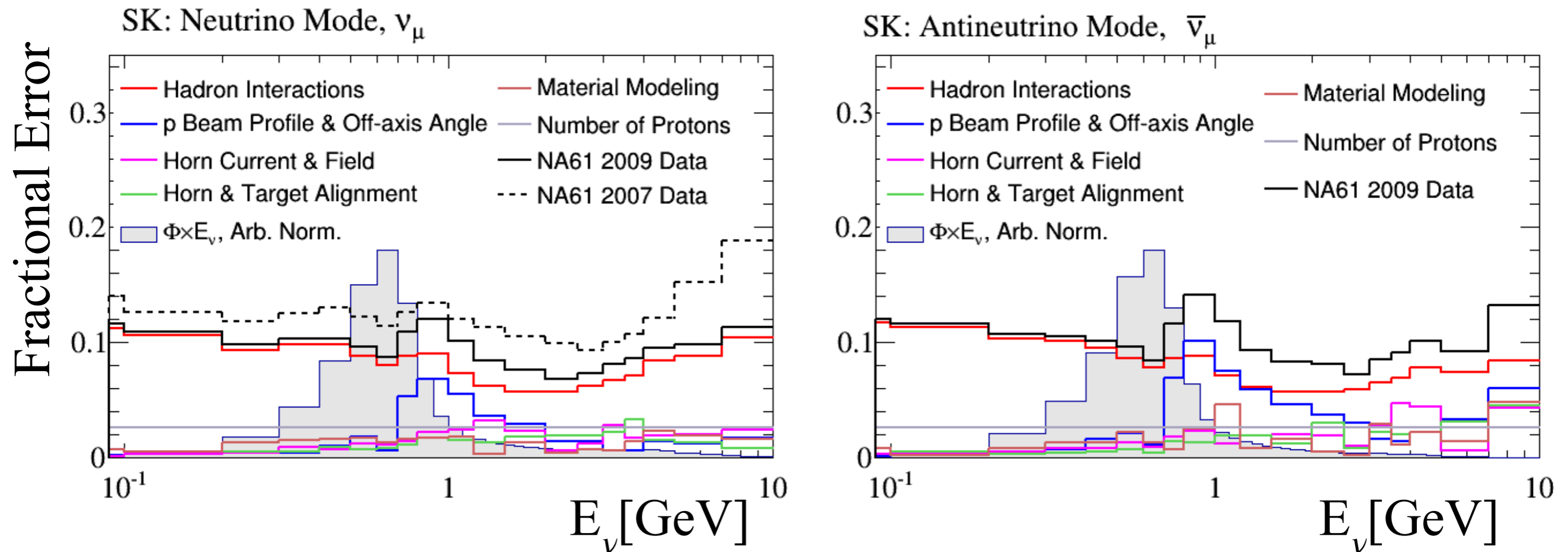
Neutrino fluxes



Fluxes known with uncertainties smaller than 10% based on NA61/SHINE thin-target measurements

Dominant systematics due to the hadron interactions modeling

Neutrino fluxes

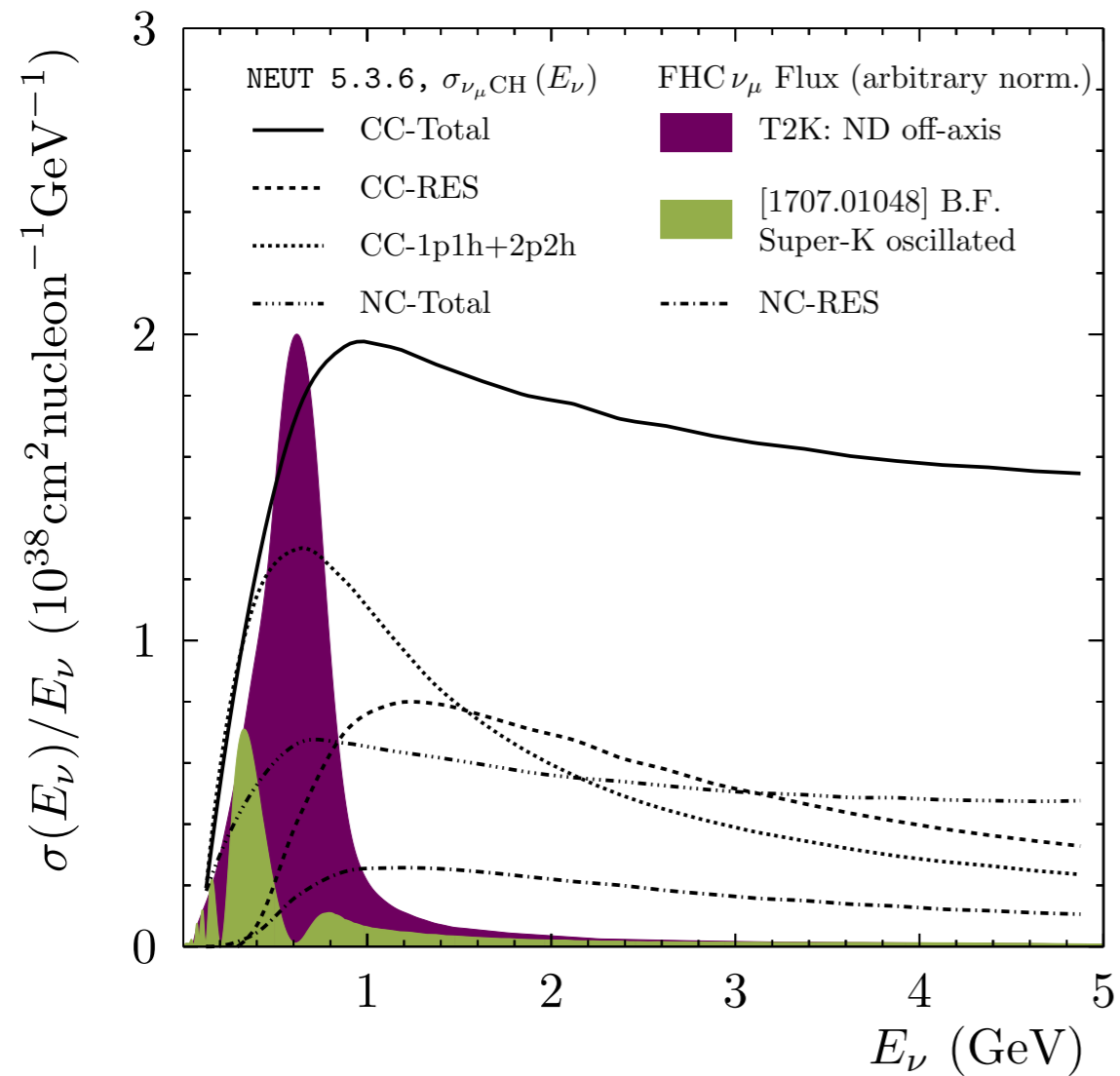


Fluxes known with uncertainties smaller than 10% based on NA61/SHINE thin-target measurements

Dominant systematics due to the hadron interactions modeling

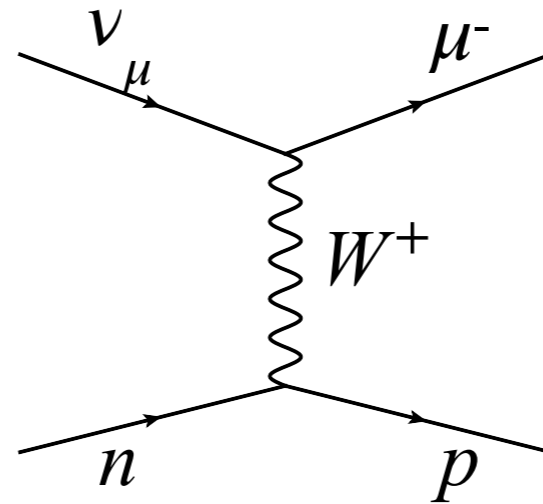
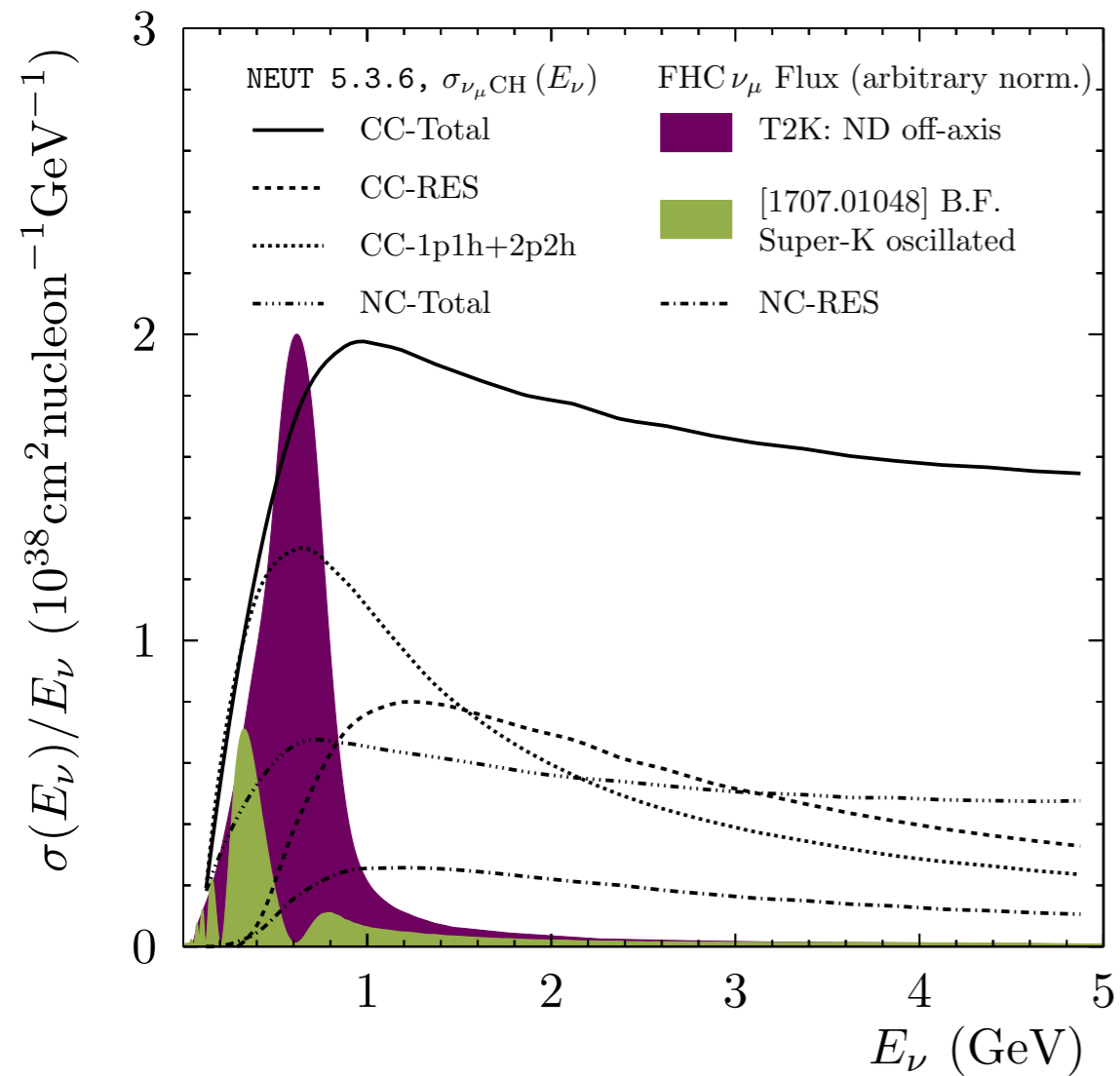
It will be reduced to $\sim 5\%$ by using NA61/SHINE measurements of T2K replica target

Relevant ν interactions at T2K



Relevant ν interactions at T2K

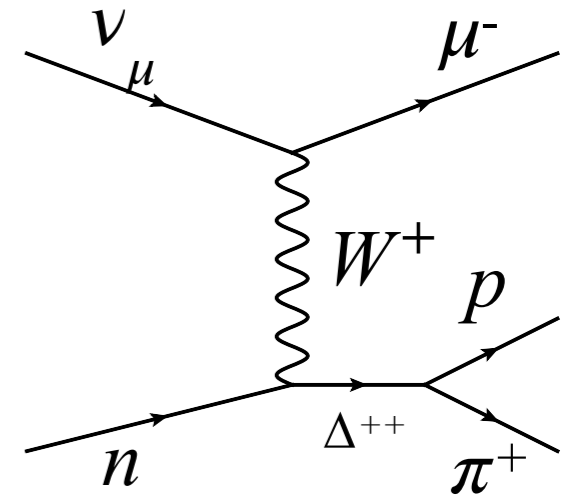
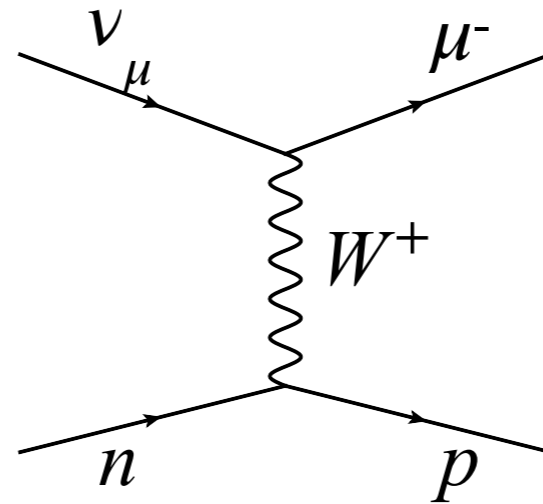
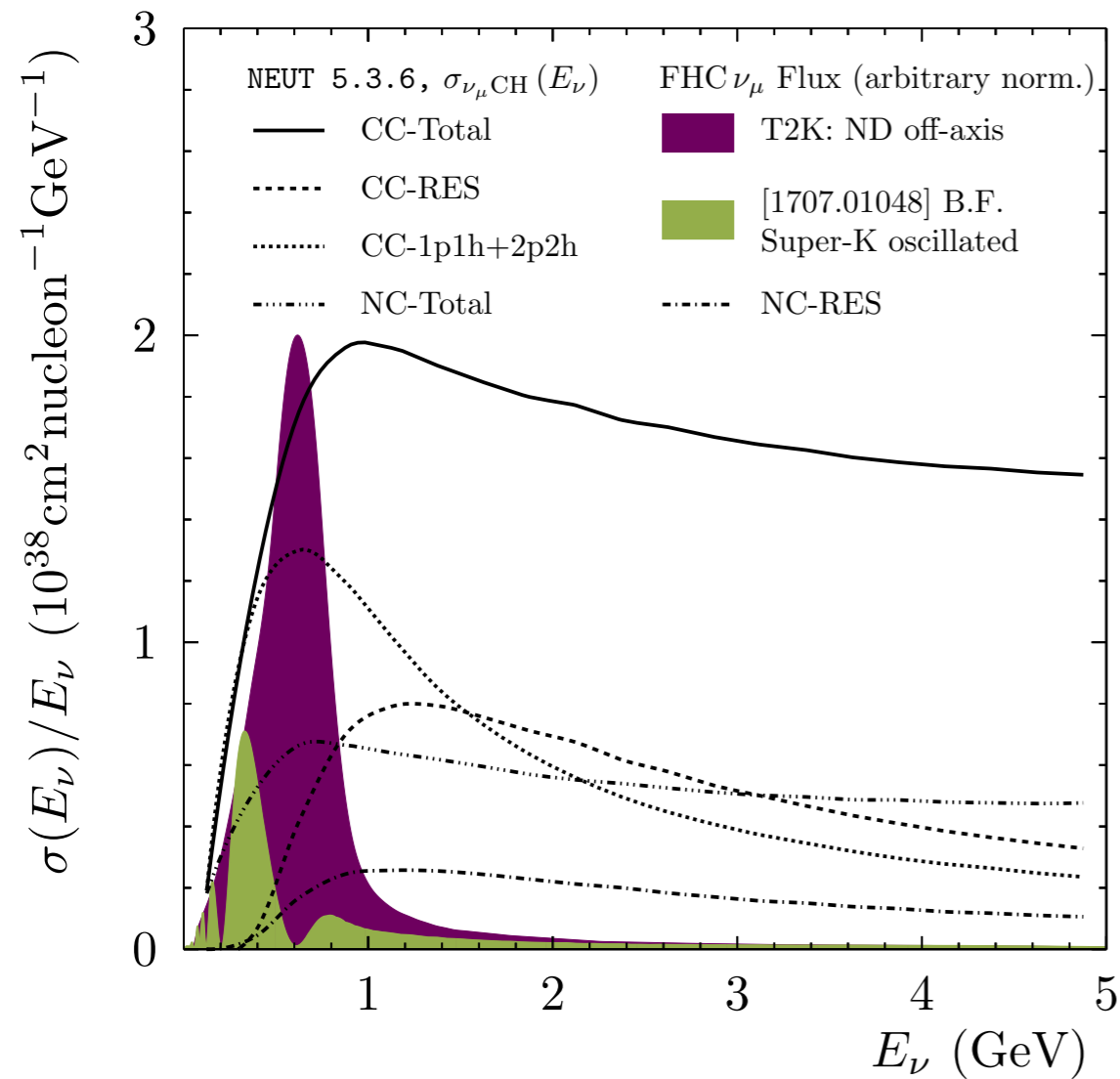
CCQE
(Charged-Current Quasi-Elastic)



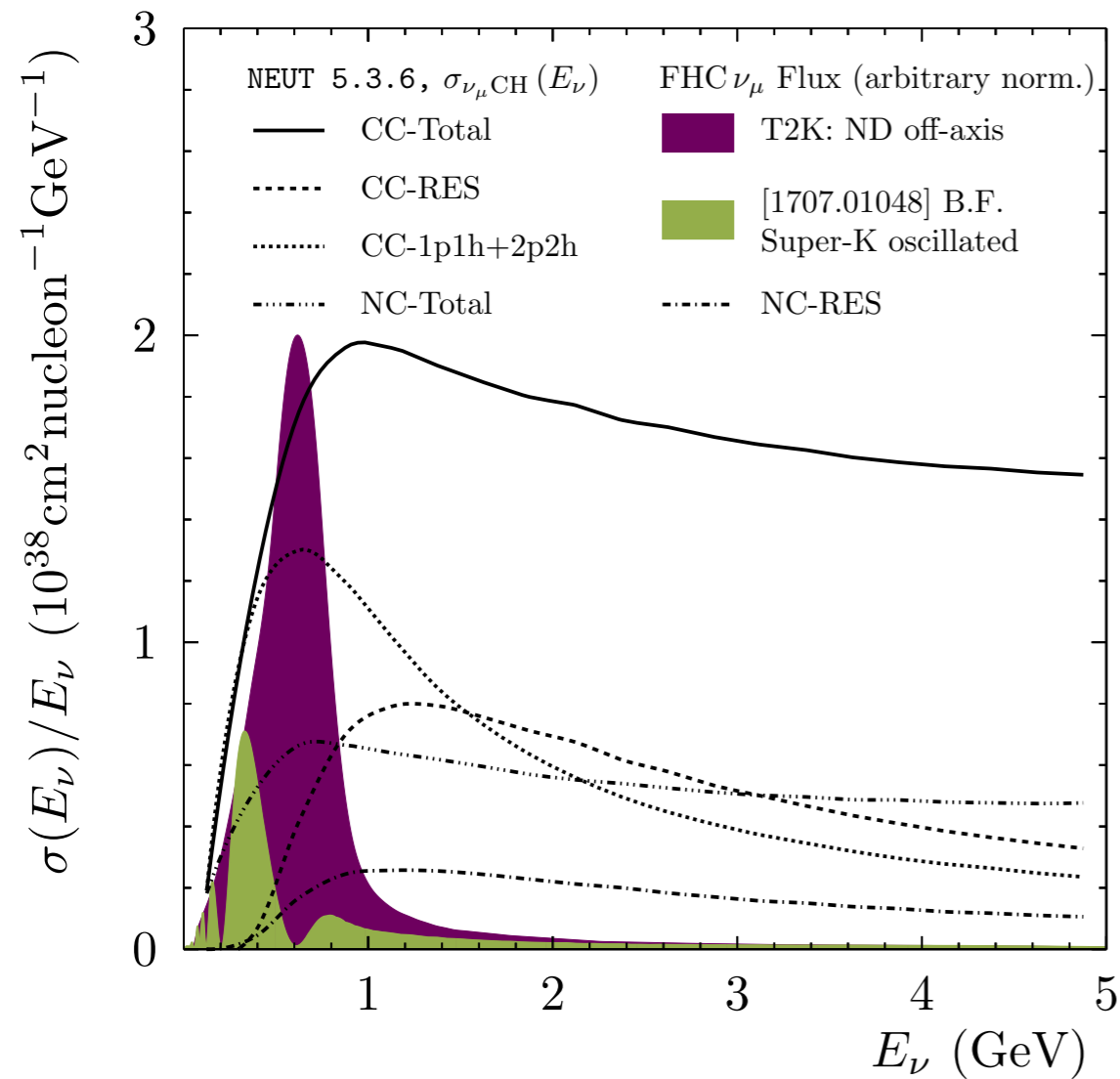
Relevant ν interactions at T2K

CCQE
(Charged-Current Quasi-Elastic)

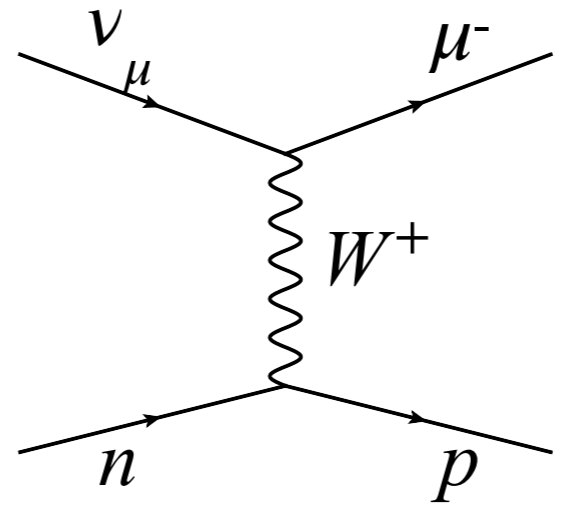
CCRES
(Charged-Current Resonant pion production)



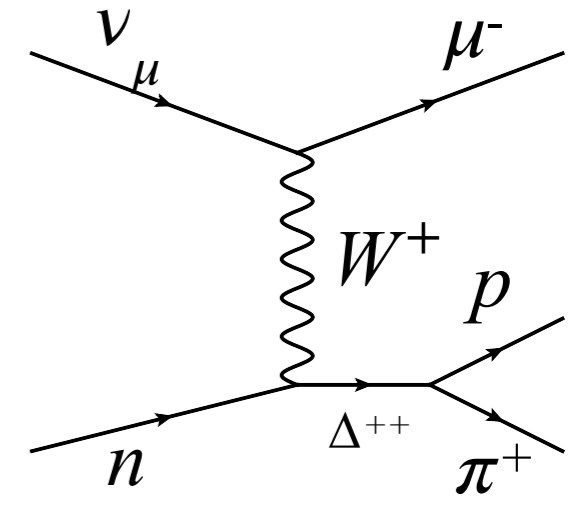
Relevant ν interactions at T2K



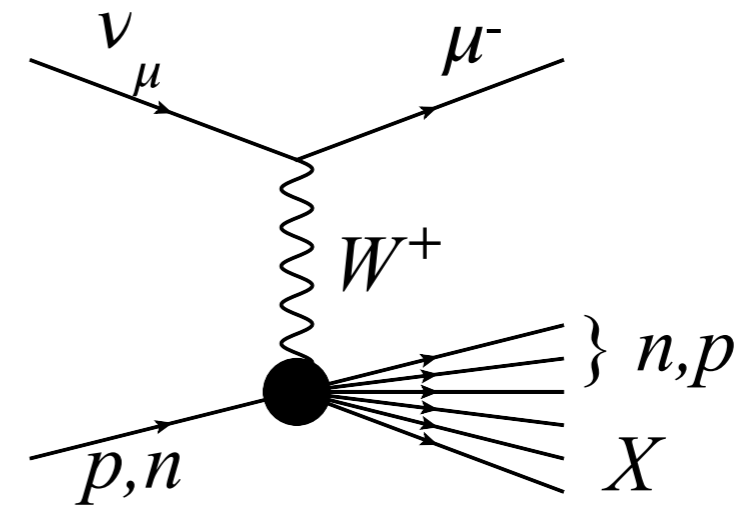
CCQE
(Charged-Current Quasi-Elastic)



CCRES
(Charged-Current Resonant pion production)



CCDIS
(Charged-Current Deep Inelastic Scattering)



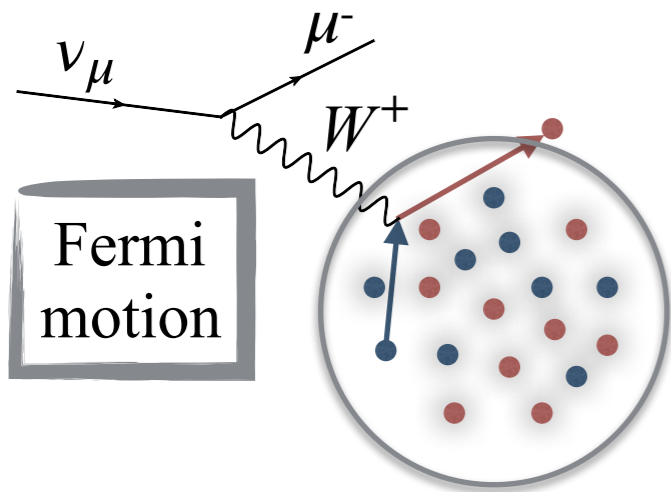
Nuclear effects

Nuclear effects

Nucleons bound in the nucleus \Rightarrow Nuclear effect!

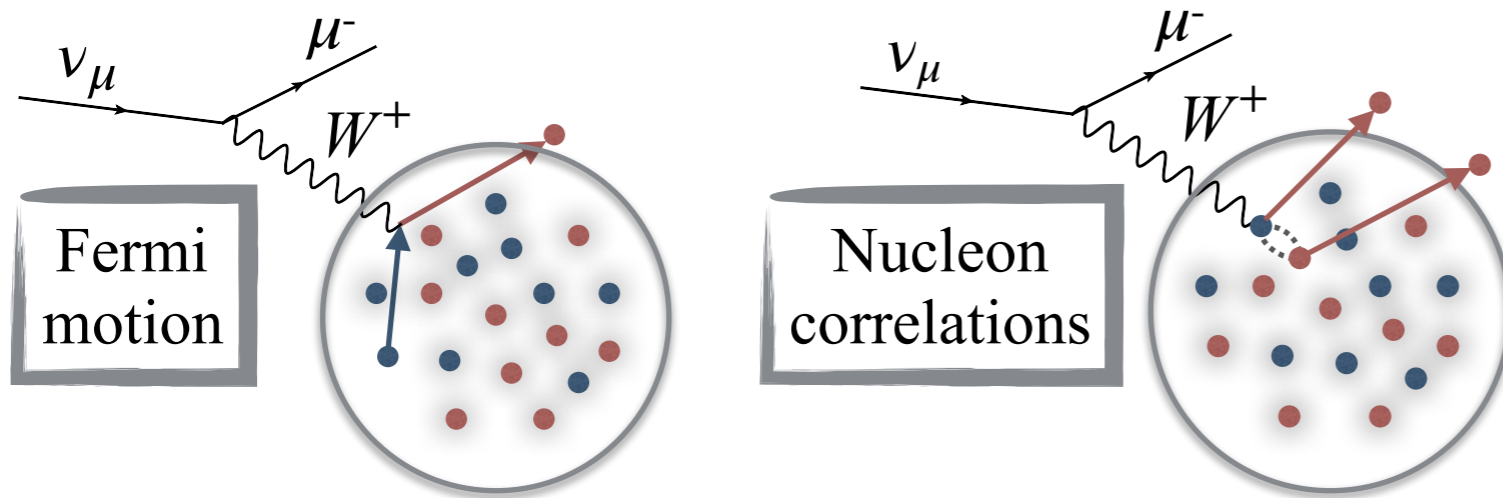
Nuclear effects

Nucleons bound in the nucleus \Rightarrow Nuclear effect!



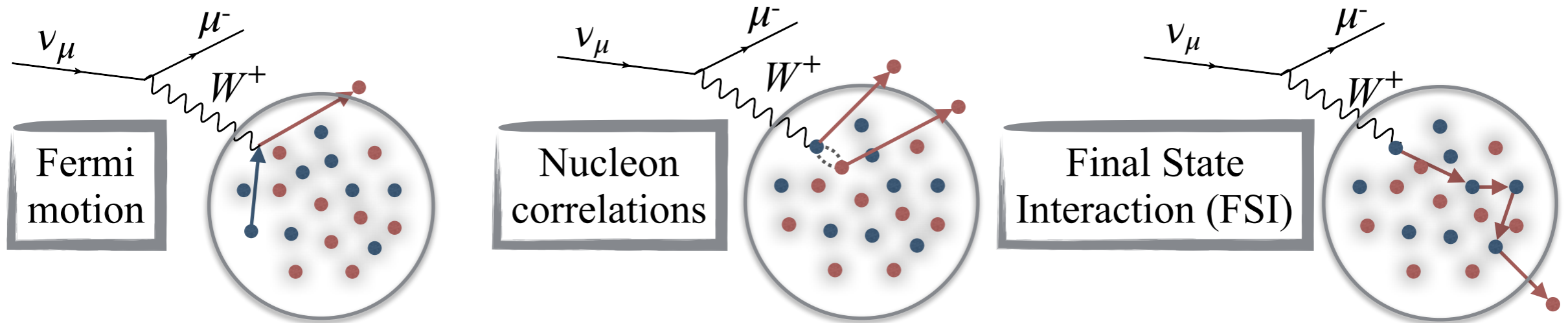
Nuclear effects

Nucleons bound in the nucleus \Rightarrow Nuclear effect!



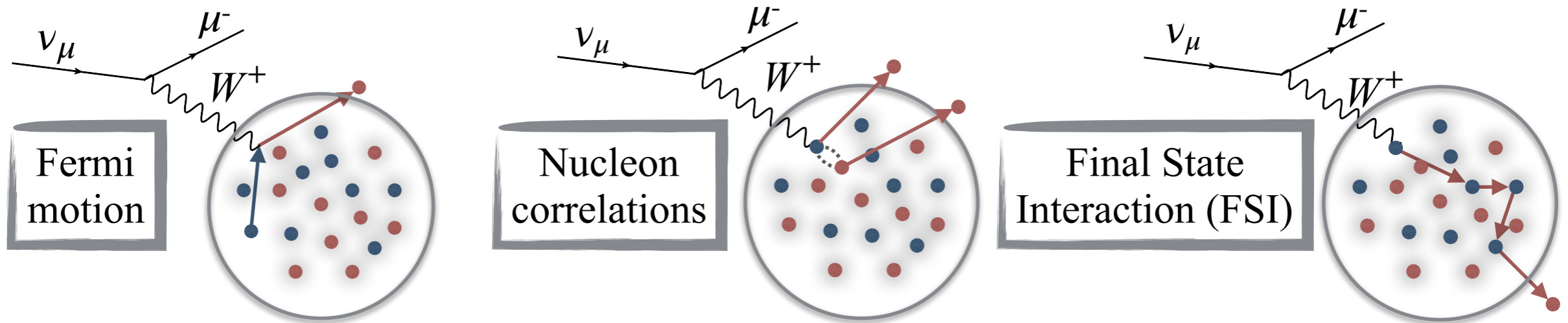
Nuclear effects

Nucleons bound in the nucleus \Rightarrow Nuclear effect!



Nuclear effects

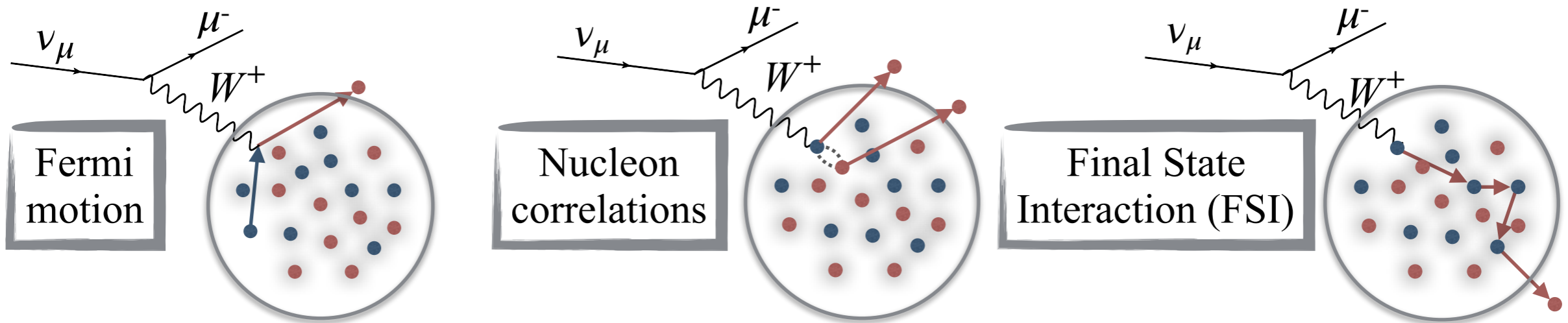
Nucleons bound in the nucleus \Rightarrow Nuclear effect!



Neutrino Energy reconstructed
using CCQE hypothesis

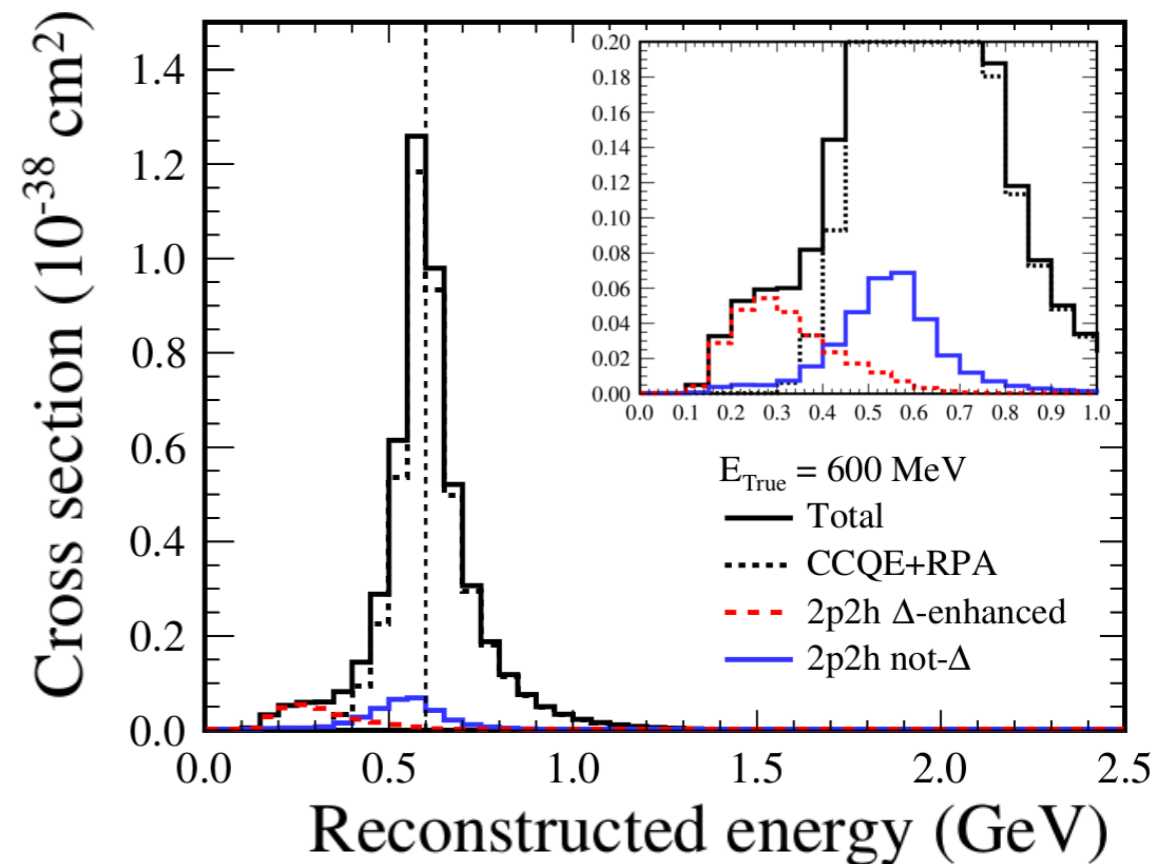
Nuclear effects

Nucleons bound in the nucleus \Rightarrow Nuclear effect!



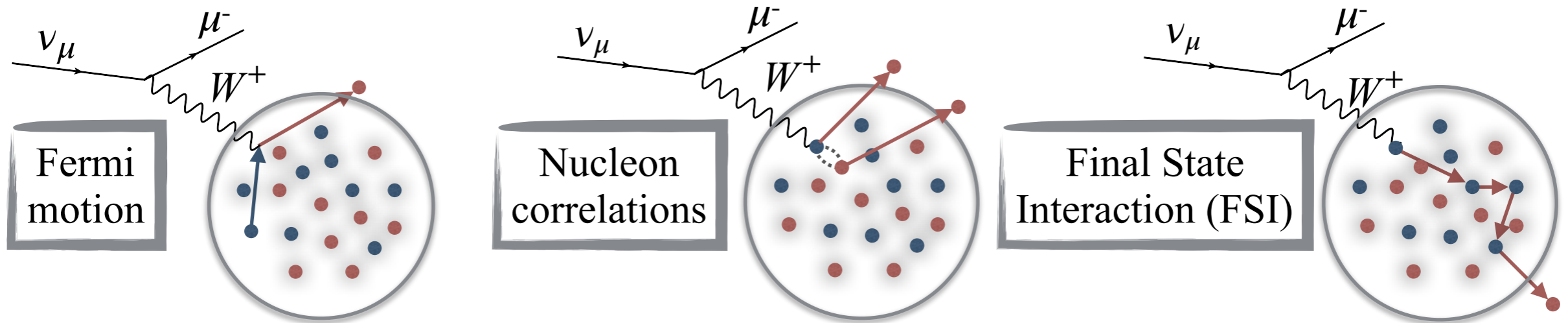
Neutrino Energy reconstructed using CCQE hypothesis

Nuclear effects introduce a bias in neutrino energy reconstruction



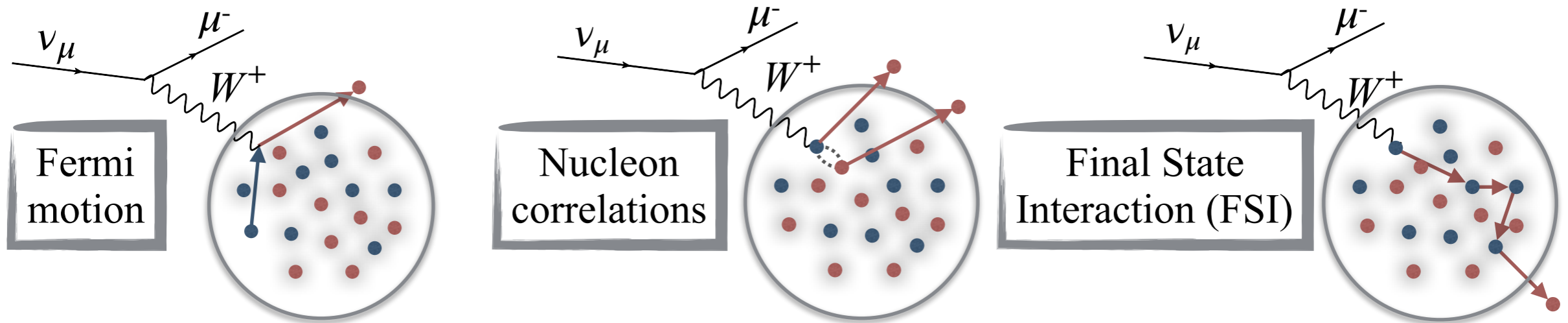
Detector acceptance

Nucleons bound in the nucleus \Rightarrow Nuclear effect!



Detector acceptance

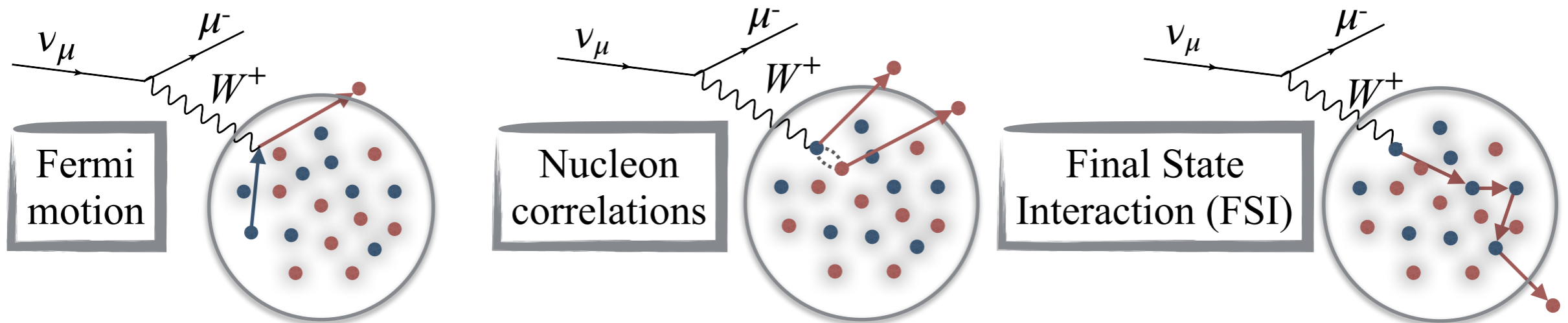
Nucleons bound in the nucleus \Rightarrow Nuclear effect!



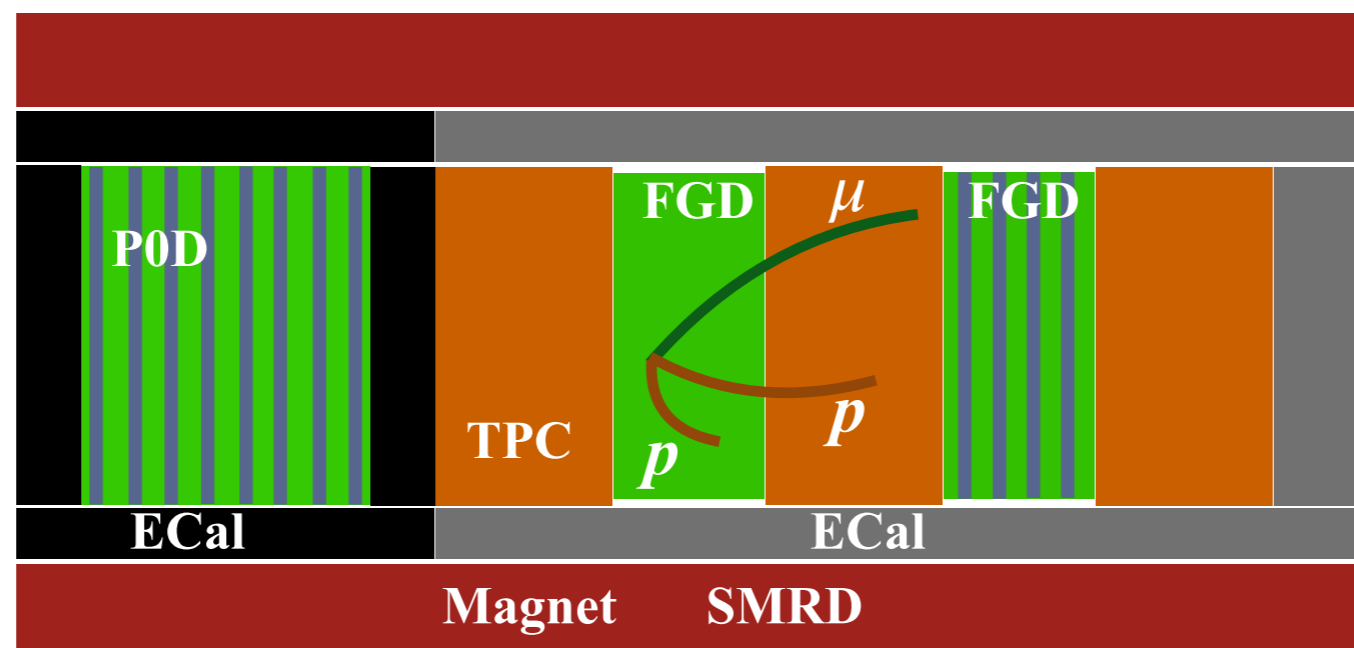
Limited detector acceptance

Detector acceptance

Nucleons bound in the nucleus \Rightarrow Nuclear effect!

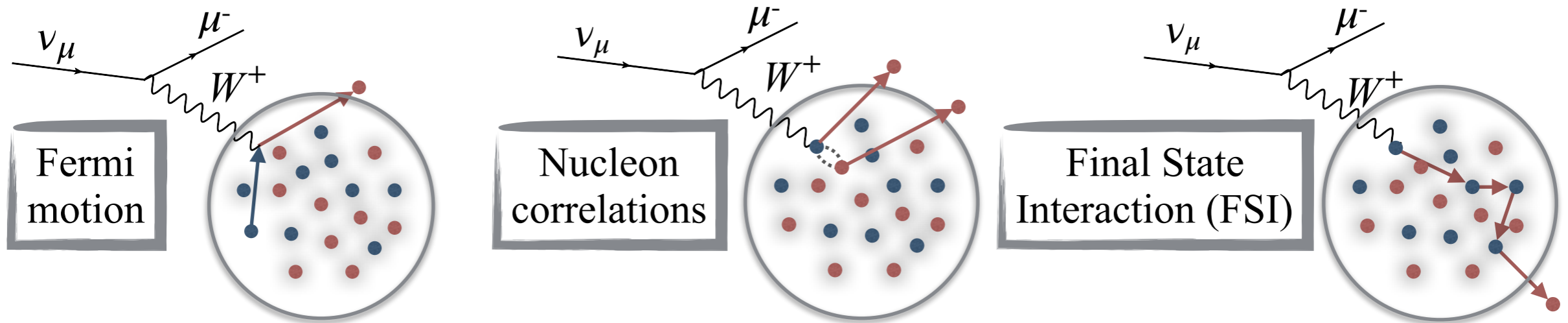


Limited detector acceptance

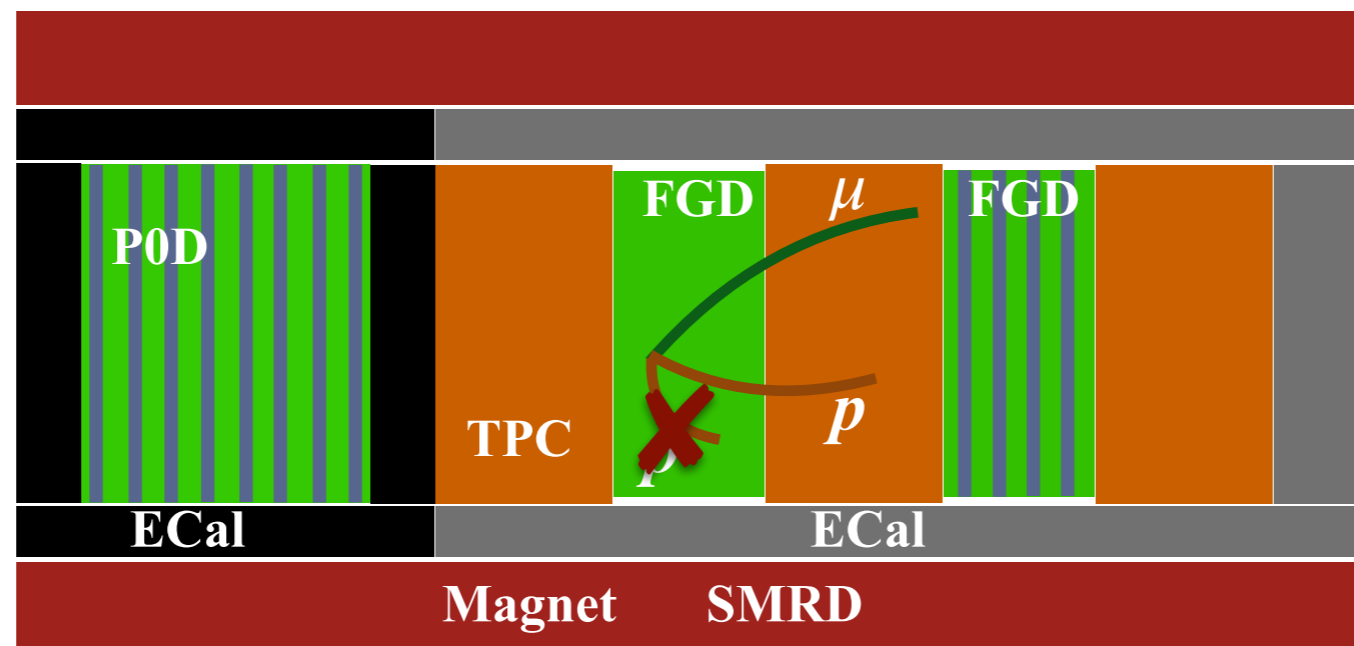


Detector acceptance

Nucleons bound in the nucleus \Rightarrow Nuclear effect!

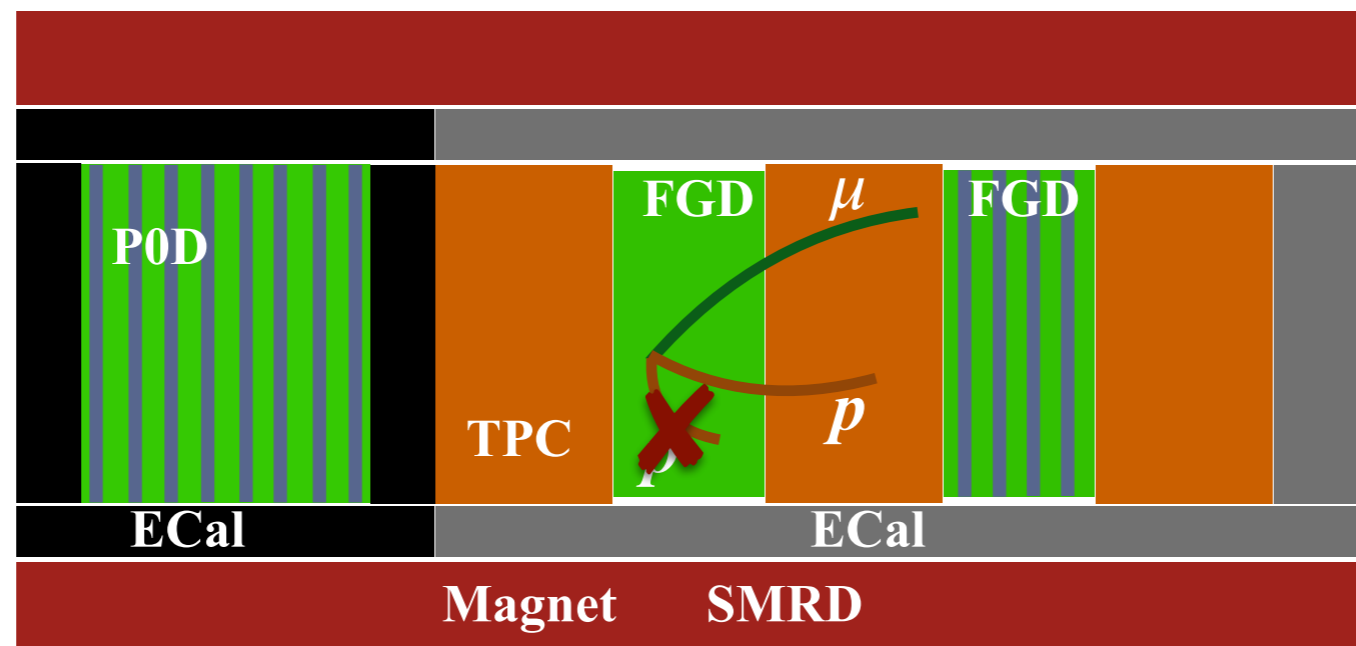
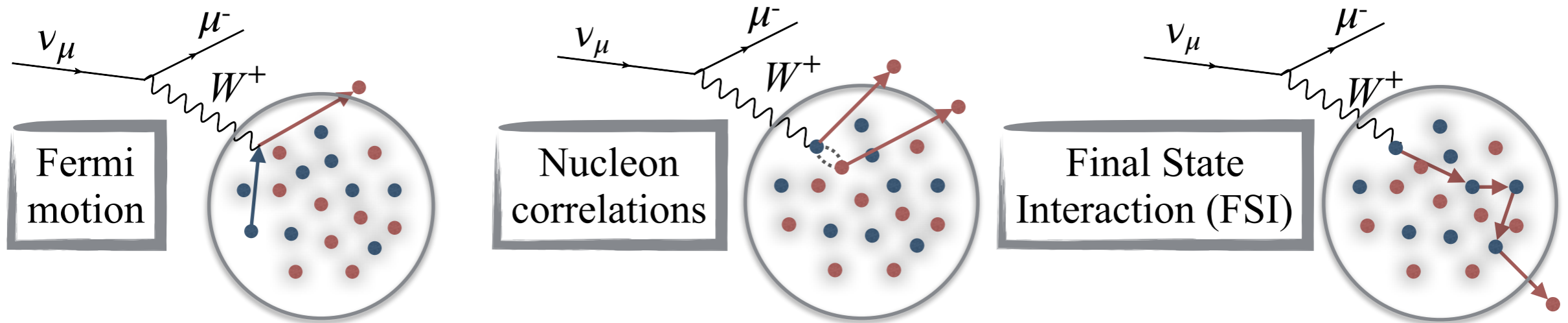


Limited detector acceptance



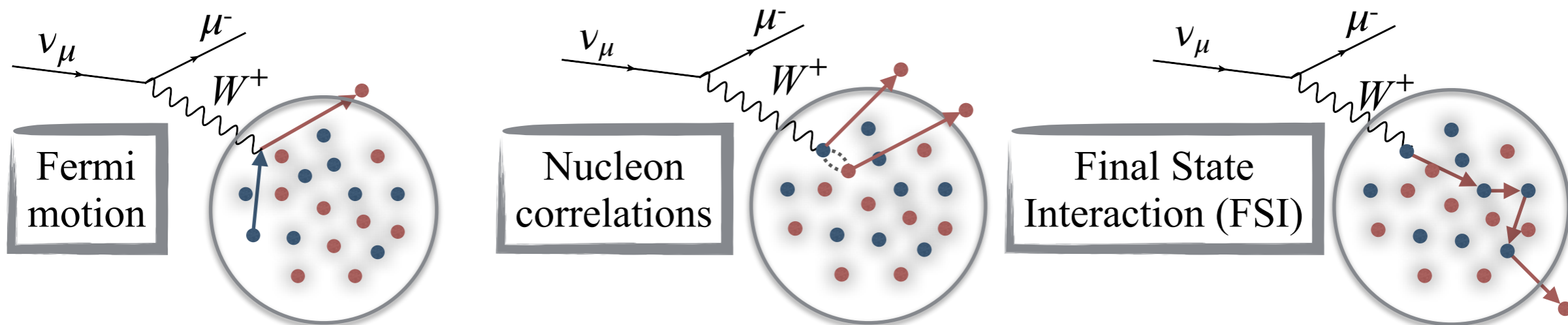
Detector acceptance

Nucleons bound in the nucleus \Rightarrow Nuclear effect!

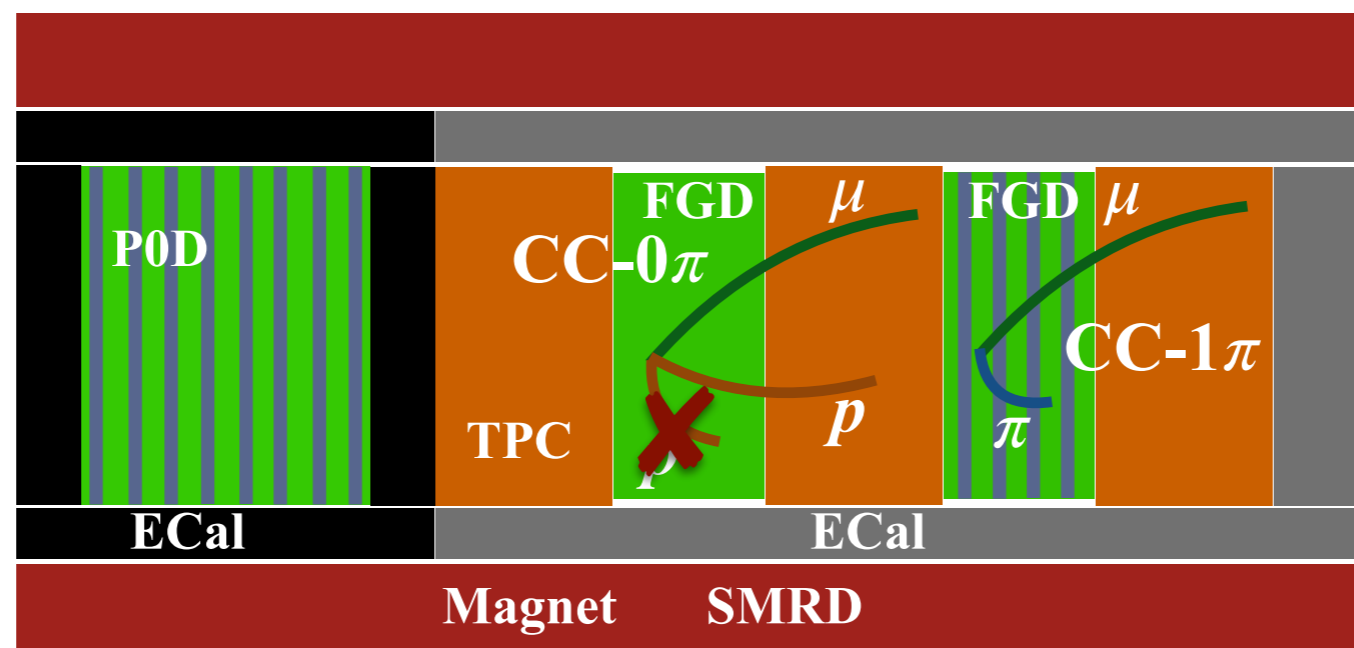


Detector acceptance

Nucleons bound in the nucleus \Rightarrow Nuclear effect!



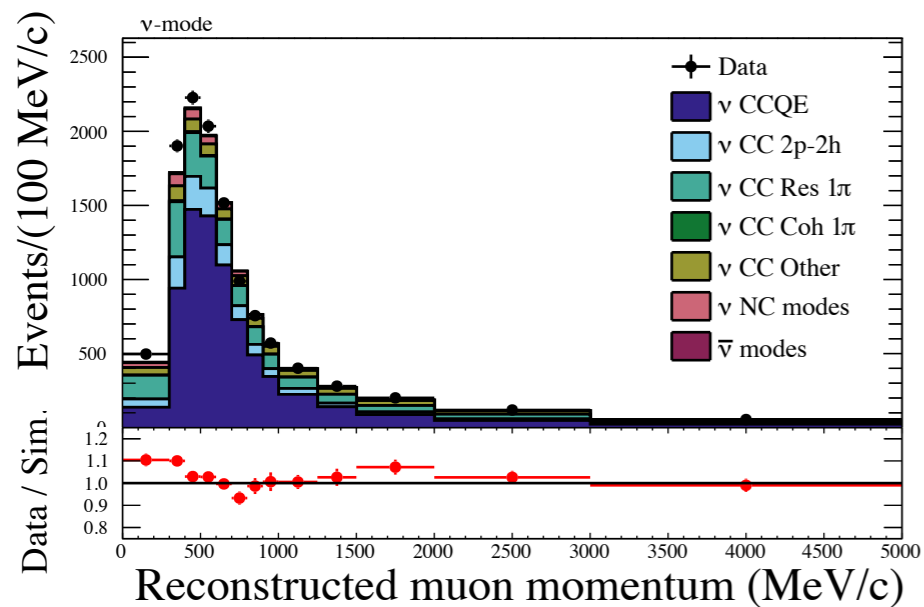
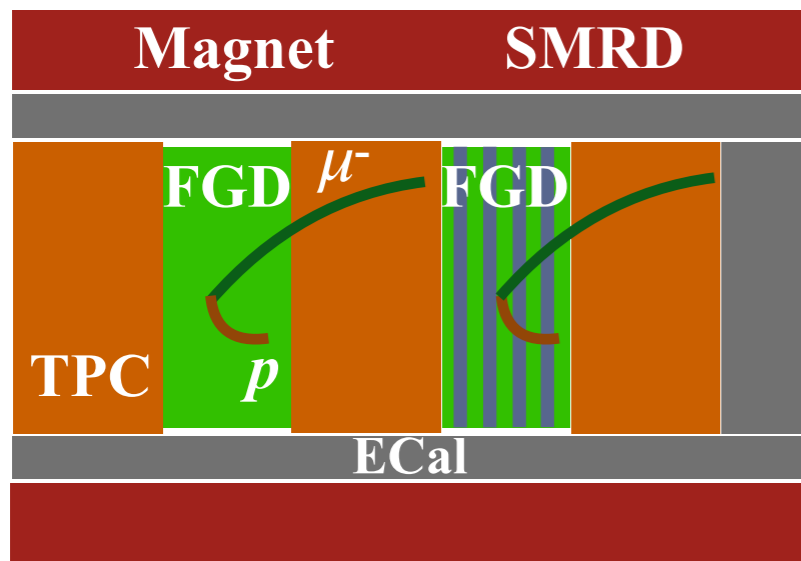
Increase acceptance and reduce the dependence from the cross-section modeling measuring interaction topologies



ND280 measurements: ν beam

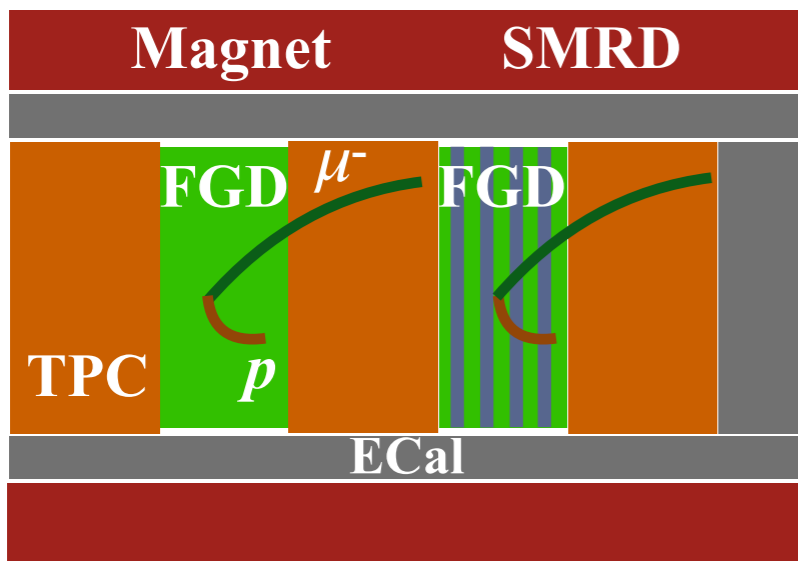
ND280 measurements: ν beam

CC- 0π

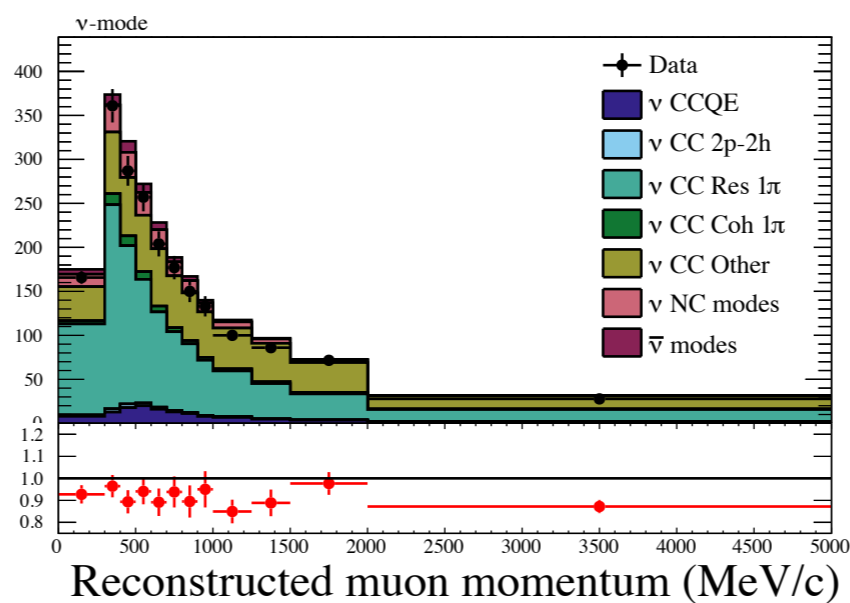
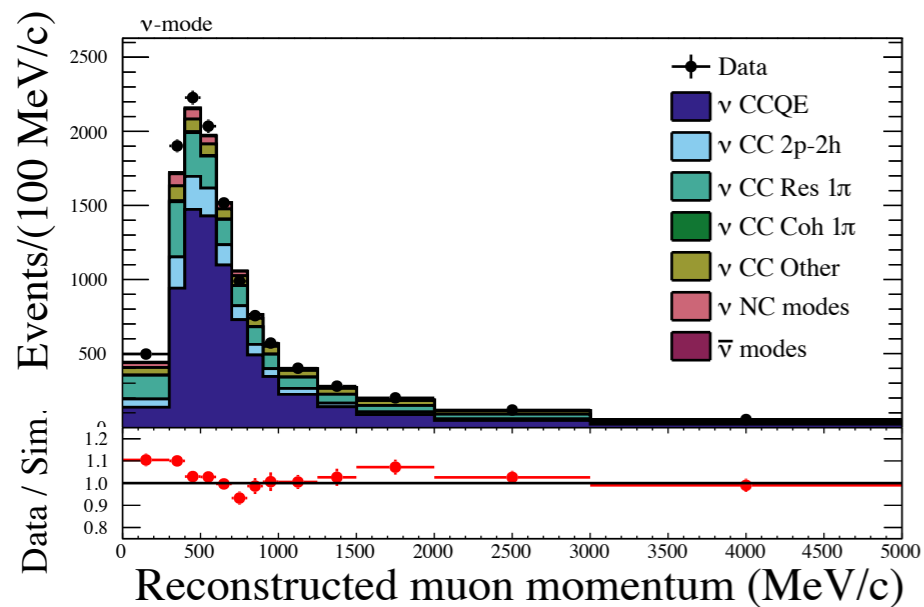
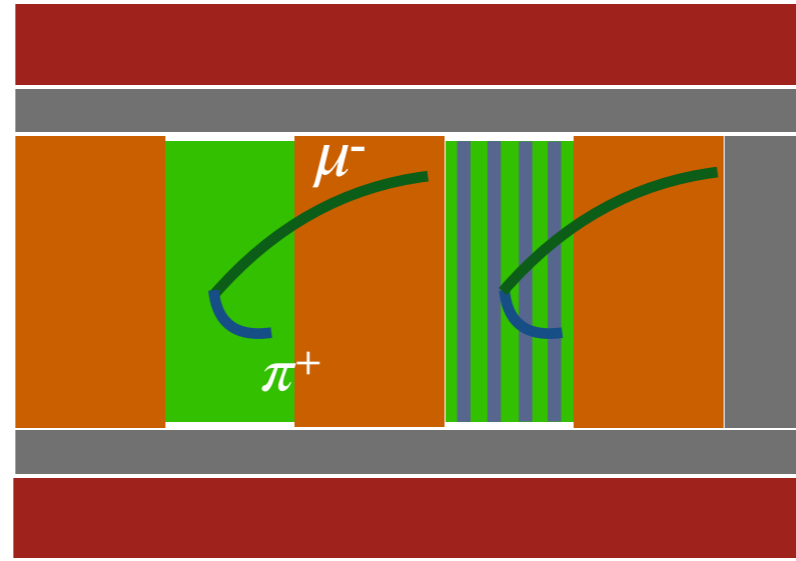


ND280 measurements: ν beam

CC- 0π

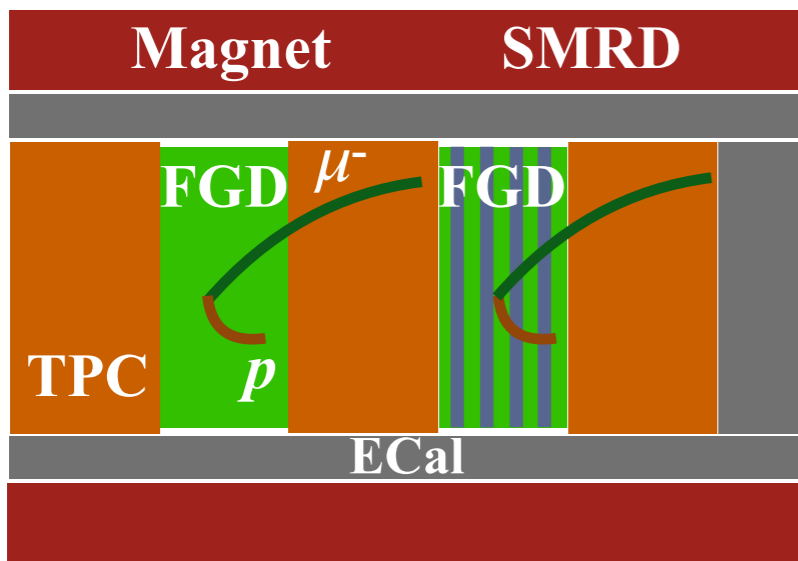


CC- $1\pi^+$

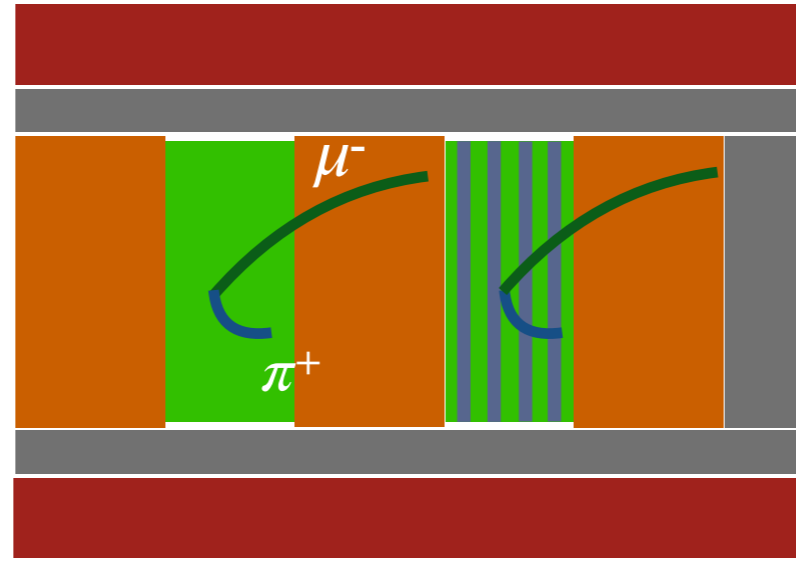


ND280 measurements: ν beam

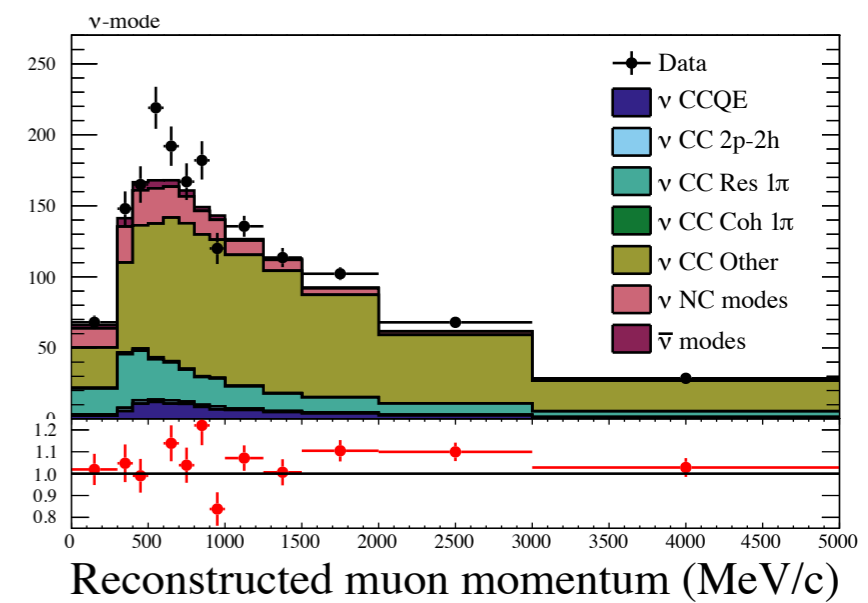
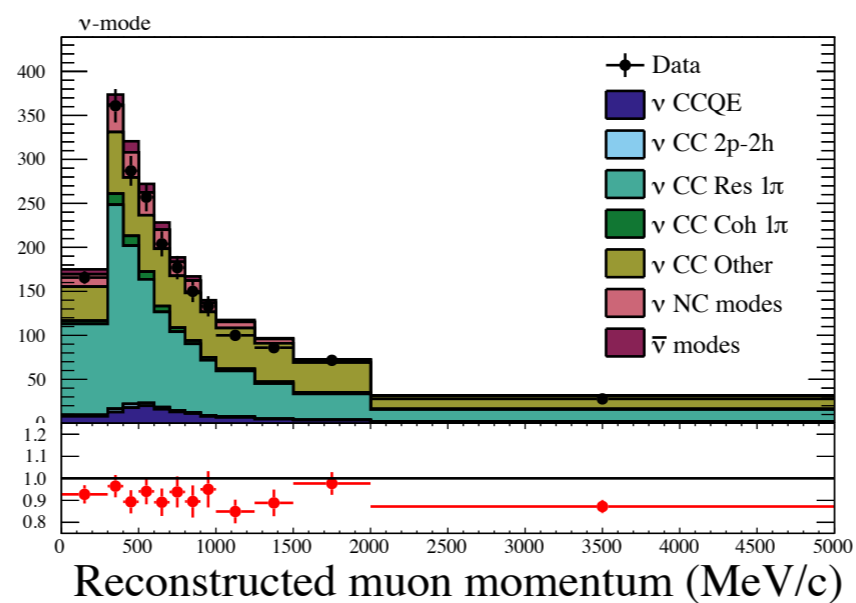
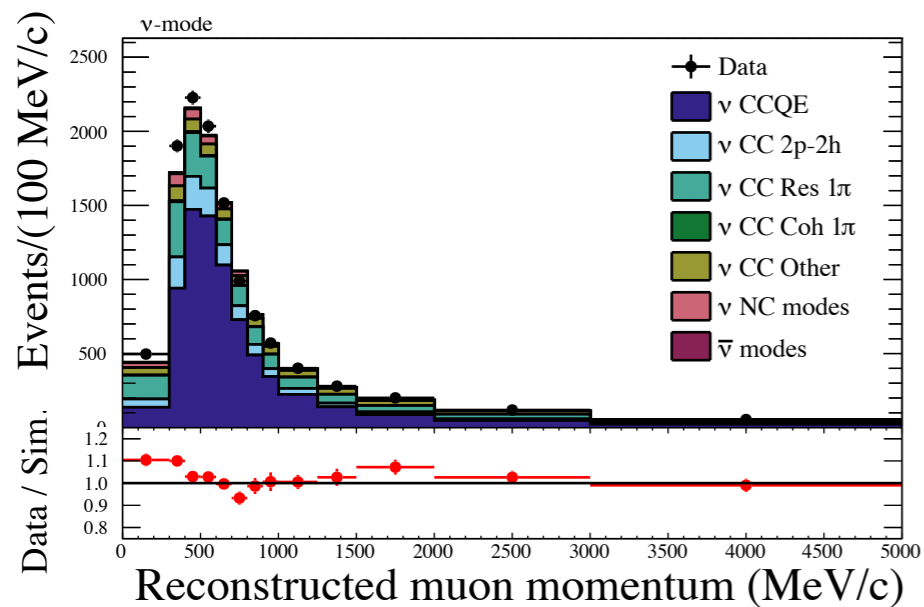
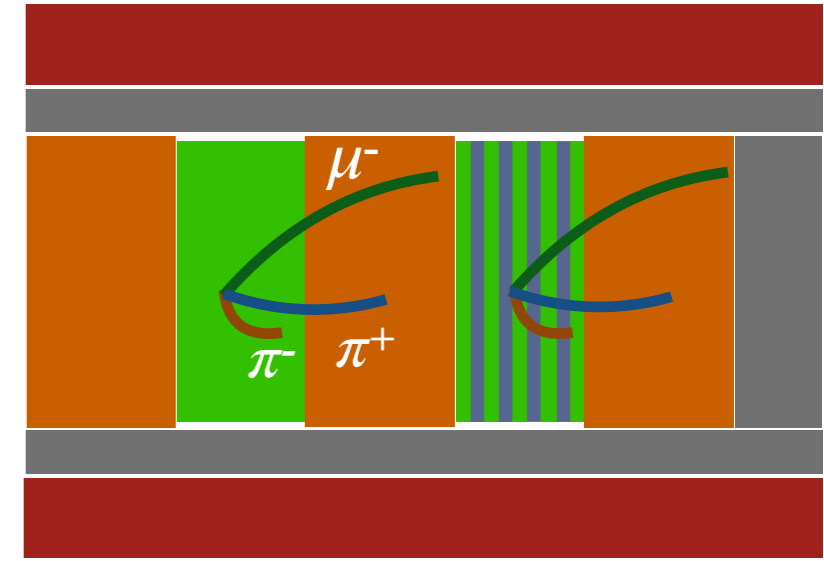
CC- 0π



CC- $1\pi^+$



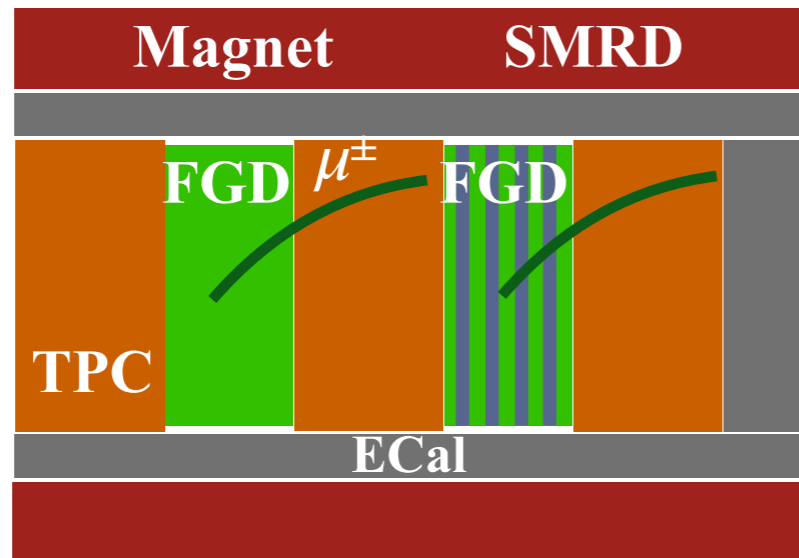
CC-Other



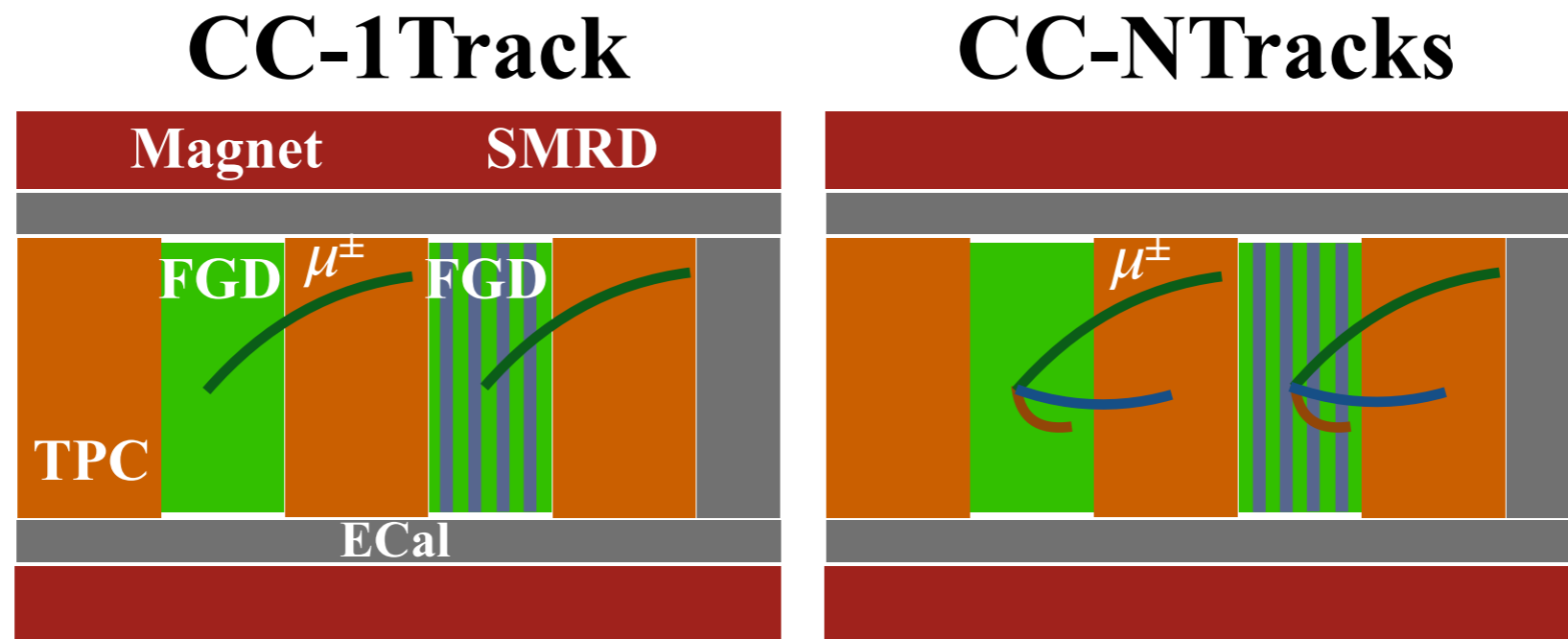
ND280 measurements: $\bar{\nu}$ beam

ND280 measurements: $\bar{\nu}$ beam

CC-1Track

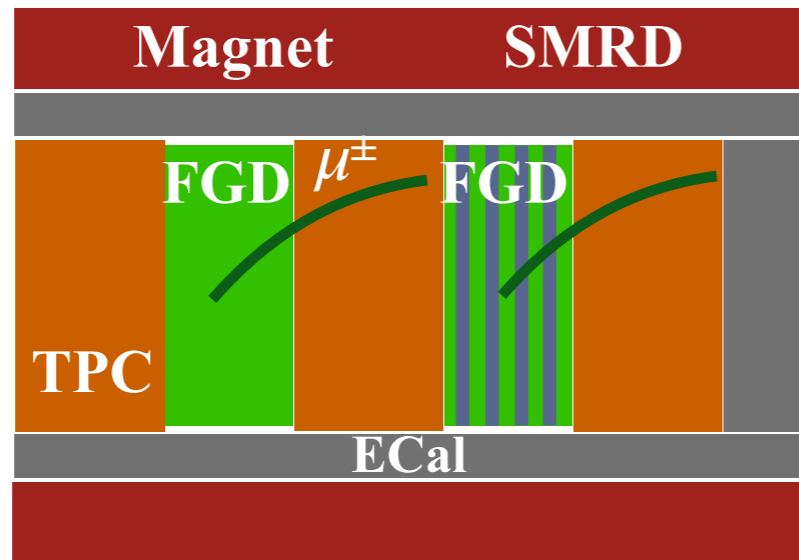


ND280 measurements: $\bar{\nu}$ beam

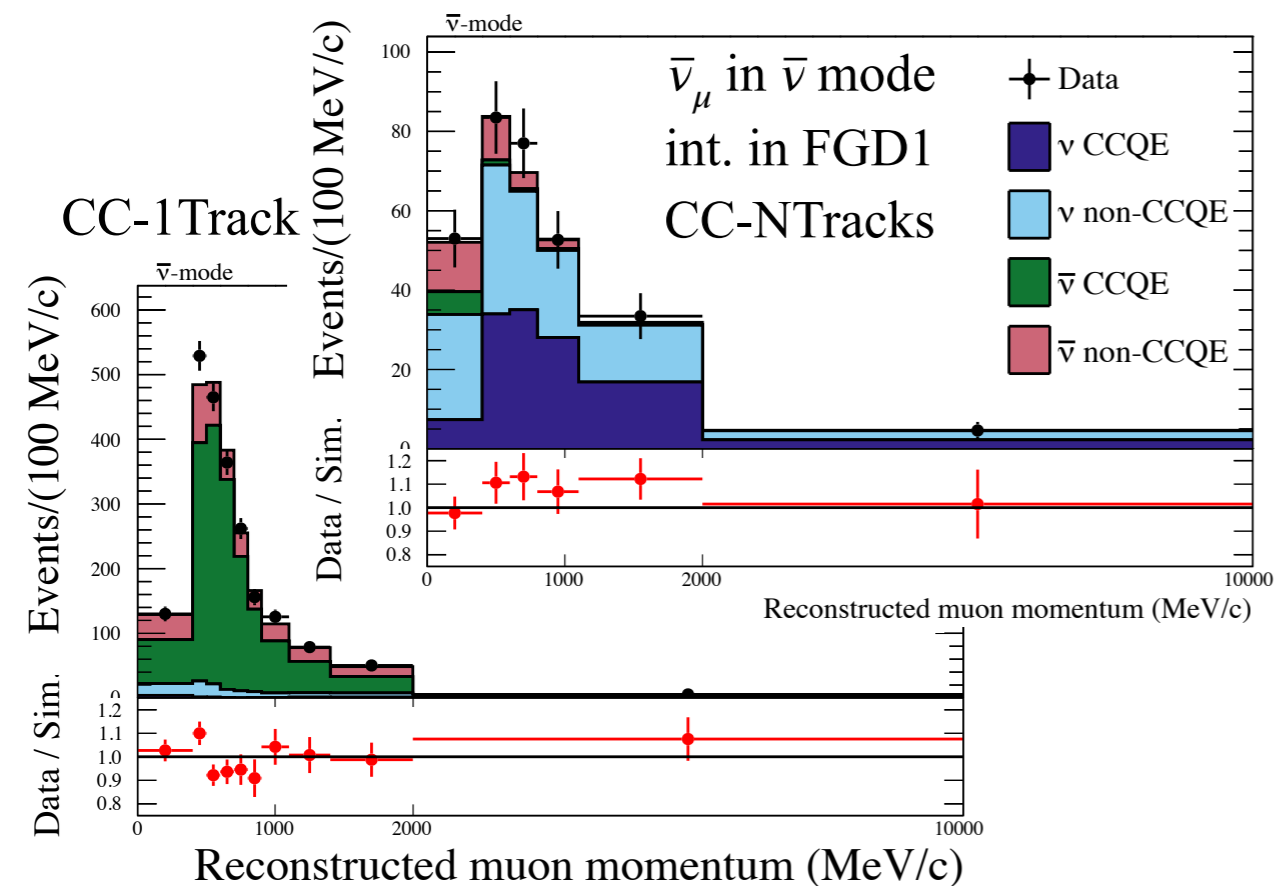
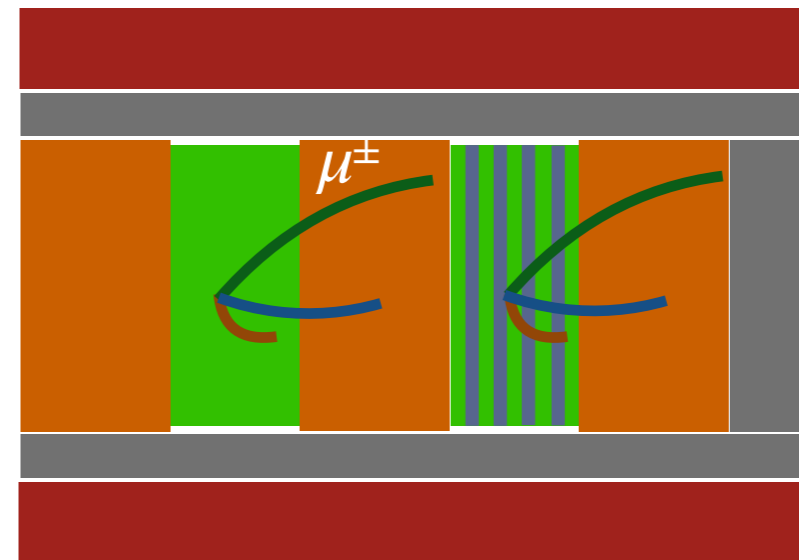


ND280 measurements: $\bar{\nu}$ beam

CC-1Track

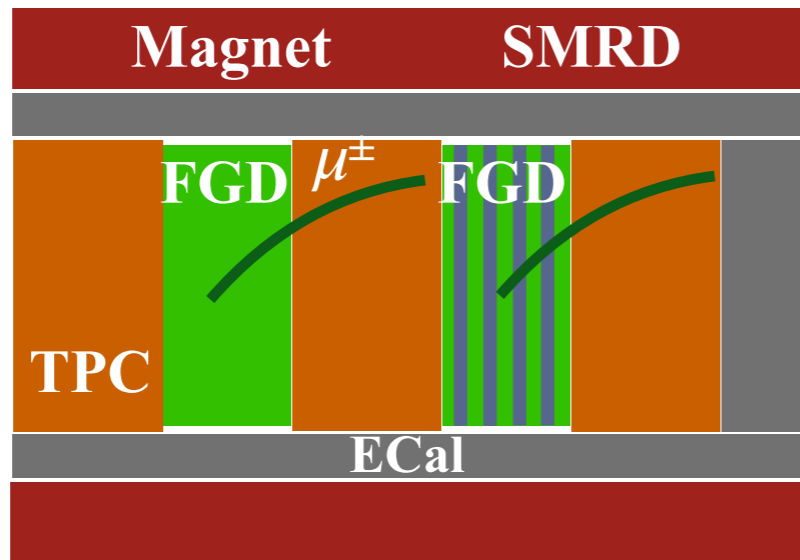


CC-NTracks

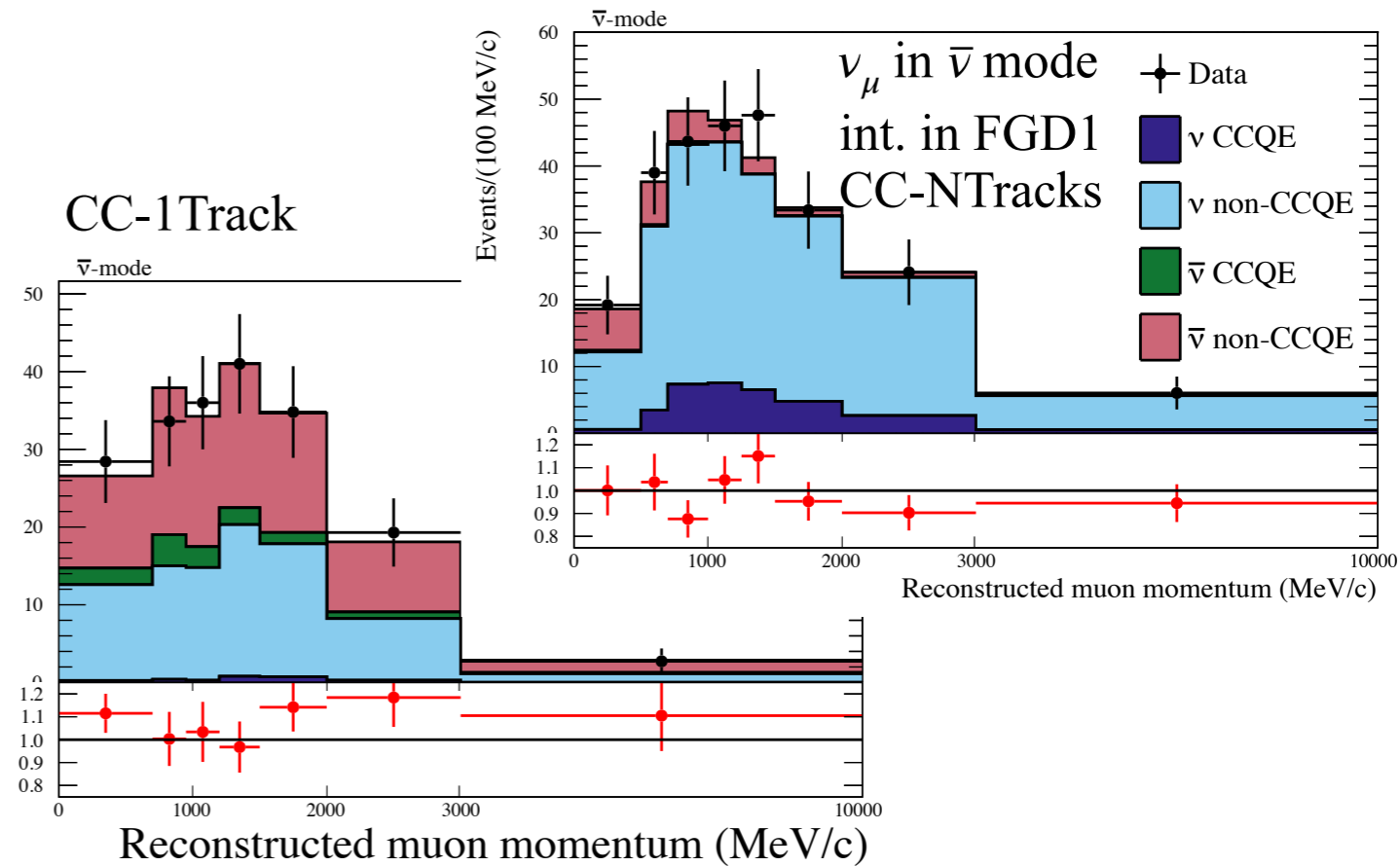
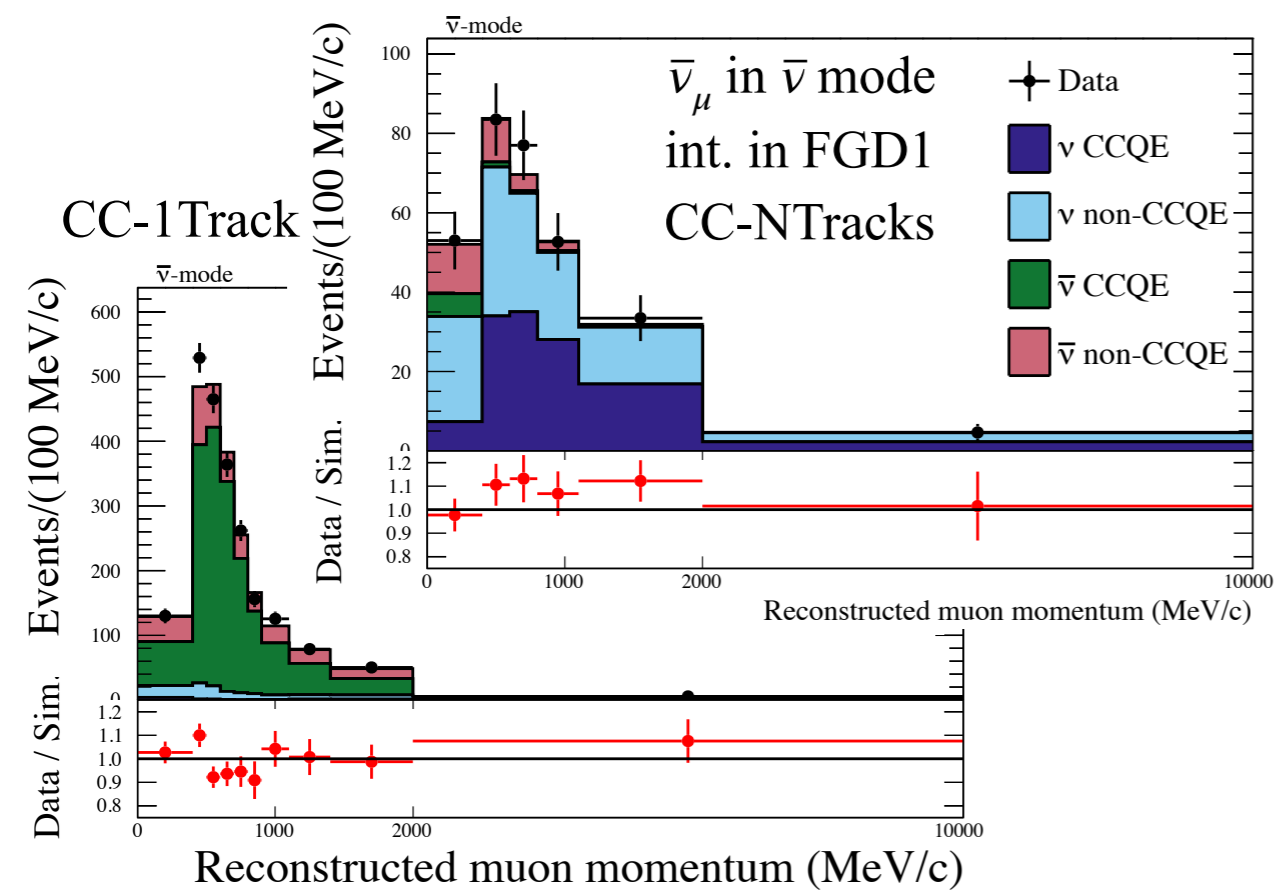
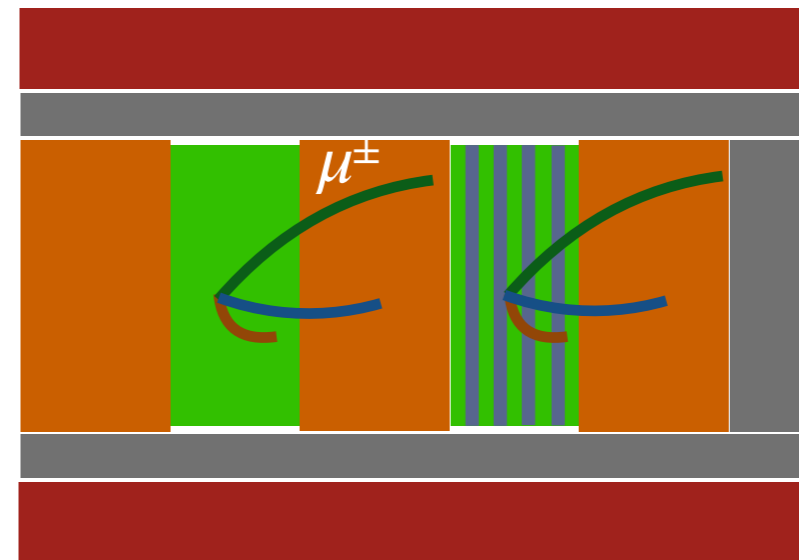


ND280 measurements: $\bar{\nu}$ beam

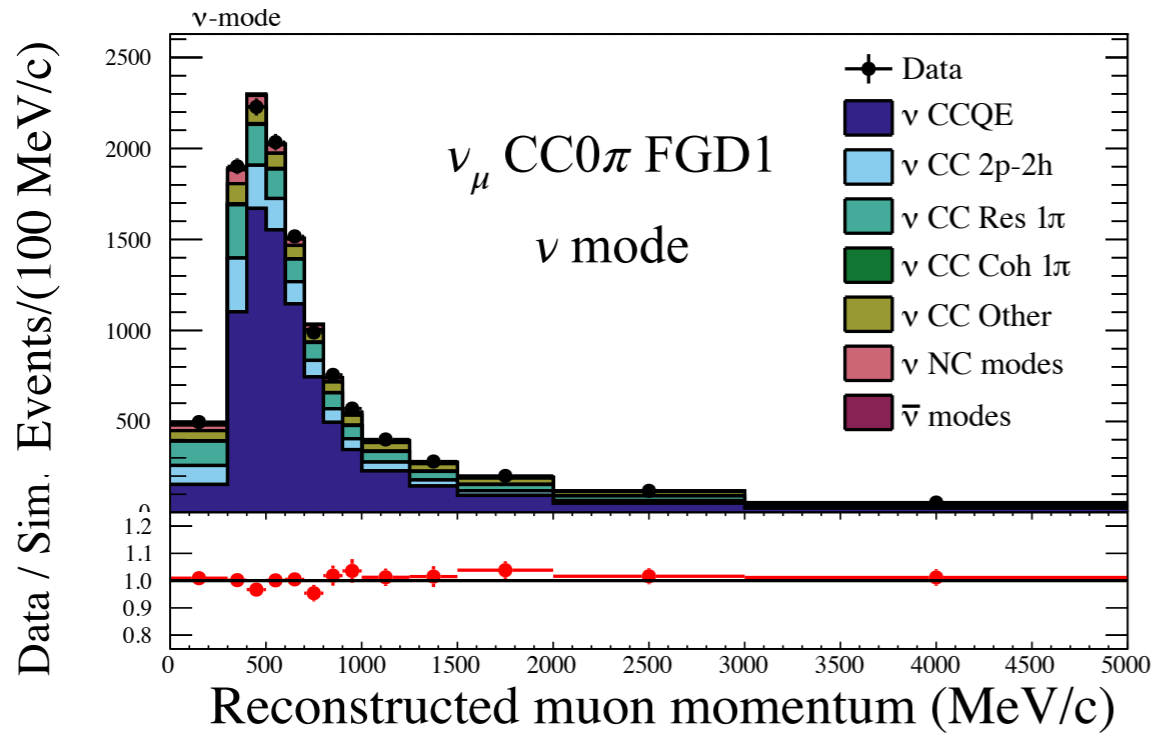
CC-1Track



CC-NTracks

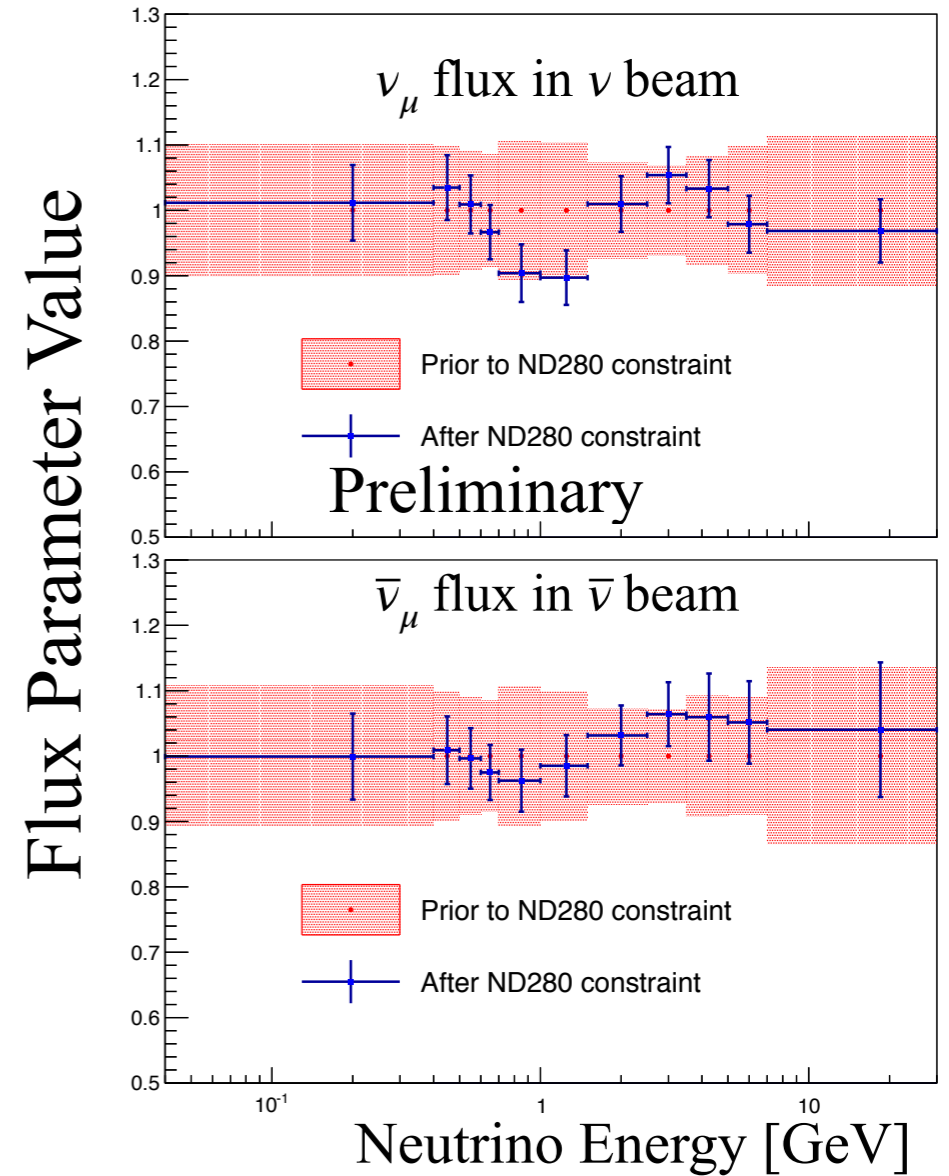


ND280 fit results

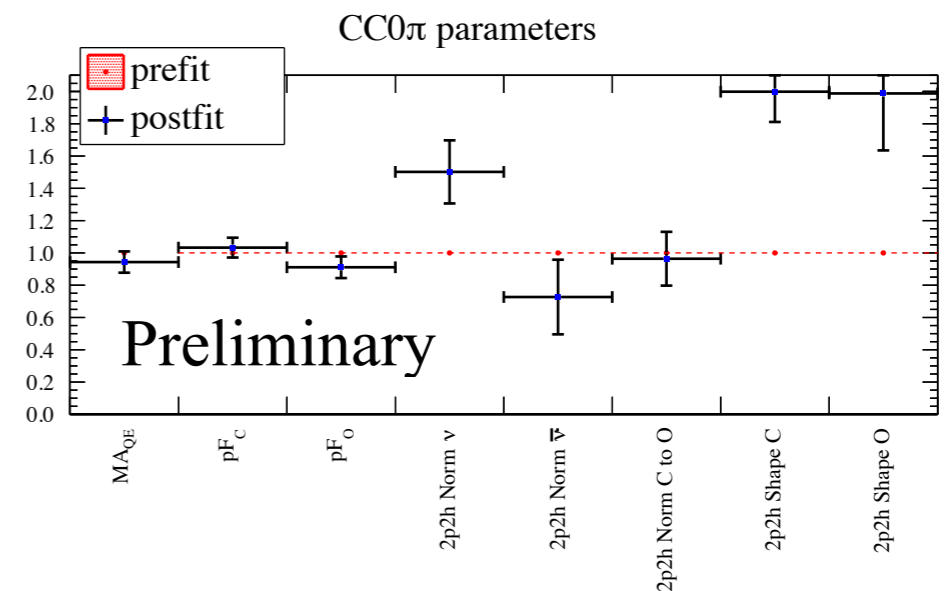


Impact on SK:

Sample	w/o ND280	w/ ND280
ν 1R μ	14,6%	5,1%
$\bar{\nu}$ 1R μ	12,5%	4,5%
ν 1Re	16,9%	8,8%
$\bar{\nu}$ 1Re	14,4%	7,1%
ν 1Re+1 π^+	22,0%	18,7%



Cross section parameter Values



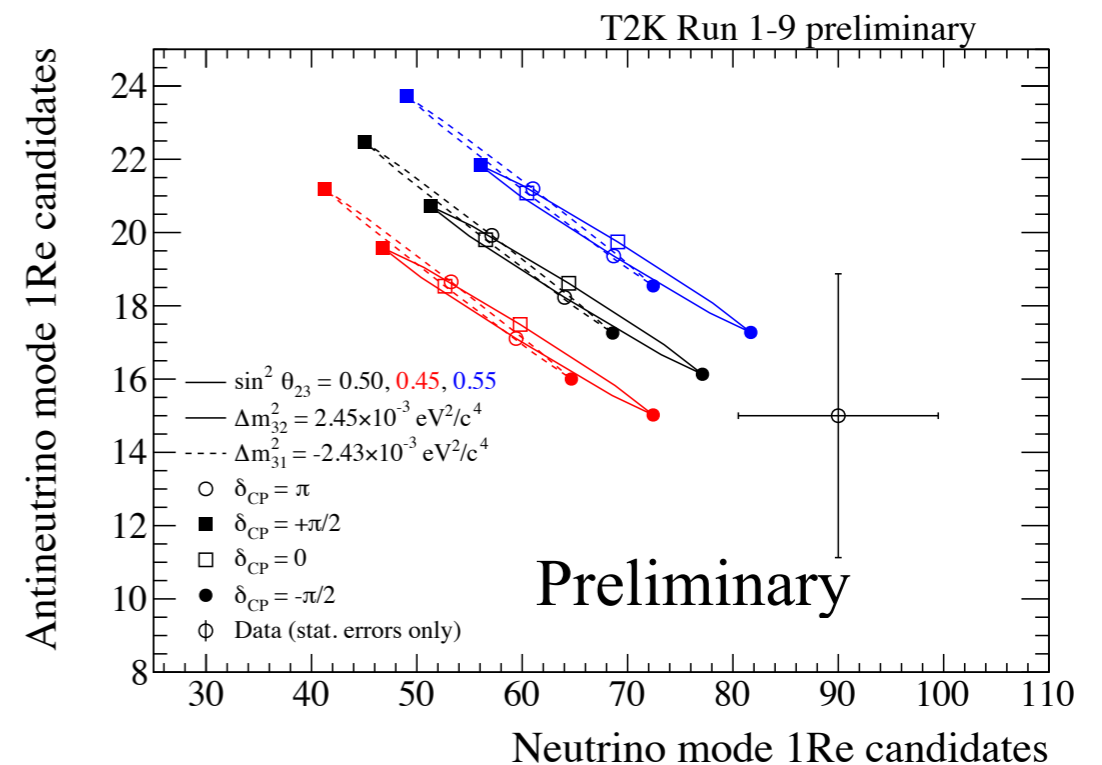
Observed events at SK

	Observed	$\delta = -\pi/2$	$\delta = 0$	$\delta = +\pi/2$	$\delta = \pi$
<i>e</i> -like ν mode	75	74.4	62.2	50.6	62.7
<i>e</i> -like+ $1\pi^+$ ν mode	15	7.0	6.1	4.9	5.9
<i>e</i> -like $\bar{\nu}$ mode	15	17.1	19.4	21.7	19.3
μ -like ν mode	243	272.4	272.0	272.4	272.8
μ -like $\bar{\nu}$ mode	140	139.2	139.2	139.5	139.9

Observed events at SK

	Observed	$\delta = -\pi/2$	$\delta = 0$	$\delta = +\pi/2$	$\delta = \pi$
e -like ν mode	75	74.4	62.2	50.6	62.7
e -like+ $1\pi^+$ ν mode	15	7.0	6.1	4.9	5.9
e -like $\bar{\nu}$ mode	15	17.1	19.4	21.7	19.3
μ -like ν mode	243	272.4	272.0	272.4	272.8
μ -like $\bar{\nu}$ mode	140	139.2	139.2	139.5	139.9

T2K data prefer $\delta_{CP} = -\pi/2$: maximize ν_e appearance and minimize $\bar{\nu}_e$ appearance

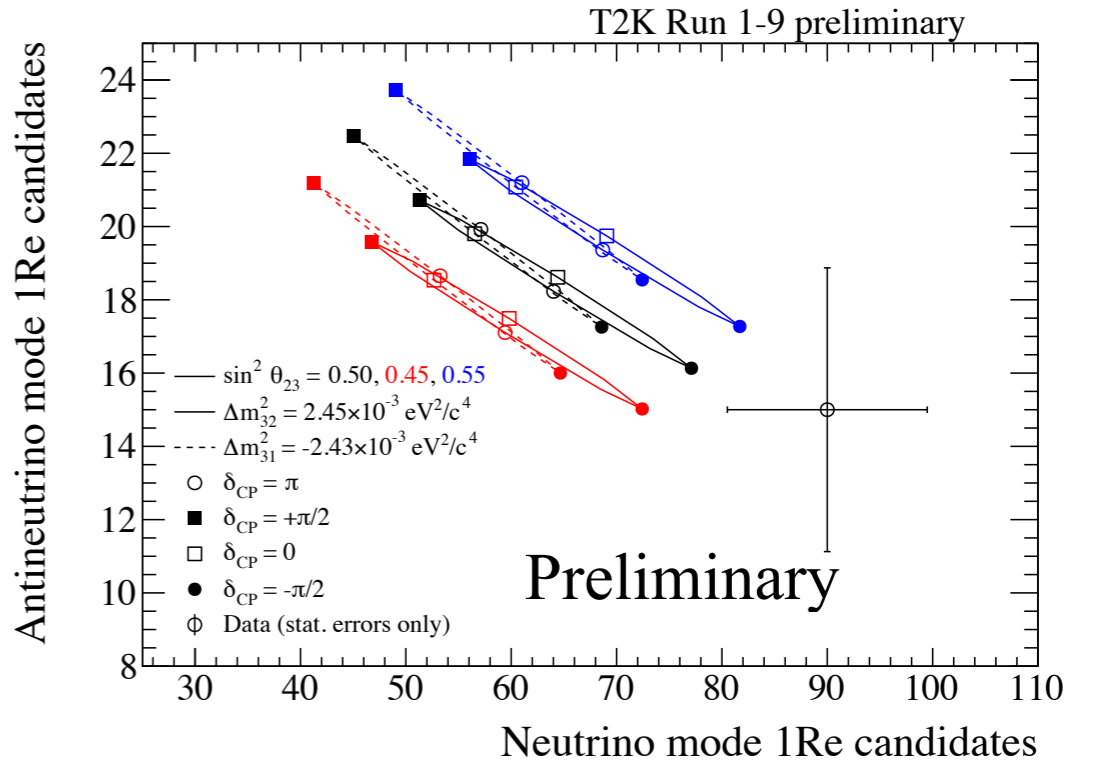


Observed events at SK

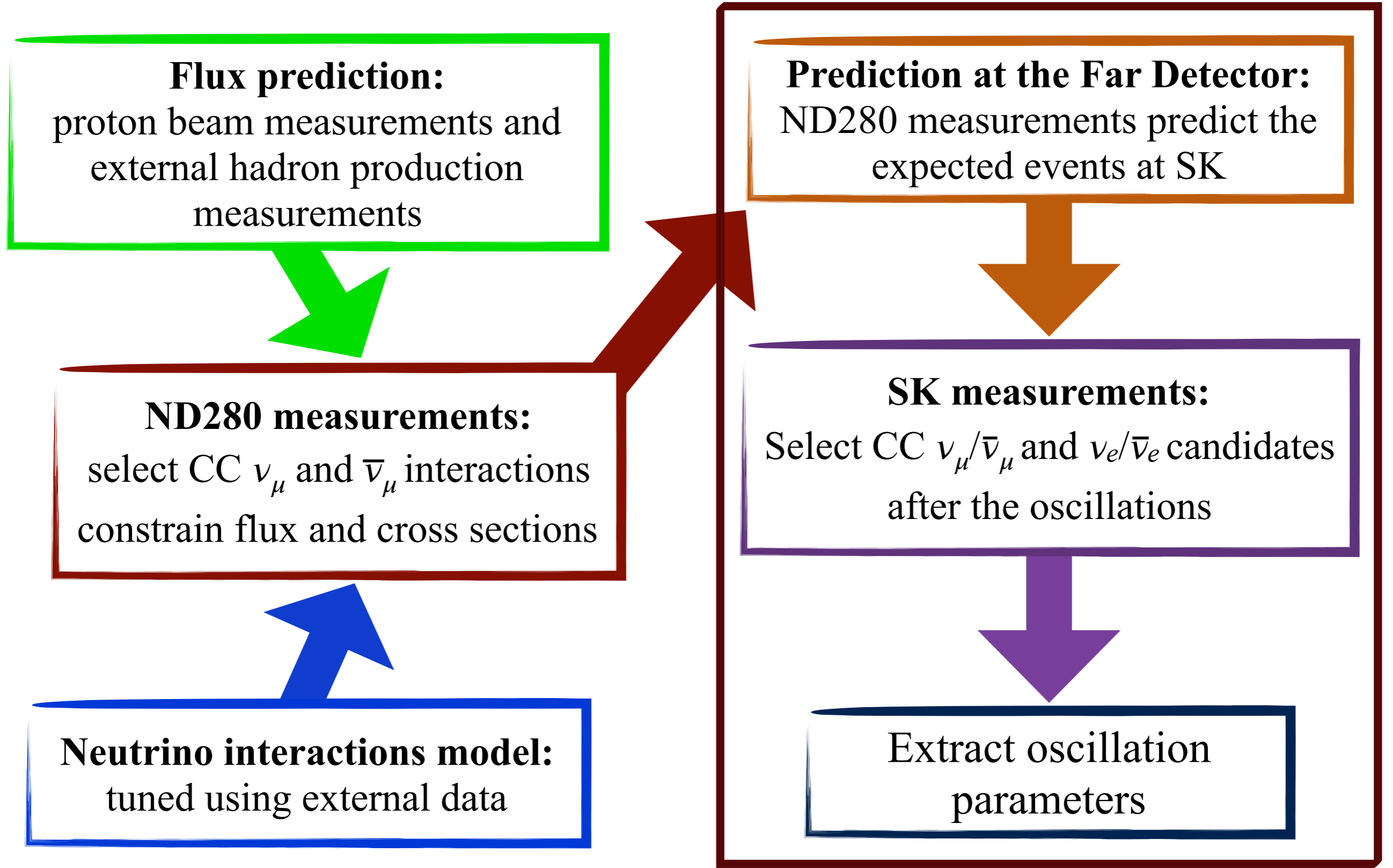
	Observed	$\delta = -\pi/2$	$\delta = 0$	$\delta = +\pi/2$	$\delta = \pi$
e -like ν mode	75	74.4	62.2	50.6	62.7
e -like+ $1\pi^+$ ν mode	15	7.0	6.1	4.9	5.9
e -like $\bar{\nu}$ mode	15	17.1	19.4	21.7	19.3
μ -like ν mode	243	272.4	272.0	272.4	272.8
μ -like $\bar{\nu}$ mode	140	139.2	139.2	139.5	139.9

T2K data prefer $\delta_{CP} = -\pi/2$: maximize ν_e appearance and minimize $\bar{\nu}_e$ appearance

In ν -mode the deficit of μ -like events is compatible with statistical and systematic uncertainties

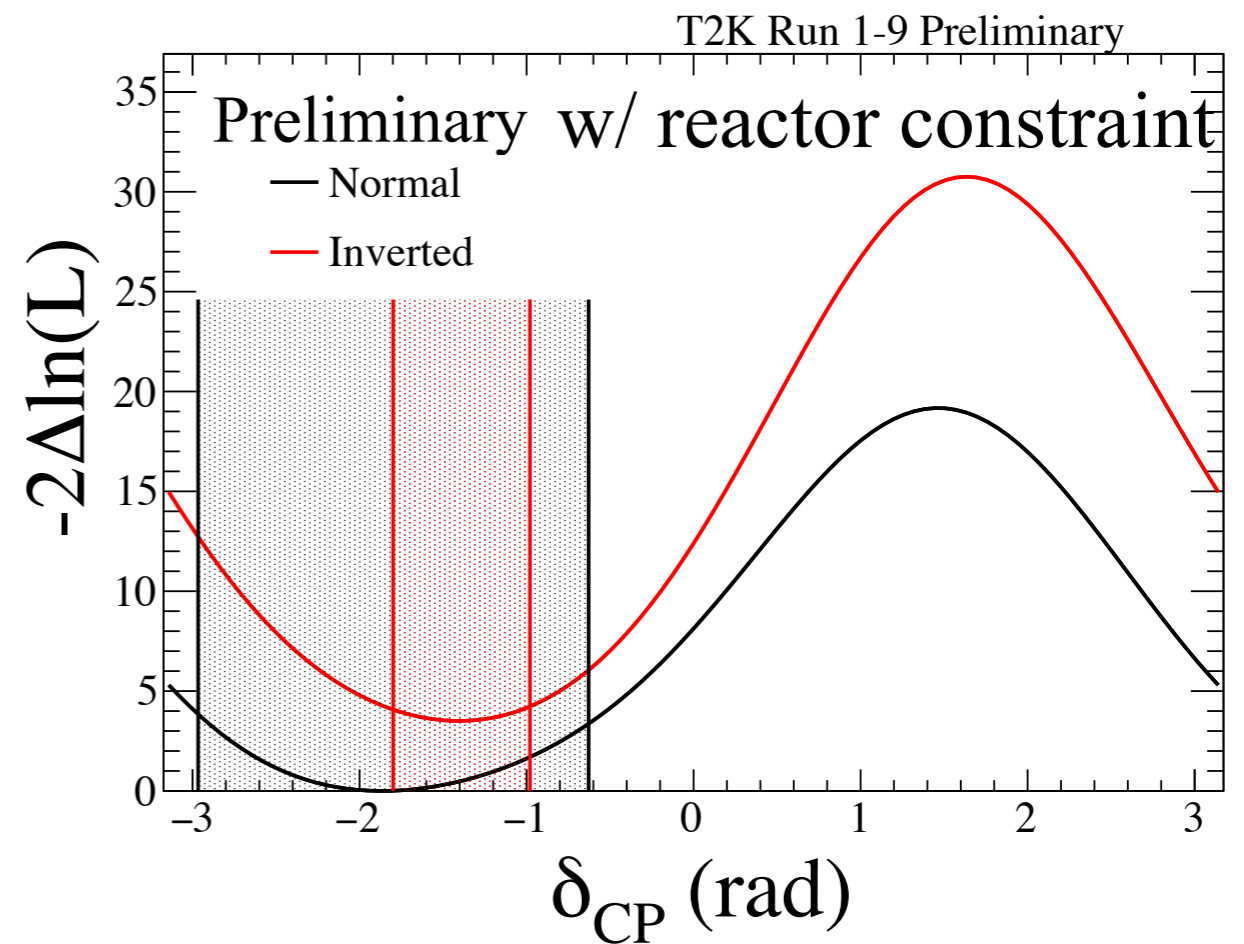
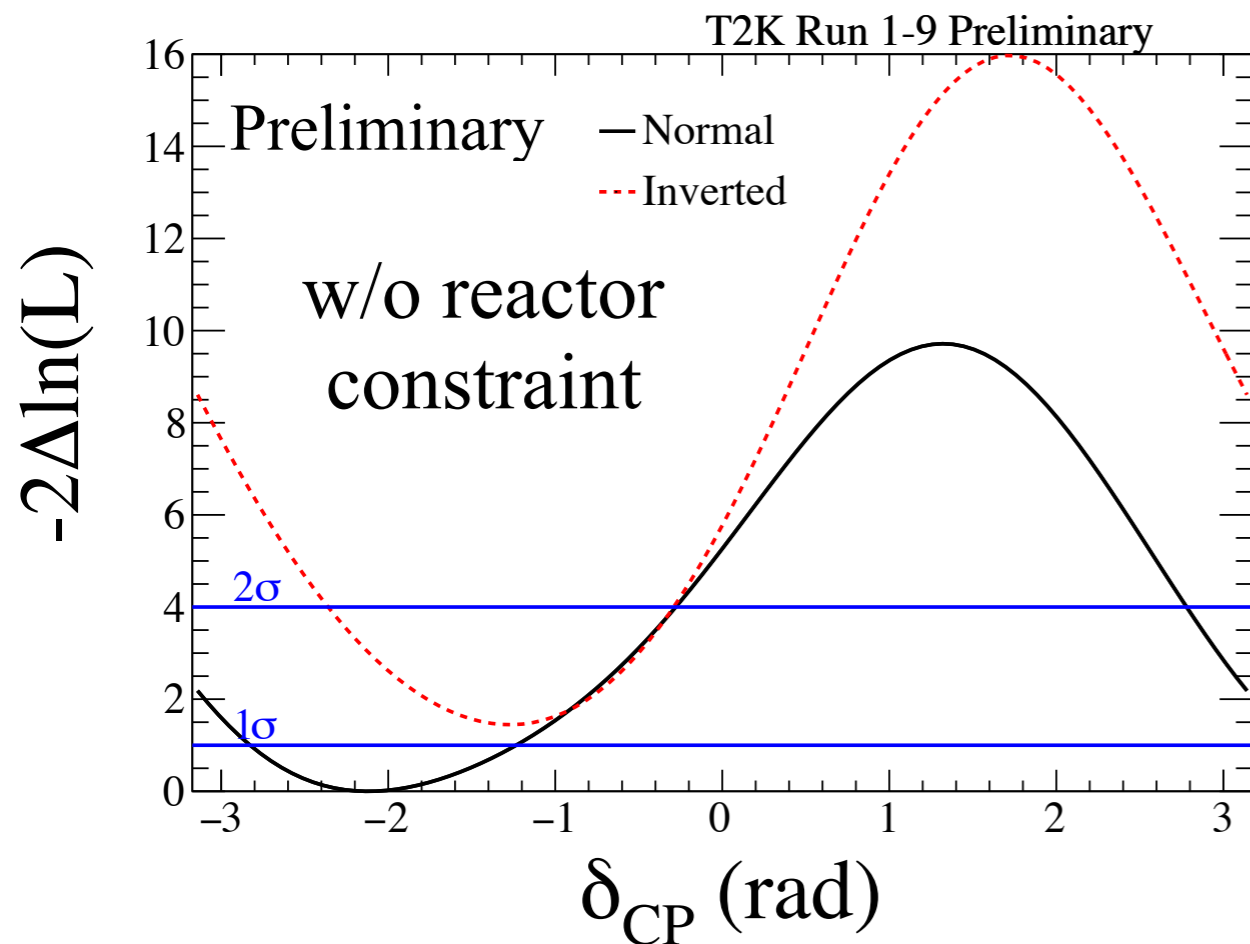


T2K oscillation analysis strategy



δ_{CP} measurement

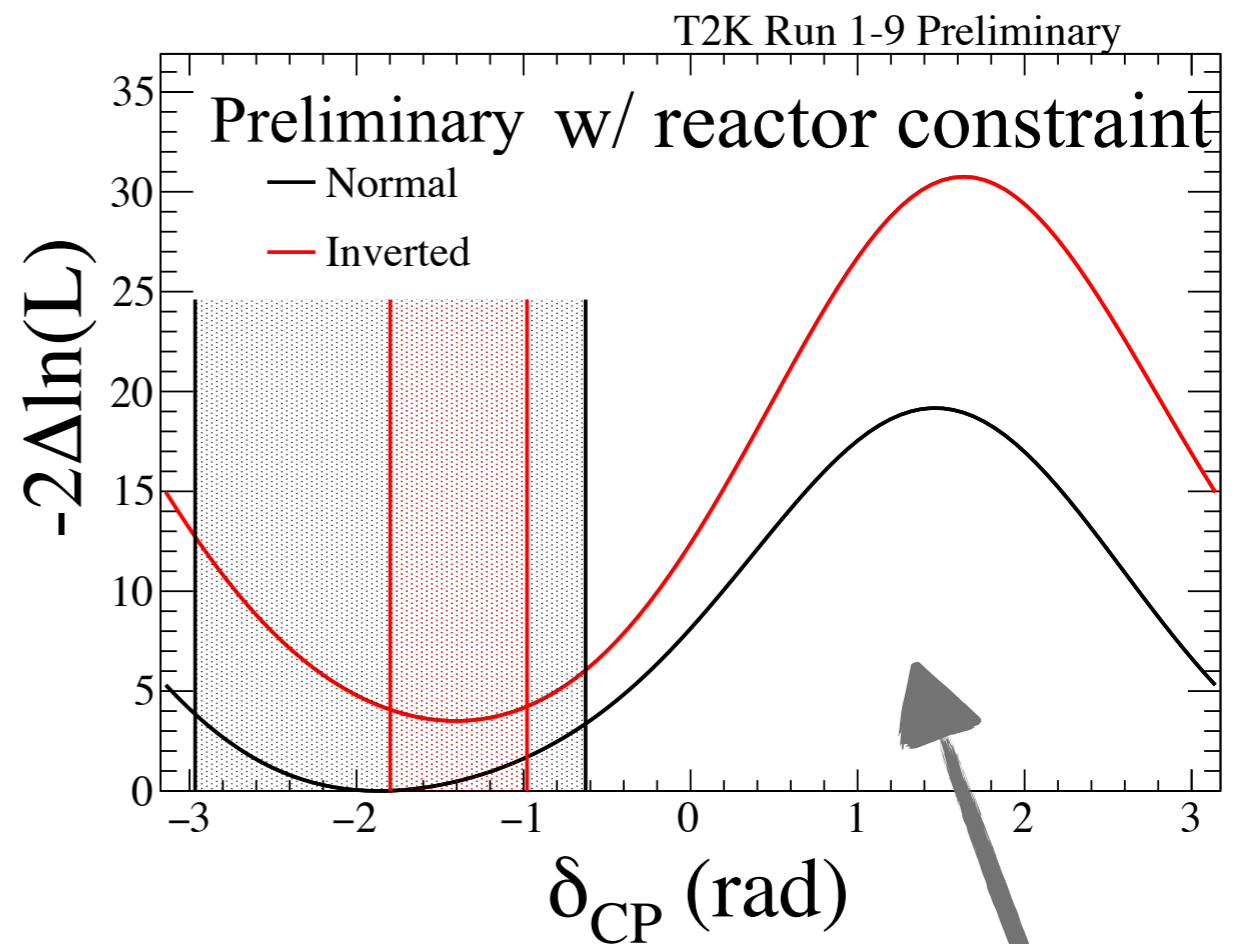
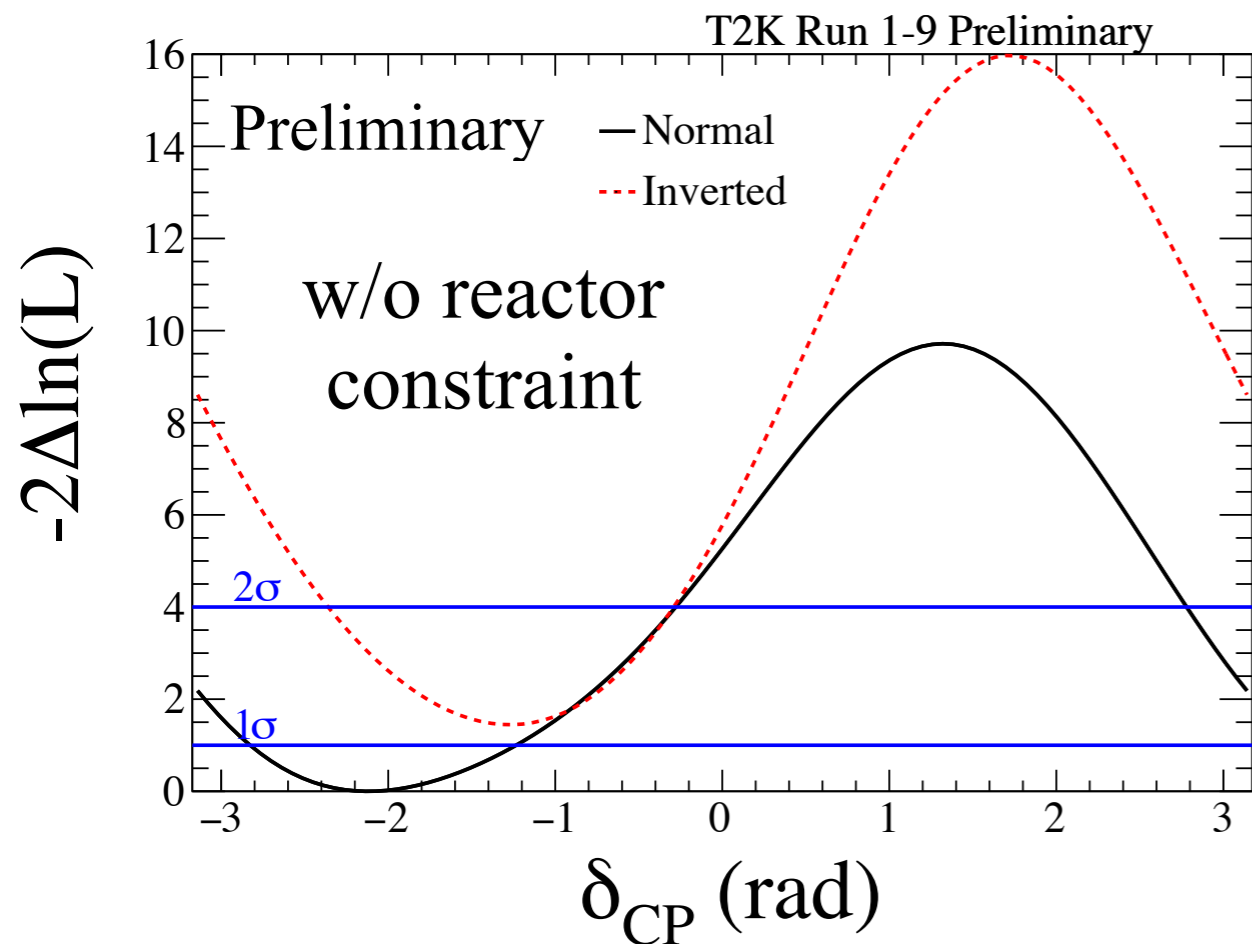
T2K data prefer values of $\delta_{CP} \sim -\pi/2$ mostly driven by the large number of events observed in the e -like sample in neutrino mode



C.L.	Normal hierarchy	Inverted hierarchy
68%	[-2.51, -1.26]	-
90%	[-2.80, -0.84]	-
2σ	[-2.97, -0.63]	[-1.78, -0.98]

δ_{CP} measurement

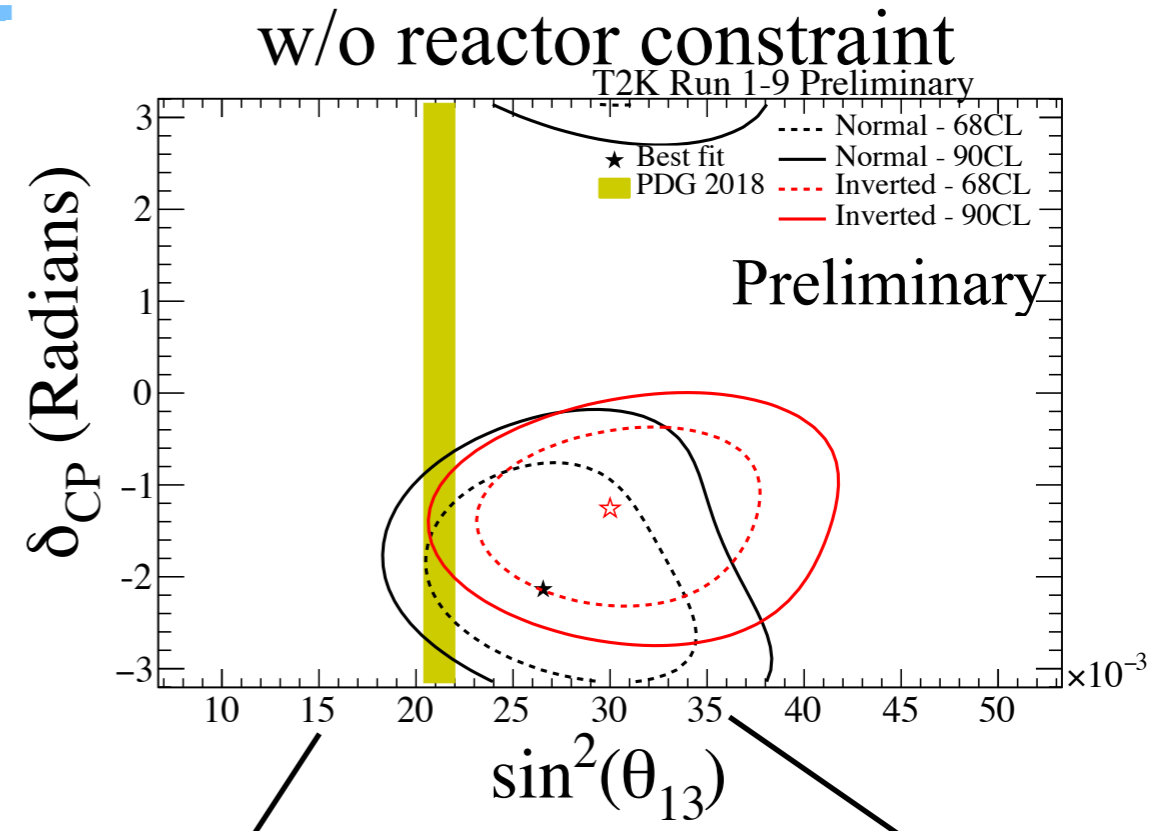
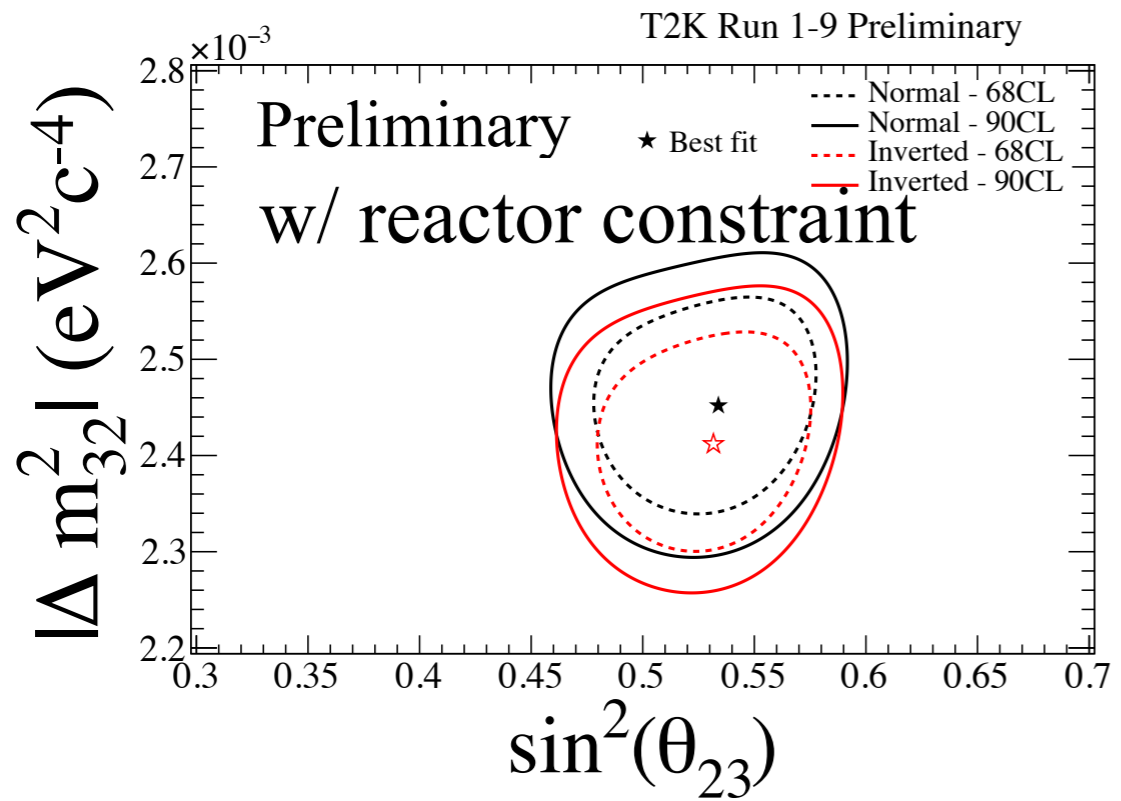
T2K data prefer values of $\delta_{CP} \sim -\pi/2$ mostly driven by the large number of events observed in the e -like sample in neutrino mode



C.L.	Normal hierarchy	Inverted hierarchy
68%	[-2.51, -1.26]	-
90%	[-2.80, -0.84]	-
2σ	[-2.97, -0.63]	[-1.78, -0.98]

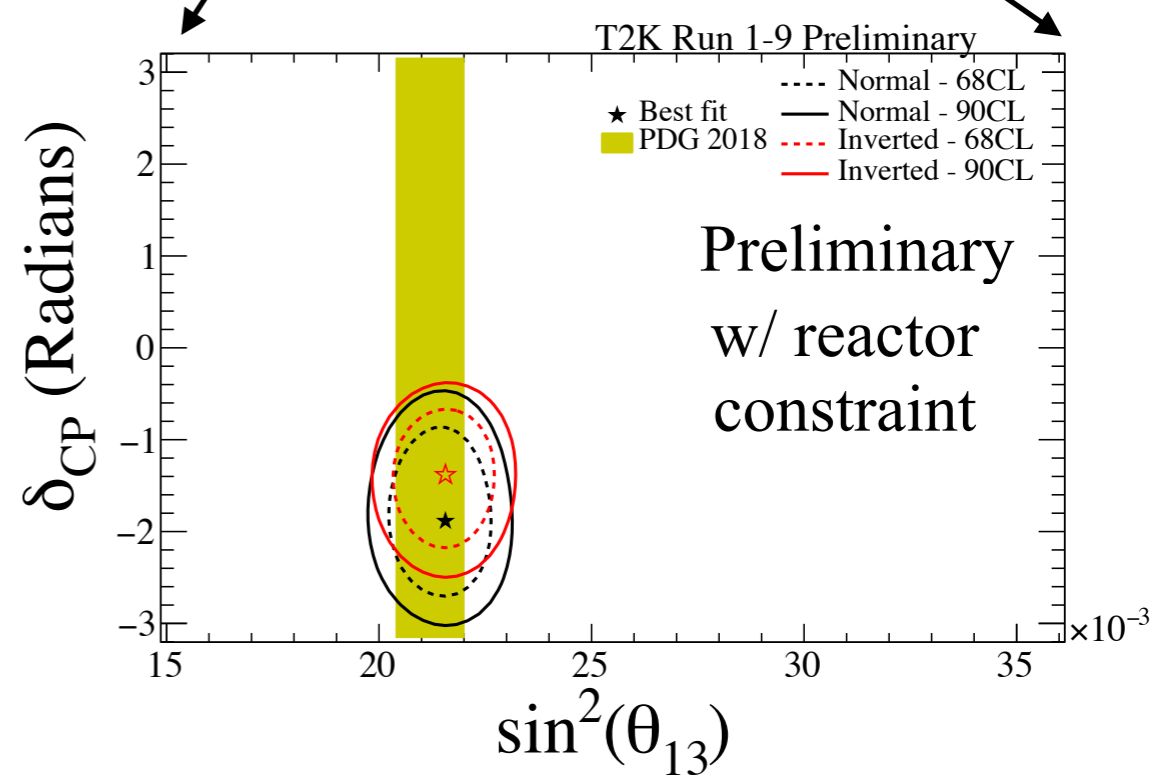
$\delta_{CP} = 0, \pi$ fall outside 2σ interval

Oscillation results (θ_{23} , $|\Delta m^2_{32}|$, θ_{13} , δ_{CP})



T2K data compatible with maximal mixing

Parameter	Best Fit NH (IH)	$\pm 1\sigma$ NH (IH)
$\sin^2\theta_{32}$	0.54 (0.53)	[0.490,0.558] ([0.496,0.560])
$ \Delta m^2_{32} \text{ (} 10^{-3}\text{eV}^2/\text{c}^4\text{)}$	2.46 (2.43)	[2.370,2.498] ([2.362,2.502])
$\sin^2\theta_{13}$	0.0268 (0.0305)	[0.0222,0.0319] ([0.0253,0.0369])



Conclusions

- T2K released results with 3.1×10^{21} POT (50% ν -mode, 50% $\bar{\nu}$ -mode)
- With these data CP conserving values are excluded at more than 2σ
- T2K data prefers maximal mixing
- Future improvements:
 - More data will come with many improvement in the analysis;
 - New antineutrino samples at the near detector;

Stay tuned!!!

Thank you for your attention

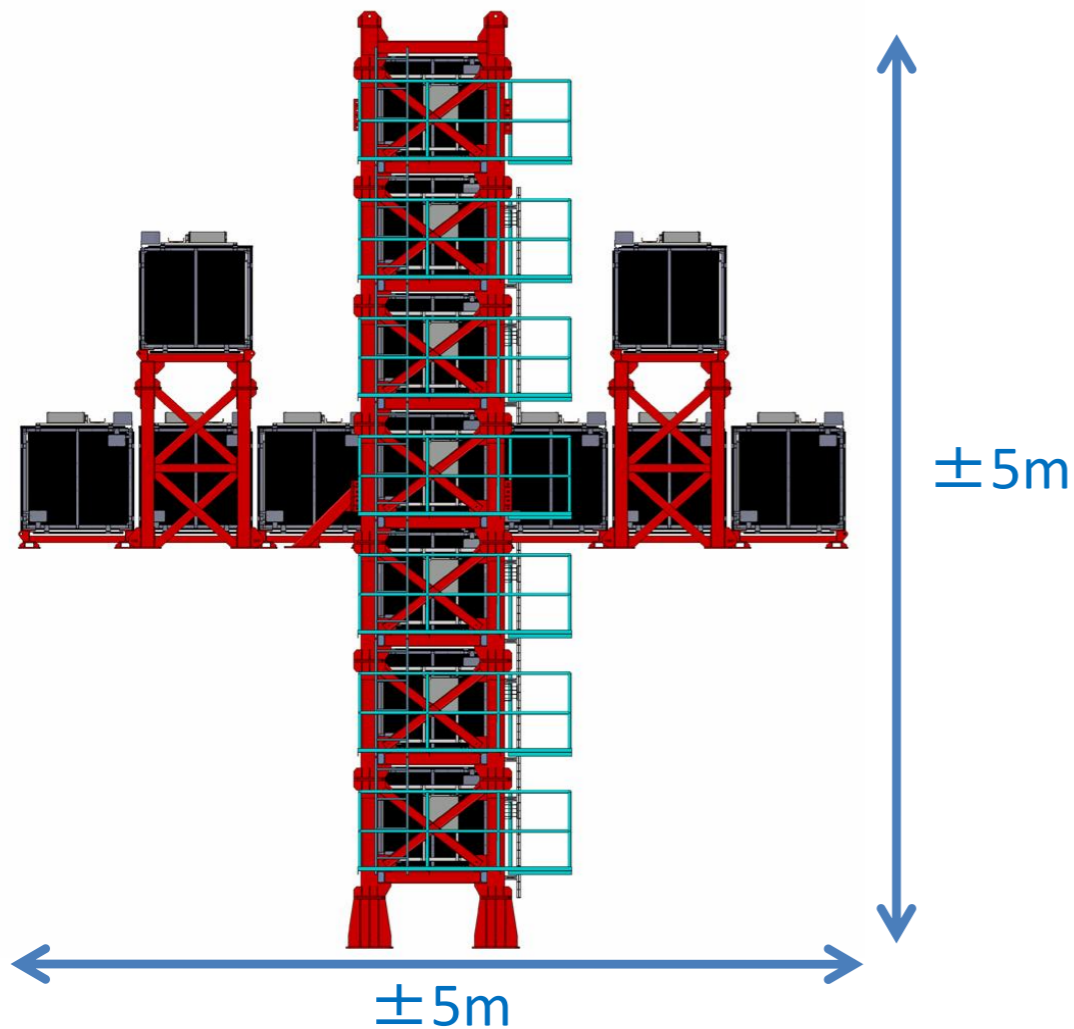
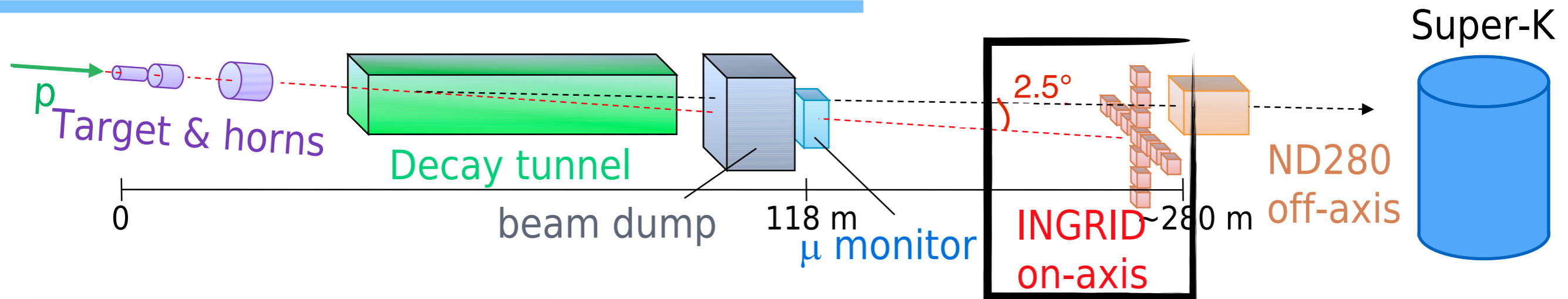


T2K Breakthrough Prize Party

January 28th, 2016 at Kuji Sunpia Hitachi

Backup

The on-axis near detector (INGRID)

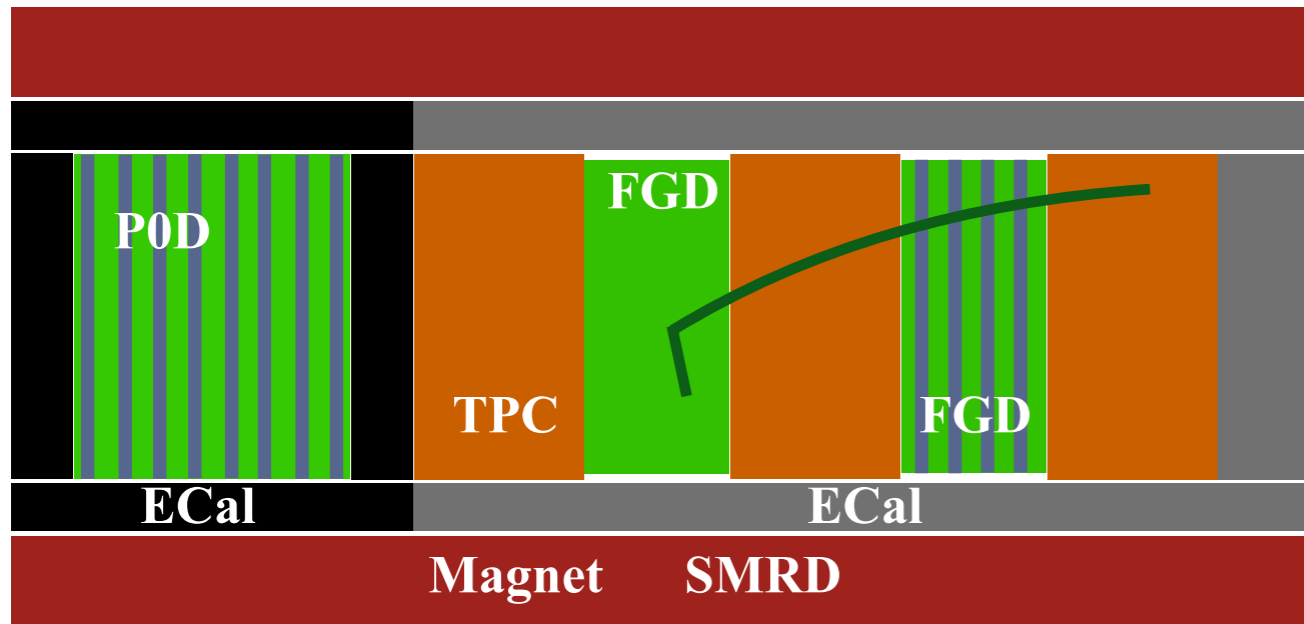


Monitor the beam stability and direction day-by-day looking at ν ($\bar{\nu}$) interactions

14 modules arranged in a cross; two others placed at off-diagonal positions

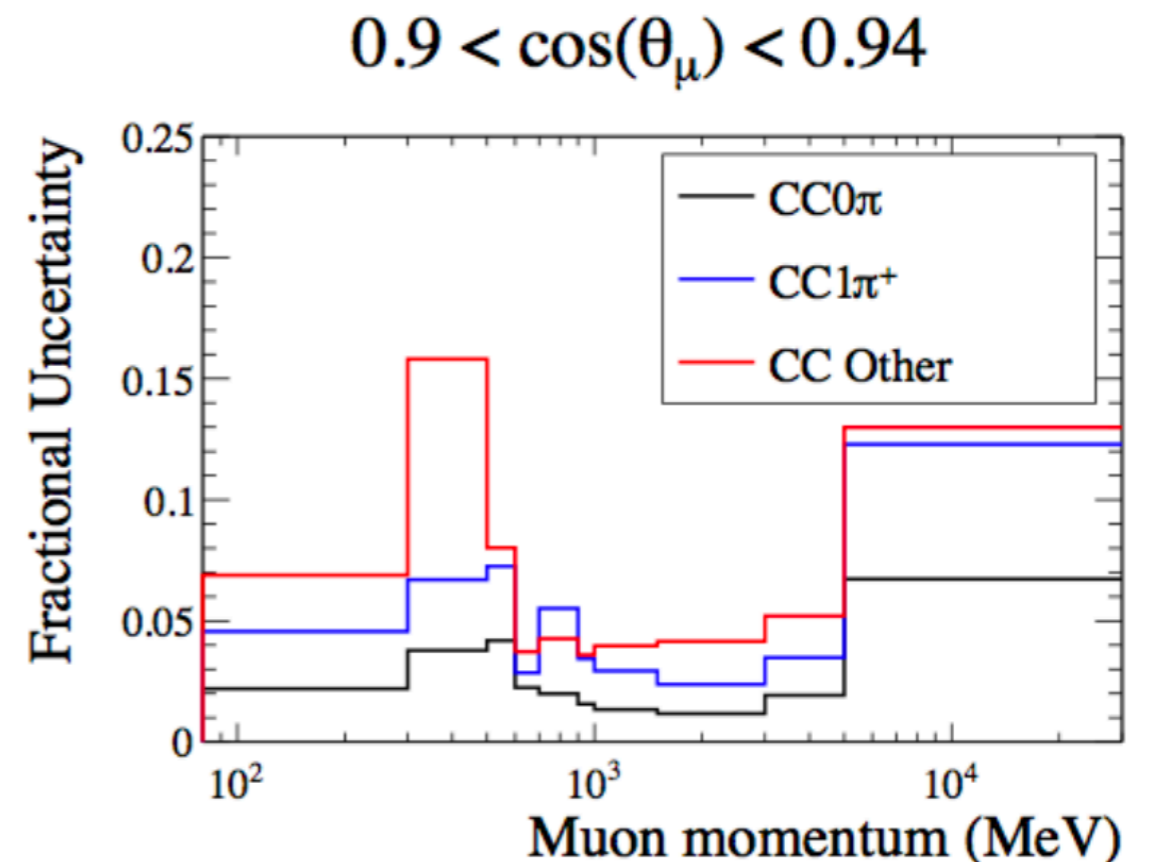
1 extra module made of scintillators and water at the center of the cross

ND280 Detector modeling



As far as possible, use data to constrain systematics; e.g. use cosmic samples to evaluate inter-detector matching

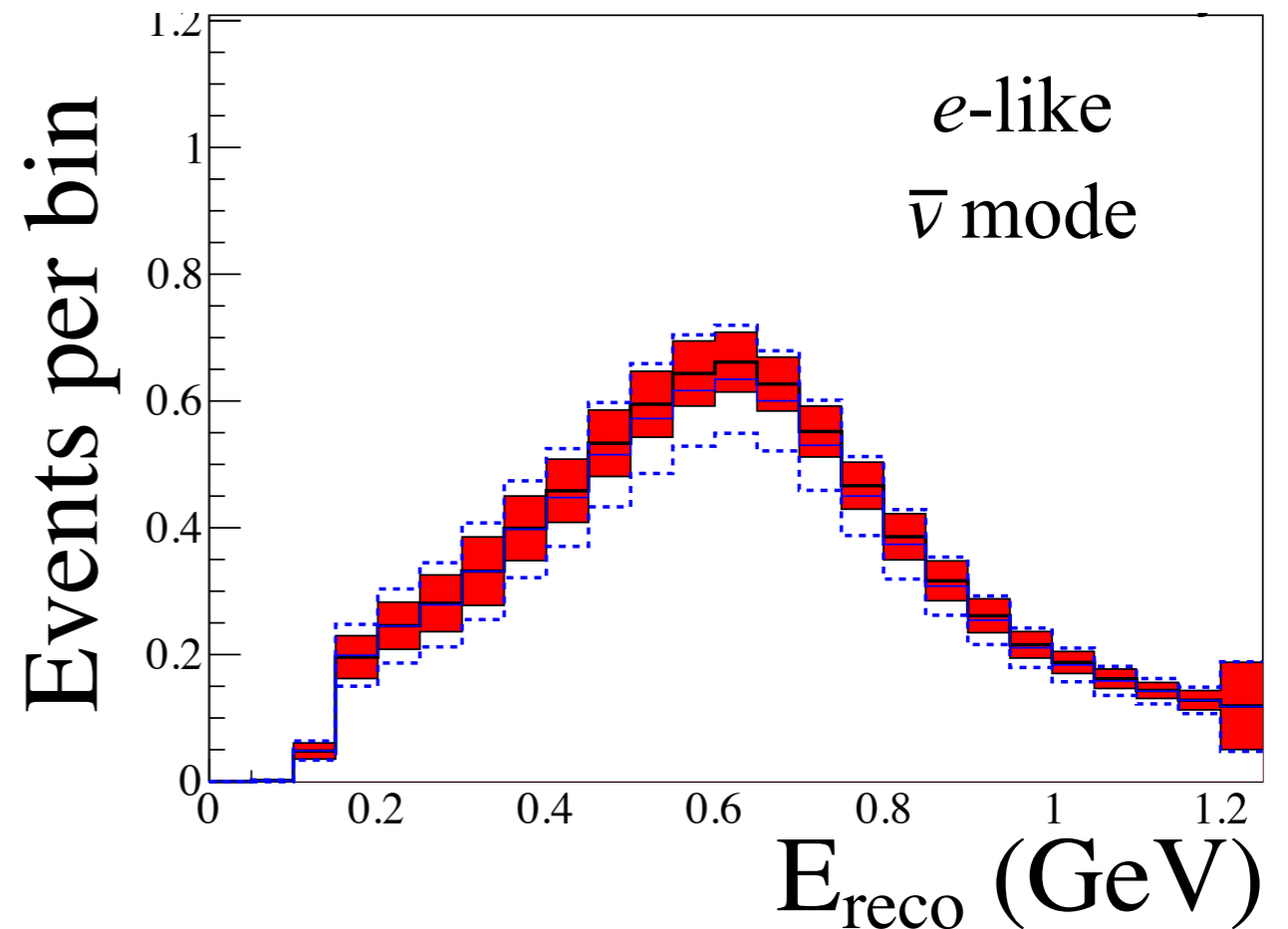
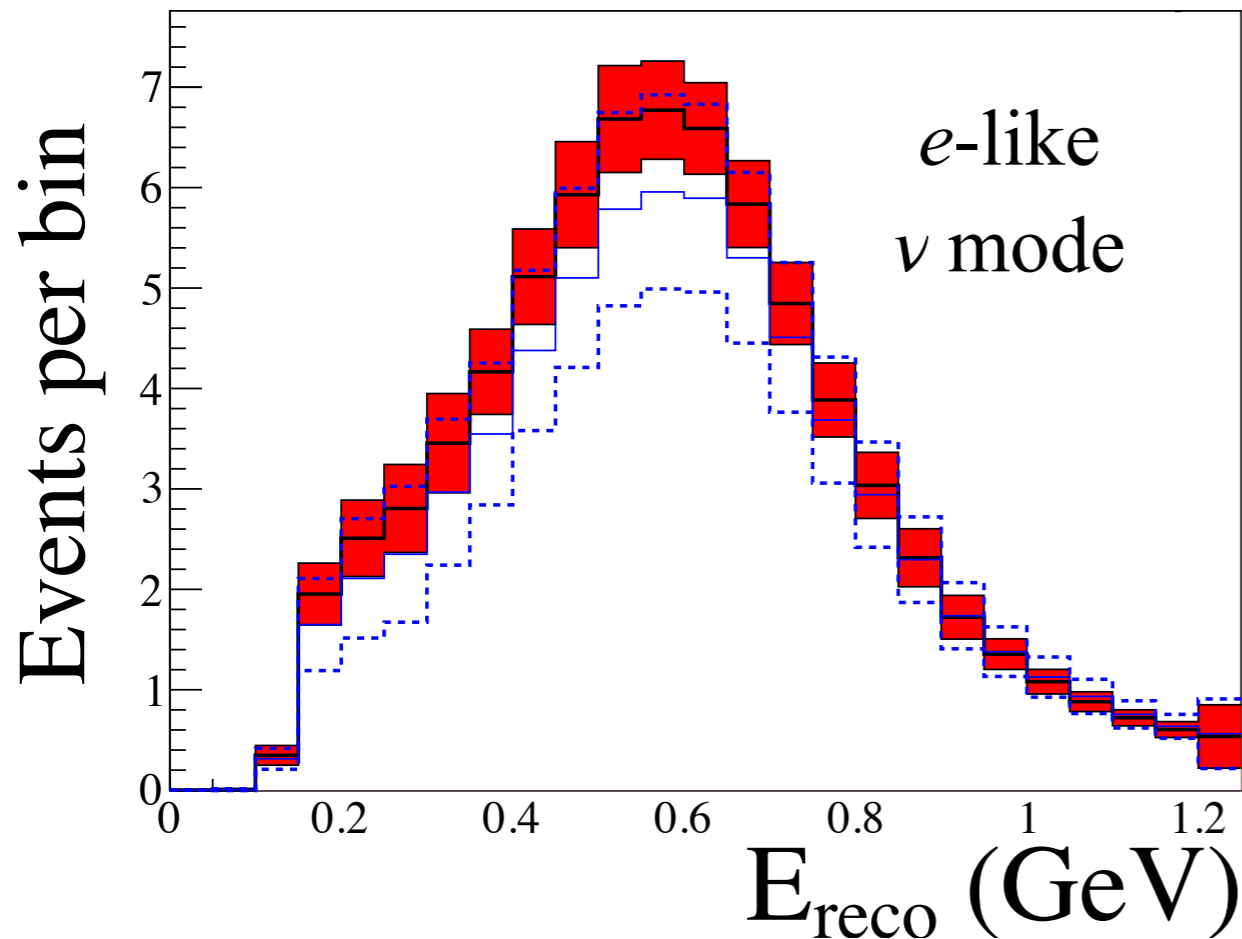
Dominant systematics are pion secondary interactions and out of fiducial volume events



Event generators: details

	NEUT 5.3.2	GENIE 2.8.0
CCQE	SF (Benhar et al., 2000) BBA05 (Bradford et al., 2005) $M_A^{QE} = 1.21 \text{ GeV}/c^2$ $p_F [^{12}\text{C}] = 217 \text{ MeV}/c$ $E_B [^{12}\text{C}] = 25 \text{ MeV}$	RFG (Bodek et al., 1981) BBA05 (Bradford et al., 2005) $M_A^{QE} = 0.99 \text{ GeV}/c^2$ $p_F [^{12}\text{C}] = 221 \text{ MeV}/c$ $E_B [^{12}\text{C}] = 25 \text{ MeV}$
2p2h	Nieves et al., 2011	-
CCRES	<u>$W < 2 \text{ GeV}$</u> Rein-Sehgal, 1981 FF (Graczyk et al., 2008)	<u>$W < 1.7 \text{ GeV}$</u> Rein-Sehgal, 1981 FF (Kuzmin et al., 2016)
CCDIS	<u>$W > 1.3 \text{ GeV}$ (w/o single π)</u> GRV98 PDF (Glück et al. 1998) BY corr. at low Q^2 (Bodek et al. 2003)	<u>$W > 1.7 \text{ GeV}$ (for $W < 1.7 \text{ GeV}$ is tuned)</u> GRV98 PDF (Glück et al. 1998) BY corr. at low Q^2 (Bodek et al. 2005)
Hadronization	<u>$W < 2 \text{ GeV}$</u> KNO scaling (Koba et al. 1972) <u>$W > 2 \text{ GeV}$</u> PYTHIA/JETSET	<u>$W < 2.3 \text{ GeV}$</u> AGKY (Koba et al. 1972) <u>$2.3 \text{ GeV} < W < 3 \text{ GeV}$</u> AGKY (Koba et al. 1972) + PYTHIA/JETSET <u>$W > 3 \text{ GeV}$</u> PYTHIA/JETSET
FSI	Intra-nuclear cascade	Intra-nuclear cascade (INTRANUKE hA)

Expectation at SK

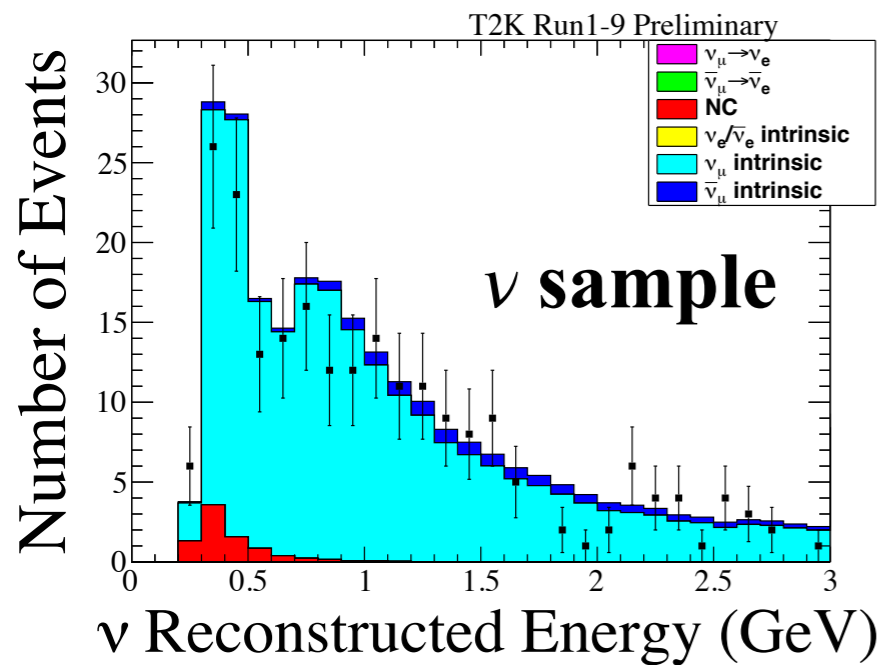


ND280 constraints are crucial for oscillation analysis precision

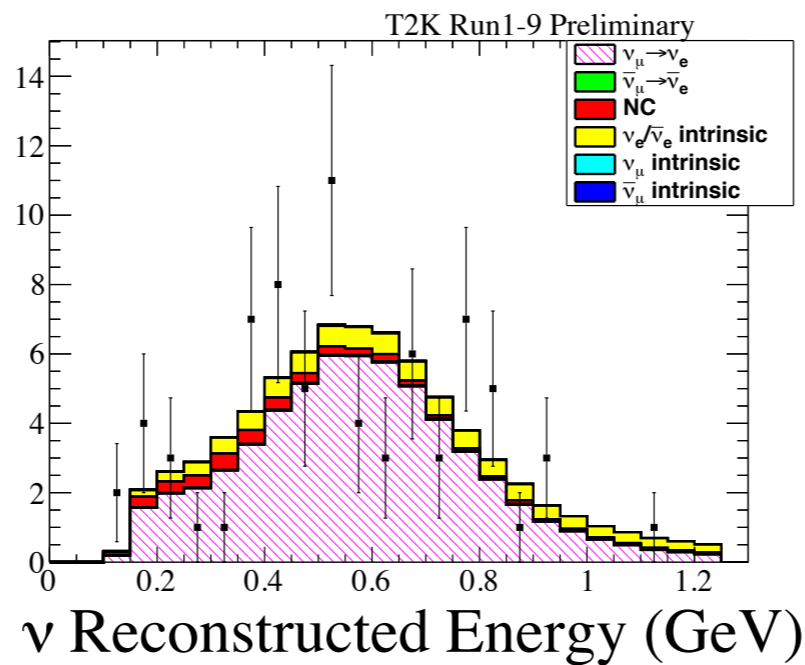
	ν mode			$\bar{\nu}$ mode	
	μ -like	<i>e</i> -like	<i>e</i> -like+ $1\pi^+$	μ -like	<i>e</i> -like
Total w/o ND280	14.6%	16.9%	22.0%	12.5%	14.4%
Total w/ ND280	5.1%	8.8%	18.7%	4.5%	7.1%

SK Samples

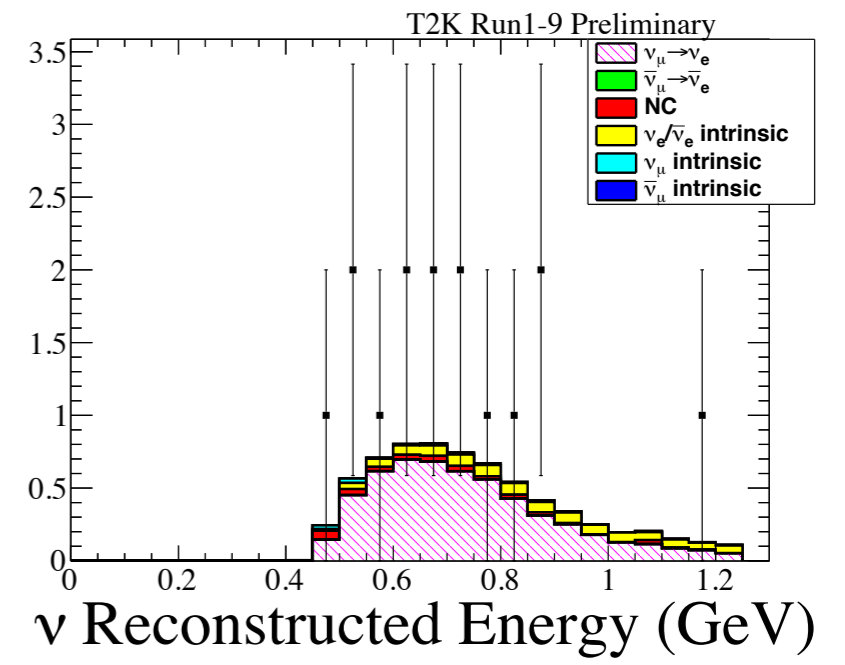
1 μ -like ring



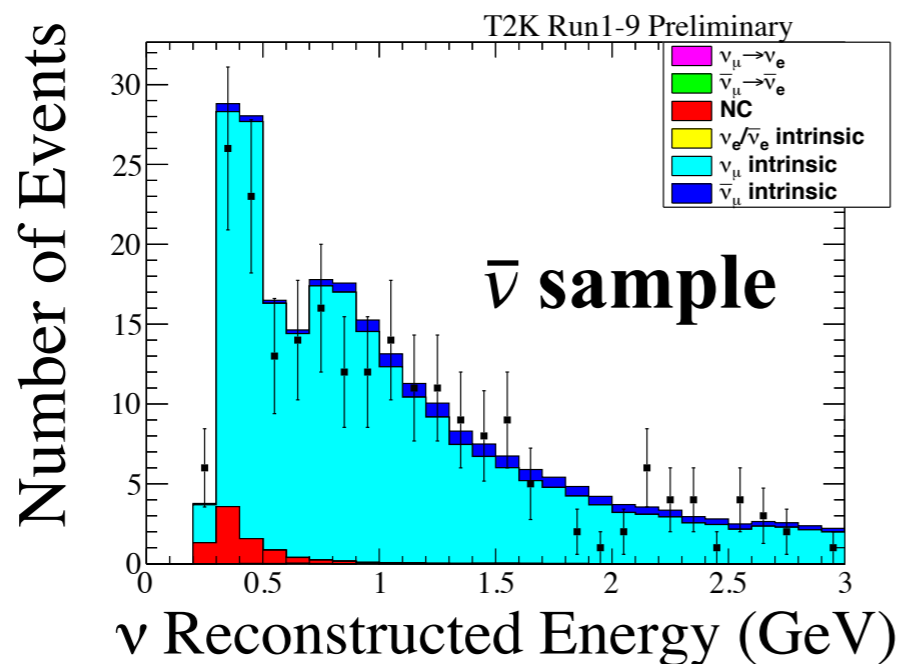
1 e -like ring



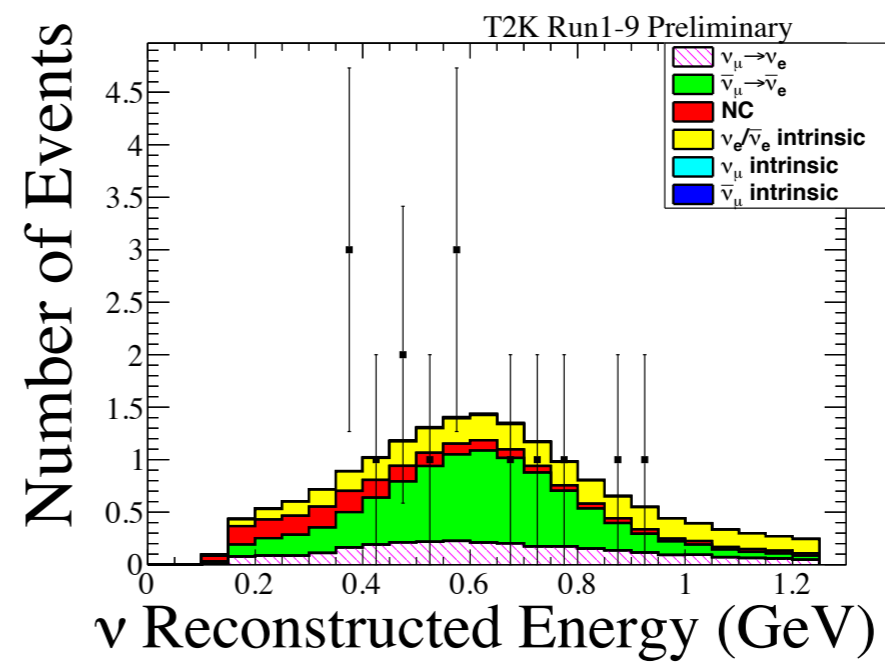
1 e -like + 1 Michel- e -like ring



1 μ -like ring

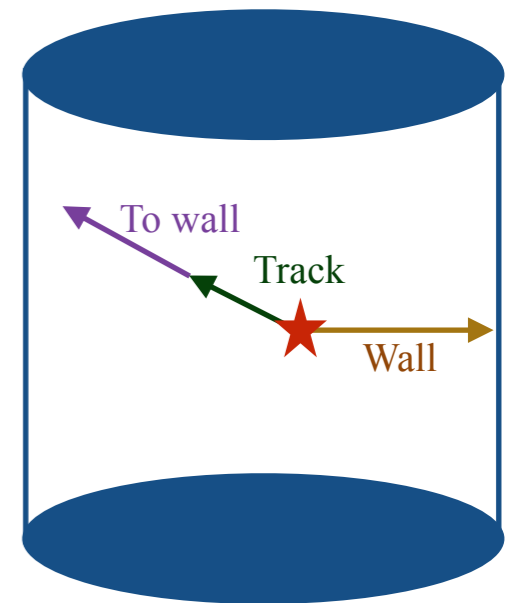


1 e -like ring



SK reconstruction

- New reconstruction algorithm is used for SK
- It combines time and charge likelihood for a given ring hypothesis
- New definition of fiducial volume combining distance of the vertex from the wall and direction to the wall (previously only distance from the wall was used)
 - ~30% more statistics for ν -mode e -like samples
 - ~20% more statistic for $\bar{\nu}$ -mode e -like
 - Better purity for μ -like samples by reducing NC background



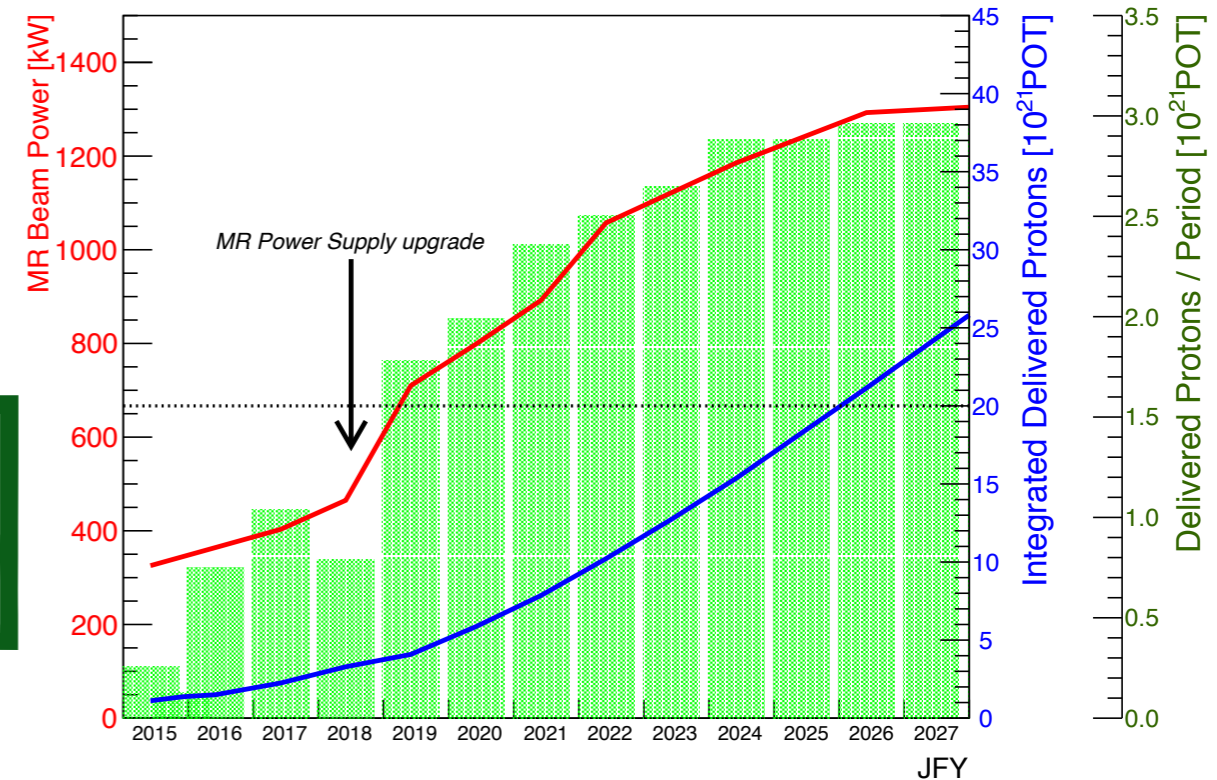
Samples	New SK selection	Old SK selection
	Purity	Purity
μ -like ν mode	80%	68%
e -like ν mode	81%	81%
e -like+ $1\pi^+$ ν mode	79%	72%
μ -like $\bar{\nu}$ mode	80%	71%
e -like $\bar{\nu}$ mode	62%	64%

Future prospects: T2K-II

T2K was originally approved to collect 7.8×10^{21} POT driven by sensitivity to θ_{13}

Proposal for an extended to collect 20×10^{21} POT

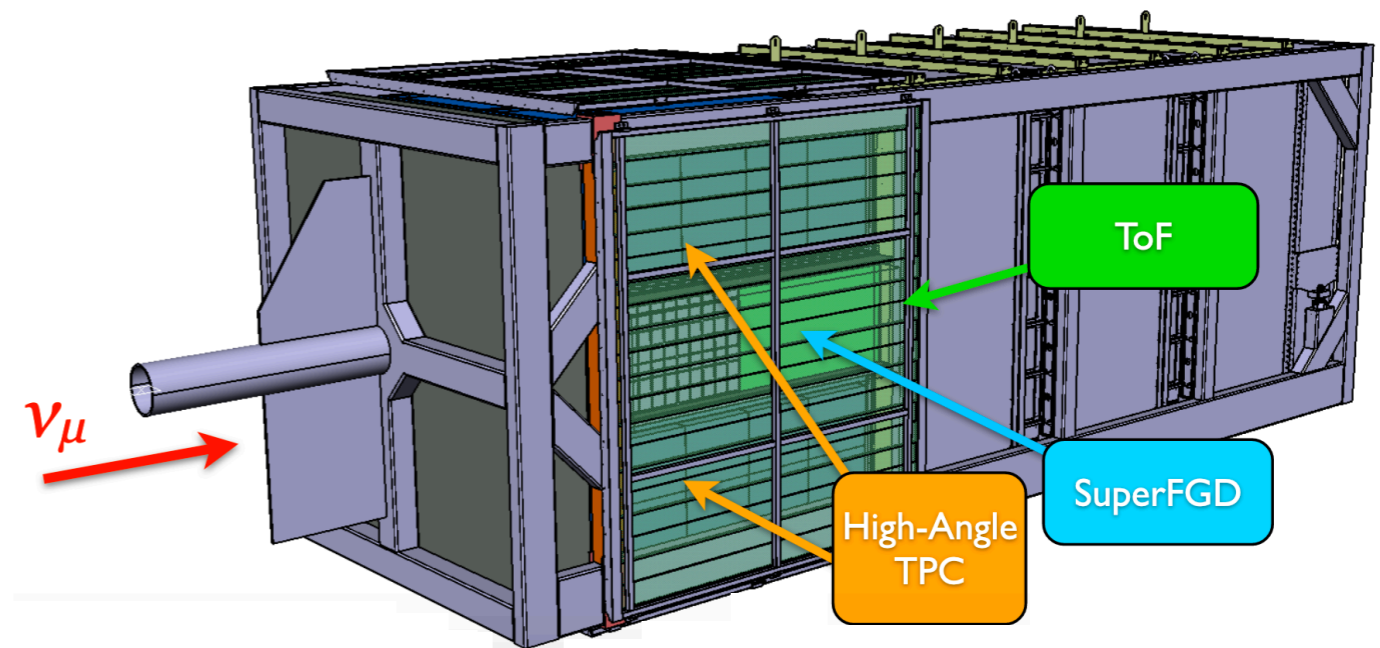
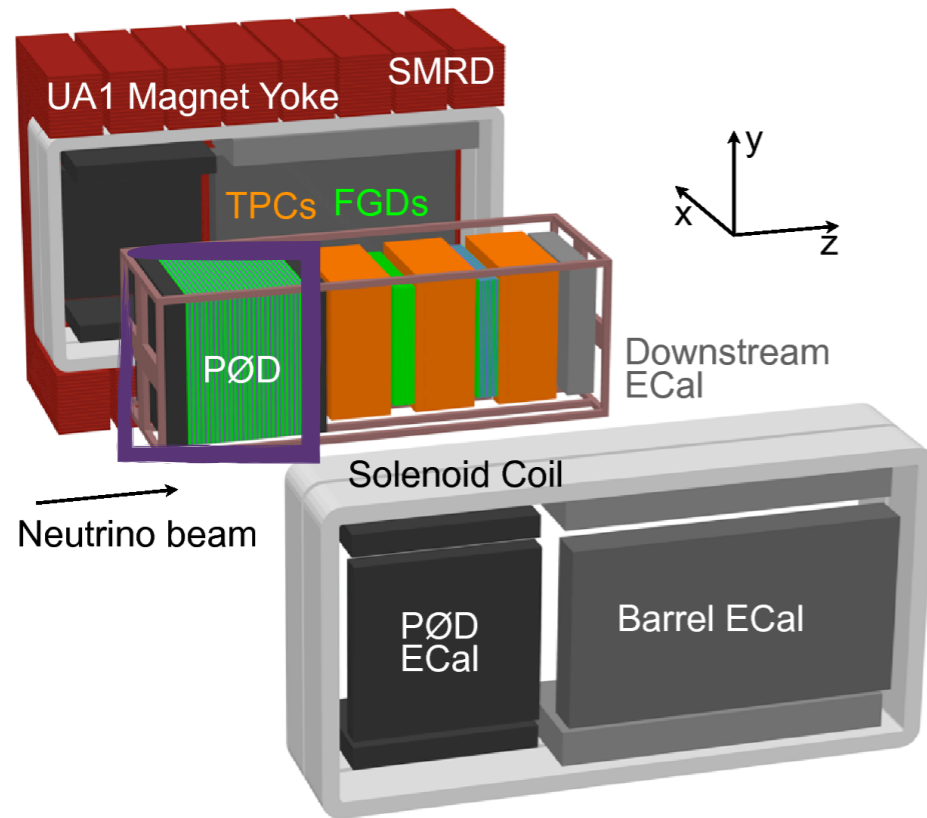
Increase beam power up to 1.3 MW and horn current up to ± 320 kA



SK plan to start to dope water with Gadolinium from next year:

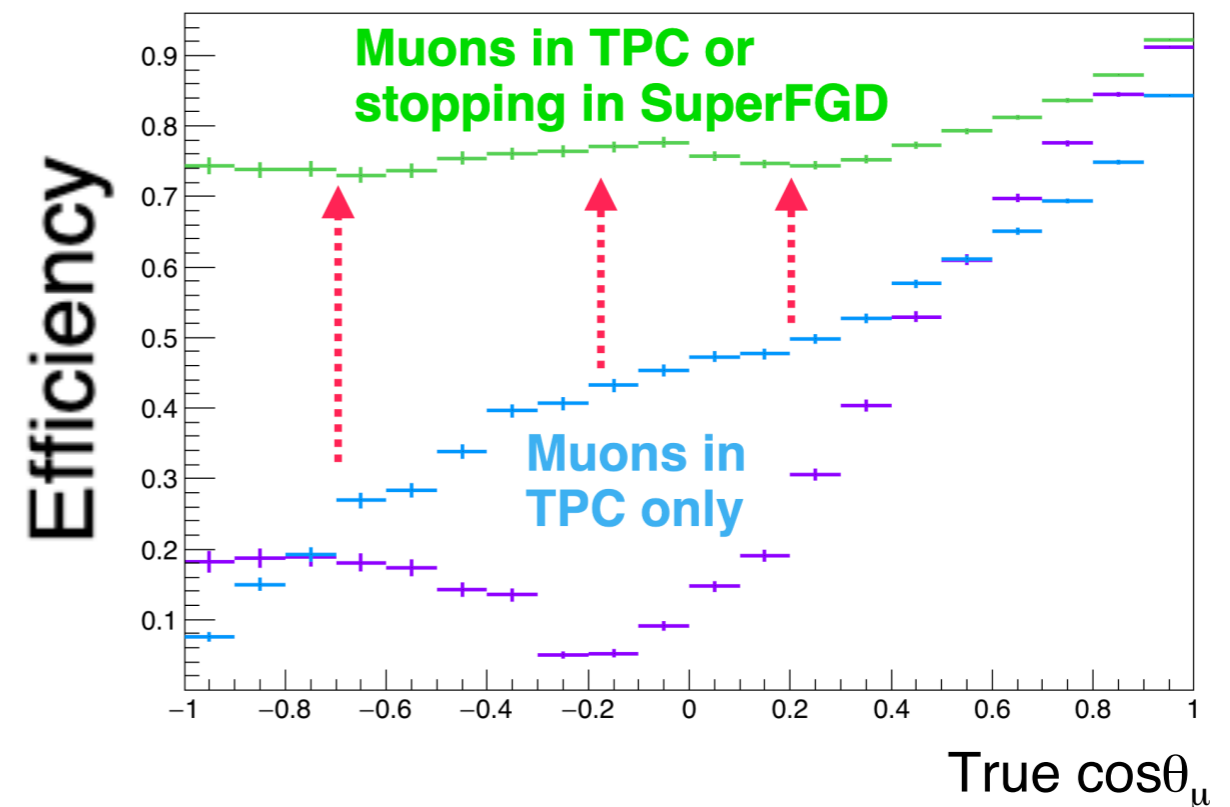
- Enhance neutron detection capability
- Improves low energy antineutrino detection
- Provides wrong sign bkg constraint in T2K antineutrino data

T2K-II: ND280 upgrade

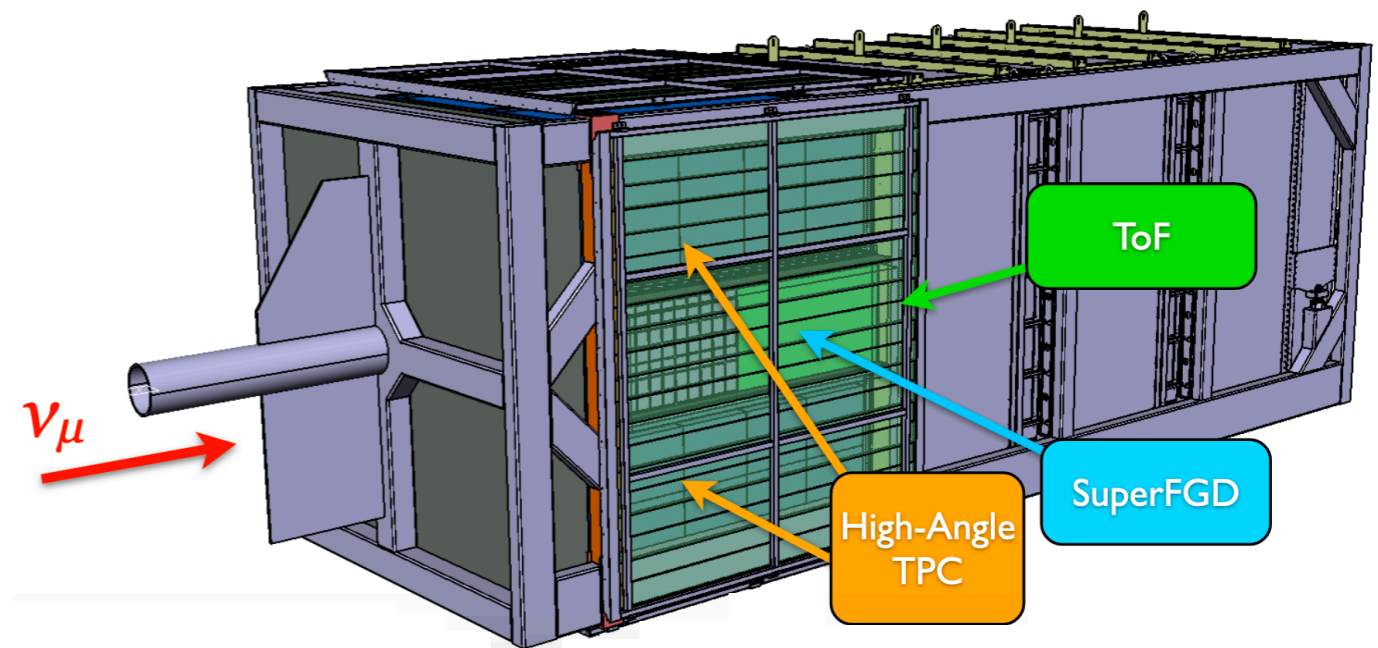
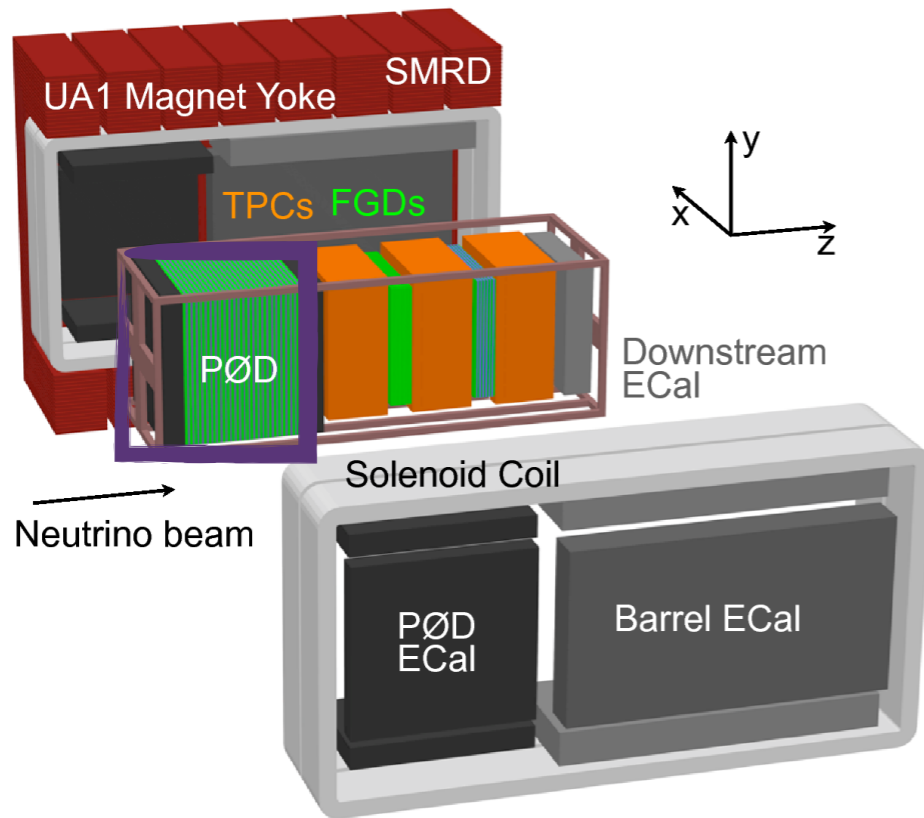


Main ND280 limitations:

- Low efficiency in the “high-angle” region
- Reduced sensitivity to cross section models
- Low threshold for protons

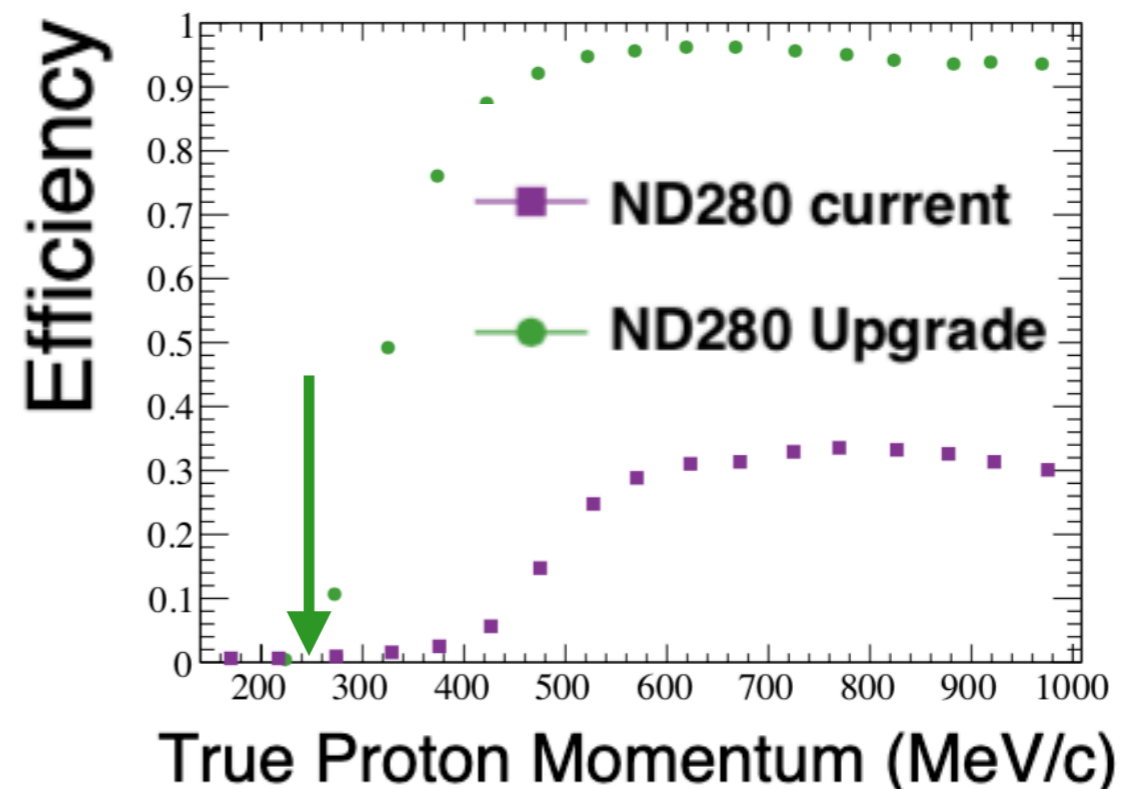


T2K-II: ND280 upgrade

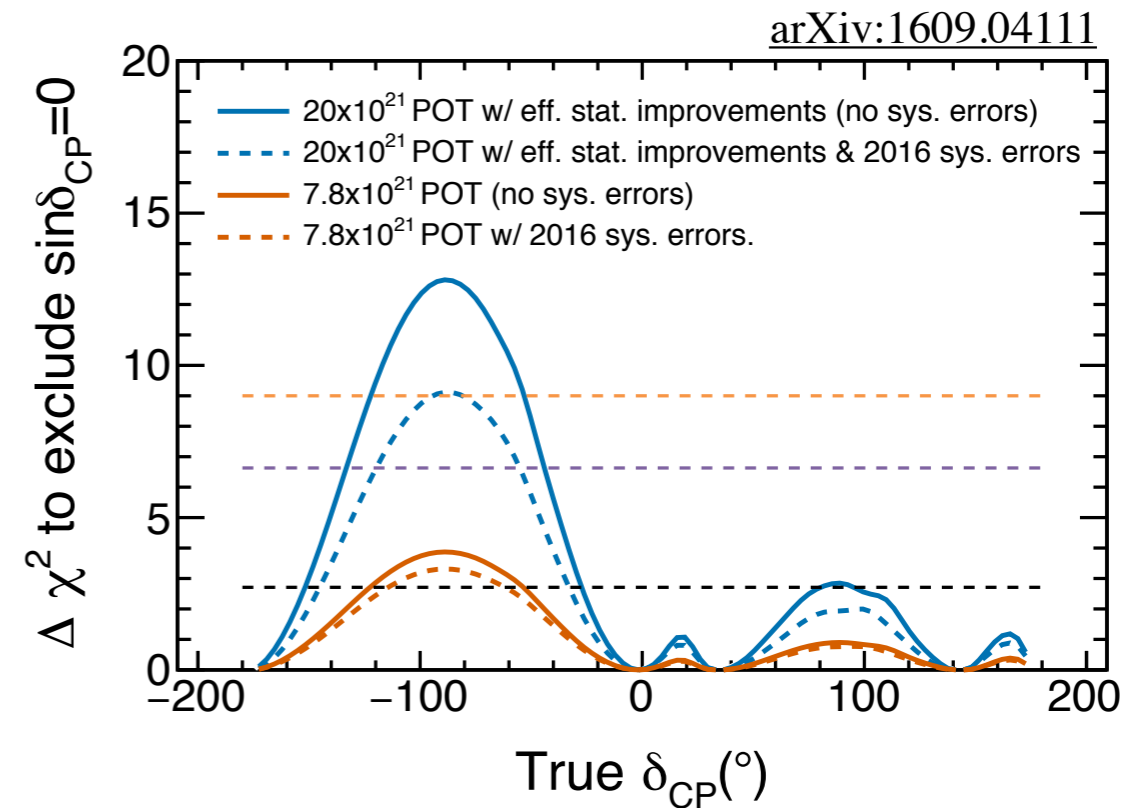
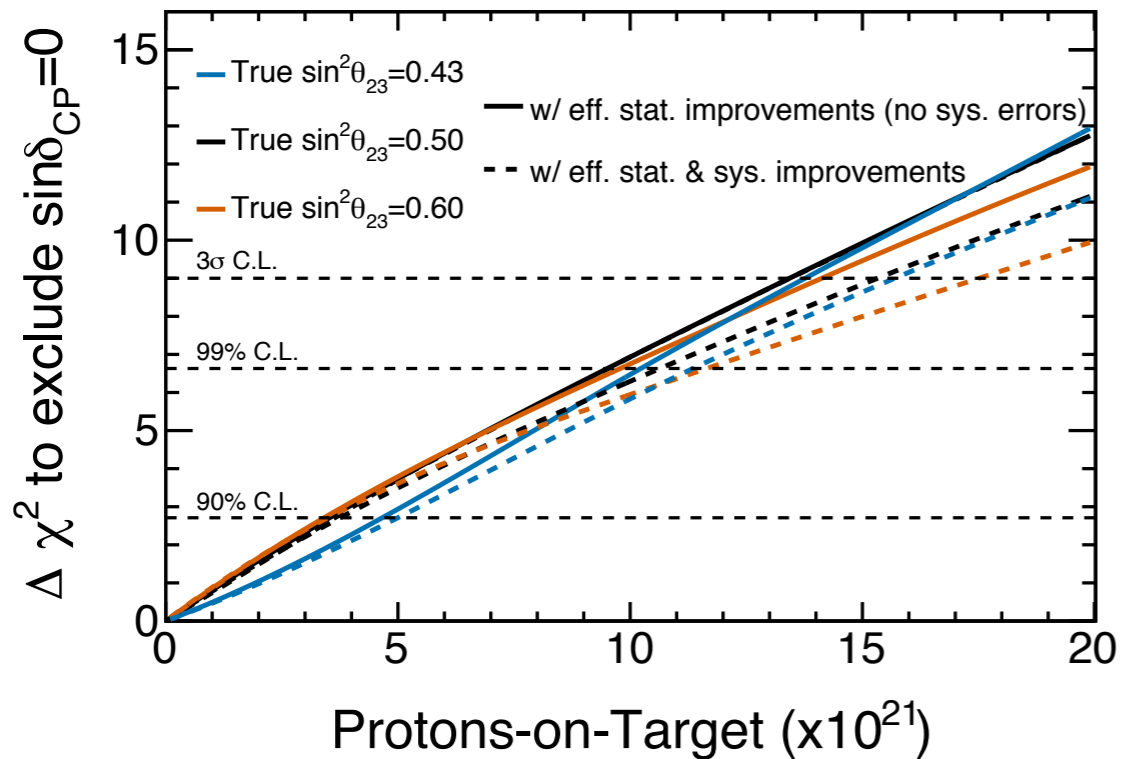


Main ND280 limitations:

- Low efficiency in the “high-angle” region
- Reduced sensitivity to cross section models
- Low threshold for protons

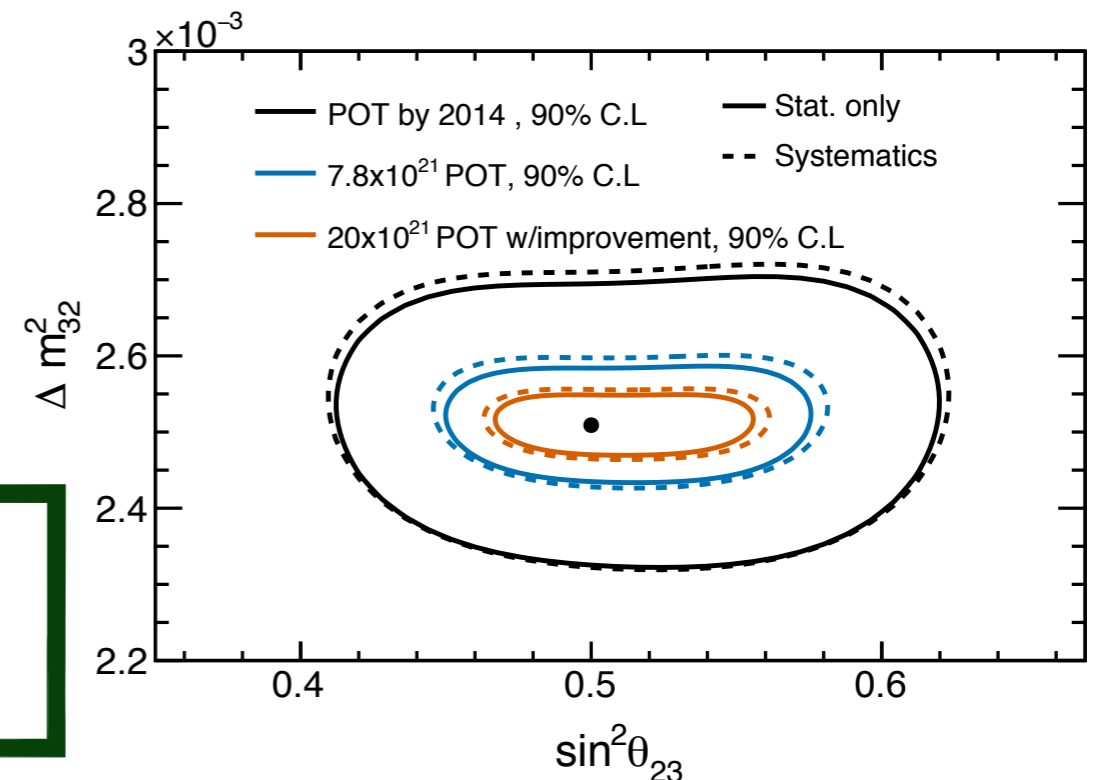


T2K-II physics case



$\sim 3\sigma$ sensitivity to CP-violation for favorable (and currently favored) parameters

Important to reduce systematics with respect to what we have today



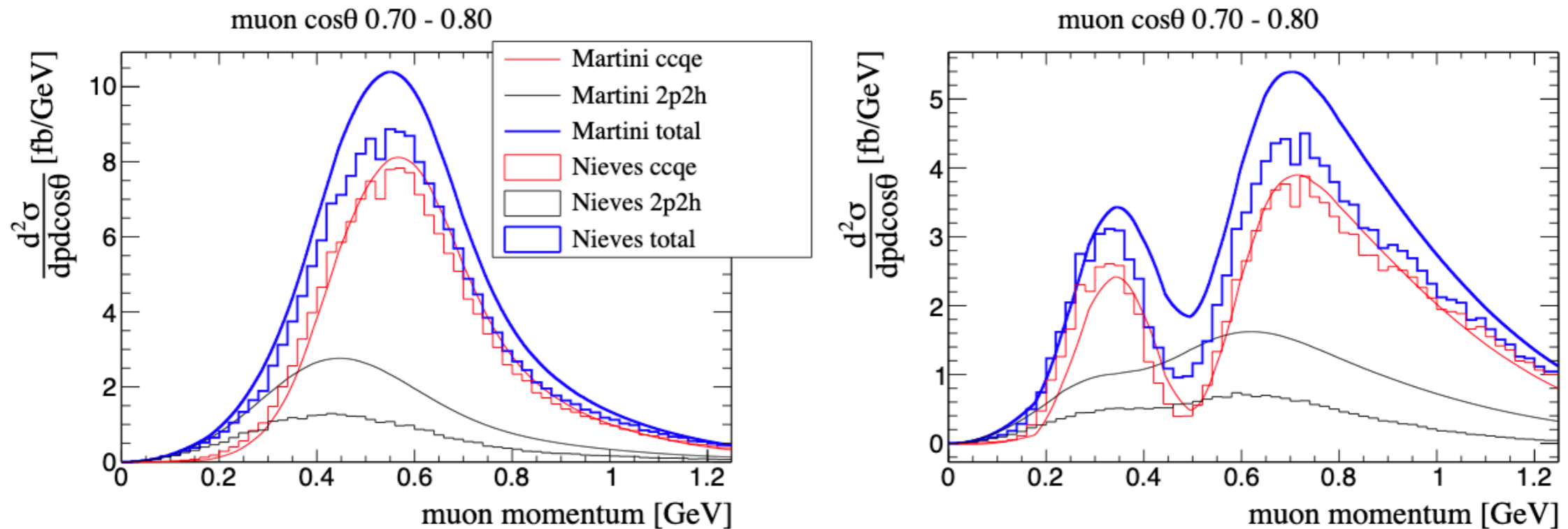
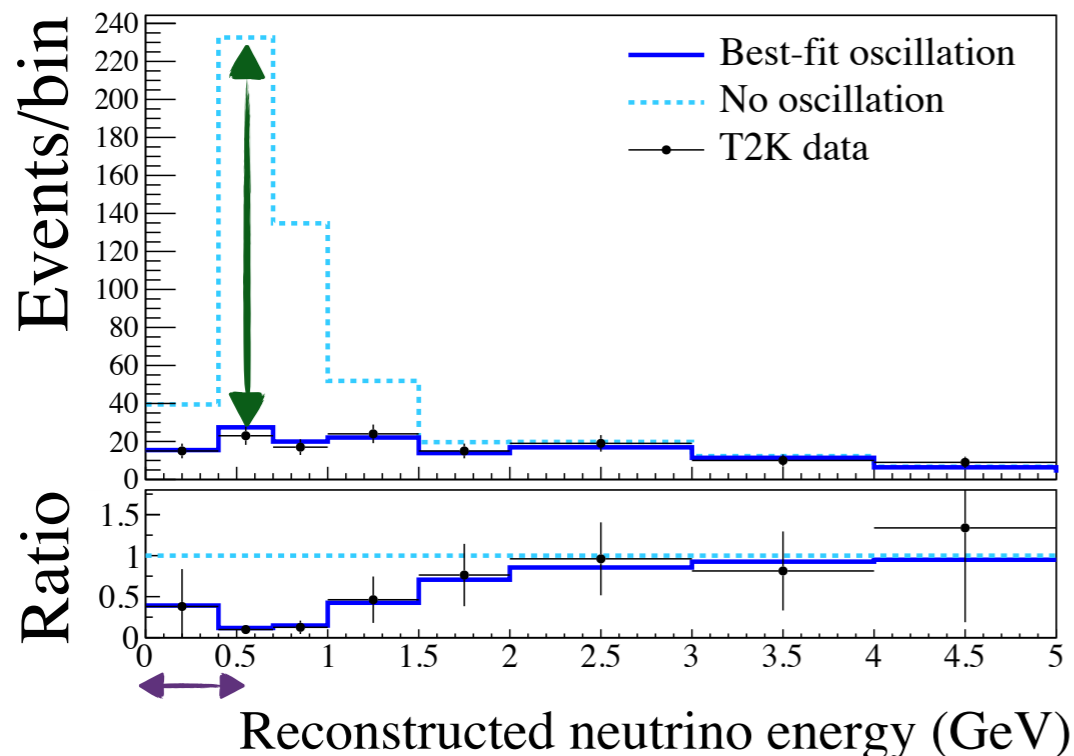


FIG. 18: Distribution of CCQE and 2p2h contributions as a function of muon momentum in the angular range $\cos\theta = [0.7, 0.8]$ at ND280 (left) and Super-K (right) as predicted in the models of Martini *et al.* [68] (continuous line) and Nieves *et al.* [69, 70] (histogram).

T2K oscillation (θ_{23} , $|\Delta m^2_{23}|$)

- Atmospheric parameters (θ_{23} , Δm^2_{32}) through ν_μ disappearance

$$P(\bar{\nu}_\mu \rightarrow \bar{\nu}_\mu) \approx 1 - \sin^2 2\theta_{23} \sin^2 \left(\frac{\Delta m^2_{32} L}{4E} \right)$$



$\sin^2 2\theta_{23}$ proportional to the depth of the dip (oscillation minimum)

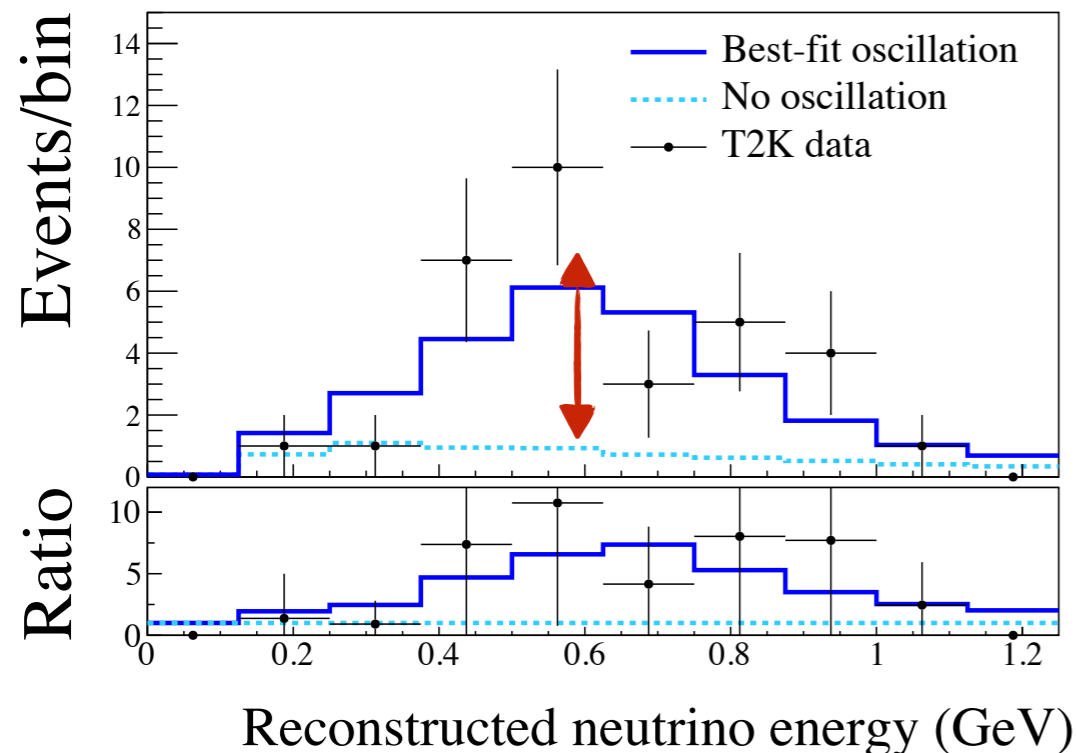
Δm^2_{23} proportional to the position of the dip

T2K oscillation (θ_{13} , δ_{CP})

- $(\theta_{13}, \delta_{CP})$ depends on the $\nu_e/\bar{\nu}_e$ appearance

$$P(\bar{\nu}_\mu \rightarrow \bar{\nu}_e) \approx \sin^2 2\theta_{13} \sin^2 \theta_{23} \sin^2 \left(\frac{\Delta m_{32}^2 L}{4E} \right) (\mp) O(\delta_{CP})$$

In the case of T2K δ_{CP} change the appearance probability by $\pm 30\%$ while the mass ordering has a $\sim 10\%$ effects



$\sin^2 2\theta_{13}$ proportional to the oscillation maximum

θ_{13} compatible with the one measured by experiments at reactors.